TEXTILE RESEARCH JOURNAL

VOLUME XXV August 1955 *NUMBER 8*

PUBLICATION OF

TEXTILE RESEARCH INSTITUTE

Editorial Office: 10 East 40th Street, New York 16, N. Y.

FOR MAXIMUM CROCK-FASTNESS

IN PIGMENT DYEING AND PRINTING—

RHOPLEX AC-33*

RHOPLEX AC-33 is an acrylic resin emulsion which imparts excellent crock resistance when used as a binder for pigment dyeing and printing.

It also exhibits unusually high emulsion stability in storage and in application.

RHOPLEX AC-33 as a resin finish forms a crystal-like film which produces a firm, full hand of good durability.

* **RHOPLEX AC-33** *is another dependable chemical product for the textile industry made by the makers of* LYKOPON.

RHOPLEX *and* LYKOPON *are trade-marks, Reg. U.S. Pat. Off. and in principal foreign countries.*

CHEMICALS FOR INDUSTRY

ROHM & HAAS COMPANY

WASHINGTON SQUARE, PHILADELPHIA 5, PA.

Representatives in principal foreign countries

TEXTILE RESEARCH JOURNAL

VOL. XXV, NO. 8 AUGUST 1955

IN THIS ISSUE

RESILIENCE OF SCOURED WOOL. Adnan Demiruren and R. H. Burns . 665

DIGESTIBILITY OF CHEMICALLY-MODIFIED WOOLS IN PAPAIN-BISULFITE UREA. F. G. Lenox 676

VISUAL OBSERVATIONS OF THE BEHAVIOR OF SOIL PARTICLES IN DILUTE AQUEOUS SOAP SYSTEMS. Charles W. Hock . . 682

AN EVALUATION AND COMPARISON OF EVENNESS TESTERS. William T. Waters 686

STRESS-STRAIN RELATIONSHIPS IN YARNS SUBJECTED TO RAPID IMPACT LOADING. *PART III:* EFFECT OF WAVE PROPAGATION. Jack C. Smith, Frank L. McCrackin, and Herbert F. Schiefer 701

APPLICATIONS OF THERMODYNAMICS TO THE STRETCHING OF CELLULOSE FIBERS. W. E. Roseveare and Louise Poore 709

THE MECHANISM OF SUPERCONTRACTION IN KERATIN. G. M. Jeffrey, J. Sikorski, and H. J. Woods 714

EXPERIMENTAL STUDY OF THE VISCOELASTIC PROPERTIES OF TEXTILE FIBERS: DYNAMIC MEASUREMENTS FROM SUBSONIC TO SUPERSONIC FREQUENCIES. K. Fujino, H. Kawai, and T. Horino 722

Correction, Volume XXV, No. 3 737

Letters to the Editor

STUDIES ON WOOL GELATIN: ISOLATION OF ACID PEPTIDES FROM ROOM-TEMPERATURE EXTRACTS. Helmut Zahn and Johannes Meienhofer 738

THE RELATIONSHIP OF AQUEOUS-EXTRACT *p*H TO GRADE IN RAW COTTON OF THE U. S. CROP OF 1954. Paul B. Marsh 739

Editor: Julian S. Jacobs *Production Editor:* Elizabeth Jane Cassatt

Associate Editors

H. J. Ball — W. J. Hamburger — Harold P. Lundgren
Earl E. Berkley — Milton Harris — H. Mark
Henry Eyring — K. L. Hertel — E. R. Schwarz

TEXTILE RESEARCH JOURNAL, published monthly at Prince and Lemon Streets, Lancaster, Pa., is devoted to the interest of research in textile and allied industries. It is published by Textile Research Institute.

Entered as second-class matter, April 27, 1945, at the post office at Lancaster, Pa., under the Act of August 24, 1912. Accepted for mailing at special rate of postage provided for in paragraph (d-2), Section 34.40, P. L. & R. of 1948, authorized May 9, 1950.

Manuscripts and communications should be sent to the editorial office, 10 East 40th Street, New York 16, N. Y.

Subscription rates: $15.00 per year; additional for postage, 50 cents to Canada, $1.00 to all other countries. Single copies, $1.50 each.

Contents copyrighted 1955 by Textile Research Institute. Advertising rates supplied on request.

CHEMISTS

1. PhD in organic chemistry or MS with 1 to 2 years research experience, preferably in polymers. For research related to the synthesis and application of chemical compounds connected with durable finishes for synthetic fabrics.

2. PhD or equivalent in physical chemistry, 5 to 8 years experience, some of which should have been in fiber research. To assist in planning and coordinating problems in basic fiber research covering relationship of molecular and micro structure to mechanical, thermal and other physical properties.

3. MS or PhD in physical, or in organic chemistry with strong physical background, 0 to 5 years experience. For fundamental studies on cellulose and its derivatives and in development of manufacturing processes for cellulose derivatives.

The diversity of the Celanese Corporation activities in chemicals, textiles and plastics . . . the continuing growth and expansion of the organization . . . provide opportunities for qualified men in the Research Laboratories in Summit, New Jersey, a pleasant residential community within 30 miles of metropolitan New York City.

Please submit resumes, including salary desired, to J. A. Berg.

Celanese

CORP. OF AMERICA

Morris Court Summit, N. J.

THE CSI SURFACE ABRADER

The evaluation of surface abrasion is essential to determine serviceability of most materials. The CSI Surface Abrader is a redesign of the Universal Wear Tester for surface abrasion only. The aims were to furnish a unit at a reduced cost which will utilize the laboratory air source. The method consists of inflating the test specimen by controlled air pressure and accurately controlling the pressure of the abradant on the specimen by means of dead weights. The specimen may be rotated during abrasion or abraded unidirectionally. This surface abrasion procedure makes it possible to control the tension of the specimen, the area of contact, and the pressure between the specimen and the abradant and minimizes disturbance arising from unevenness of specimen interference of fabric debris.

The test for Pilling tendencies of fabrics is an additional feature with the accessories now available upon request.

CUSTOM SCIENTIFIC INSTRUMENTS, INC.

541 Devon Street Kearny, N. J.

T.R.I.'s Annual Review of Research and Development

Review of Textile Research and Development During 1954. Prepared by the staff of Textile Research Institute, Princeton, New Jersey. Price $5.00.

Published previously in the May issue of TEXTILE RESEARCH JOURNAL, the "Review" for 1954 with classified bibliography of 2000 literature references is now ready for distribution as a bound report. It will not appear in the JOURNAL.

Orders for copies should be sent to:

Textile Research Institute

Princeton, New Jersey

TEXTILE RESEARCH JOURNAL

VOL. XXV, NO. 8 AUGUST 1955

Resilience of Scoured Wool

Adnan Demiruren[1] and R. H. Burns

Wool Department, University of Wyoming

Abstract

The 6 inherent fiber properties, tensile strength, fiber length, fiber thickness, contour (major-minor axis), crimp length to depth ratio, and crimp depth were responsible for 31% of the variations in the compressional-bulk resilience of wool. In the case of maximum load or stiffness, these same 6 inherent fiber properties were responsible for 85% of the variations. In both cases, the most important inherent property was tensile strength. It accounted for 17% of the variations in the compressional-bulk resilience of wool and for 66% of the variations for maximum load or stiffness. Fiber thickness was the least important while the other inherent factors were intermediate, with contour and crimp affecting resilience and fiber length and crimp affecting maximum load or stiffness. Compressional-bulk resilience has a very narrow range of figures in the three wool types studied, while maximum load has over 4 times the range obtained for resilience. Resilience varies within wool types and is lowest in the fine wools and highest in the medium wools, with long wools intermediate. Stiffness or maximum load is highest in fine wools, lowest in long wools, and intermediate in the medium wools. Only 31% of the variation in compressional bulk resilience of wool can be accounted for by the variation in the 6 fiber characteristics measured.

Introduction

Wool has furnished protection to both sheep and humans for centuries against the ever-changing meteorological and climatic conditions. Man has used wool as a textile fiber ever since he was able to spin and weave it into a rough fabric. Since that time, man has changed the physical dimensions of the wool fiber and produced excellent types of apparel wools through systematic breeding and improvement of his sheep flocks and intensification of the undercoat portion of the primitive sheep breeds. The results are the various types and breeds of domestic or improved sheep. As wool is a biological product, man has very little control over the chemical or physical structure of the wool fiber. Both were taken for granted and studied only for a better insight into the wisdom of Nature.

We now know much about the chemical structure of wool, and the electron microscope has revealed to us some features of the physical structure of the wool fiber. One property of wool, namely its resilience in relation to inherent fiber properties, is rarely mentioned, and we shall now explore this quality of wool.

Review of Literature

The property of resilience has been given different definitions, the most important of which are the following: Hoffman [24] proposed that resiliency and (modulus) be used in referring to a substance, such as glass, nylon, rubber, wool, etc., and that resilience (and stiffness) be used in referring to an entity,

[1] Prepared from Ph.D. thesis of A. Demiruren, July, 1954.

such as woolen fabric, a nylon yarn, or a steel spring, in each case one of specified dimensions and construction.

Smith [36] defined resilience as the ability to absorb work without suffering permanent deformation.

Fox and Schwarz [18] state that the resilience is the potential energy due to strain.

Rees [31] defined resilience in bulk as the amount of energy returned by the material between the same limits of pressure. For a perfectly elastic material, the resilience would be 100%, while for a perfectly plastic material it would be zero.

Hamburger [21, 22] defined resilience as the amount of strain energy present in a stressed system.

Beckwith and Barach [6] state that resilience is the ratio of work returned upon release of a compressional load to the total work done in compressing.

Mark [26] states that if a given fiber such as wool, cotton, rayon, nylon, etc., is to be classified as resilient, such a bunch of irregular fibers should perform as follows: (a) it must offer a moderate resistance to compression; and (b) it must spring back vigorously upon relaxation, even after being in compression for a considerable time. Mark further states that the extent to which the suit keeps its shape and drape, the absence of bulges at the knees and elbows, and the disappearance of wrinkles which are formed during daily use after hanging overnight will characterize the fabric as to the extent of its resilience. He also points out that the character of the fibers from which the fabric is built is of great influence on the resilience of the latter.

Gruntfest and Gagliardi [20] state that the wrinkle resistance of a fabric is determined by its multifilament character and by the ability of its separate fibers to recover from tensile deformation.

Cassie [11] states that heat insulation in fabrics is normally supposed to be due to "entrapped" air. An investigation of the problem of "entrapped" air shows that it really implies the drag on the air movement given by the large total surface of all the fibers in a fabric. The accessibility of the fiber surfaces to air is probably the most important factor in determining the "warmth" of different fibers. It is shown that this is related to the elastic properties of the fibers and wool is an ideal fiber for this purpose. He also states that the general properties required of underwear fabrics are that they must provide heat insulation with light weight and that they must not obstruct the passage of water vapor. Wool, he states, has a unique resistance to close packing, and 92% of the fiber surface in the finished fabric is available for air drag.

Buck and McCord [7] state that the wool fiber has properties almost ideally suited for providing fabrics with resistance to creasing and wrinkles and at the same time for making it possible for the fabric to hold a crease when desired.

Beckwith and Barach [6] state that some wools when walked on in carpet form flatten down readily and the portions of the pile lay in different directions, causing unattractive light-reflection patterns. This spoils the appearance of the fabric surface by giving it a "mangy" or "scraggly" appearance. Other wools do not crush as much; their surface is uniform and pleasing in appearance, with a pile laying in one direction. They suggest that the ability of the carpet pile fibers to resist the distorting effects of traffic could be evaluated by measuring their resilience.

Rees [31] points out the importance of fibrous materials in the bedding and upholstery industries, where they are used in bulk. He lists three important physical properties that determine their use as a bulk material as: (1) Filling capacity of the fibers, that volume occupied by a specified weight of the fibers; (2) compressibility of the fiber mass; and (3) the ability of the mass to recover from compression.

Hopkins [25] points out the importance of air drag in the insulation value of the fabrics, which in turn depends on their thickness. He states that only resilient fibers will maintain their thickness with light weight, and wool is one of the most resilient of all fibers under service conditions.

Finch [17] states that so far few attempts have been made to study the textile-material behavior from an overall point of view. Ordinarily, each worker investigated a particular method for a specific end purpose. This empirical approach, he points out, made no significant contribution to the general fund of knowledge.

Morey [28] states that the number of different instruments constructed and used in obtaining stress-strain curves on yarns are as numerous as the number of investigators.

Hamburger [21, 22] states that the elasticity and resilience are not properties but complex interactions of many factors, both inherent in the fiber and resulting from the geometry of the yarn and fabric structure.

Schofield [34] conducted a number of compressibility tests on wool and concluded that bulk fiber does not wholly elastically reverse the deformation. There is a decrease in volume after the wool is subjected to pressure.

Busse [10] states that the recoveries of fibers from bulk-compression tests appear to depend, in part, on the bulk properties of the fibers, like elasticity, plastic flow, strength, tensile compression, and other shear stresses.

Mutschler [29] measured the "compressed volume" and "relaxed volume" and calculated the bulk elasticity from a formula. He made measurements at 20 points from the bale all the way to ring spinning. He compared wool, cotton, and staple rayon, and found that wool has the highest elastic volume. Maximum volume is reached at the carding process.

Winson [38] attempted to measure the resilience of a volume of wool by enclosing it in a thin spherical rubber membrane whose pressure he made to vary in cycles. He states that the area of the loop (shape of the compression and decompression graph) relating the pressure and volume of the mass of wool seems to serve as a measure of the resilience of the wool.

Fox and Schwarz [19] state that when testing bulk fibers, the condition of the stock as to cleanliness should be considered. Wool in grease is quite different from scoured wool, wool from the dryer, or wool after further processing. He states that the quality of wool and the staple length effect the compressional properties.

Burns and Johnston [9] observed differences in fiber springiness within and between grades, which they stated was a factor tending to interfere with the compressional method of yield estimation. They also found that packing of the compression cylinder was a variable factor. They observed that variations in the physical characters had some influence on the density of the raw wool.

Van Wyk [37] states that crimping may have a direct effect on the relationship of resistance to compression. He found indirect evidence to suggest that the number of crimps per unit stretched length is a more relevant quantity than the normal staple length.

Cliff [12] recommends that the time factor be controlled, so that the axis of either load or extension may also serve as the axis of time. This means that either the rate of loading or the rate of extension must be kept constant.

Skinkle [35] describes the cylinder and plunger method of measuring the resilience of wool as follows: A 500-g sample of fiber is placed in a brass cylinder 7½ in. in diameter. A plunger is used to compress the sample, and the compressed depth is measured by a vernier. The pressure is applied by an inverted jack, and the apparatus is connected to a platform scale to read the load. The resilience may be measured by the area of the hysteresis loop (shape of the graph).

Edelman [15], in his investigation of methods for determining the filling power of feathers, found that the most reliable evaluation is obtained at the lowest test pressures of 0.0006 lb/sq in. and that little is gained by higher compressional values.

Buck and McCord [7] point out the ability of fabrics made from wool and silk to resist the formation of wrinkles, while fabrics made from linen, cotton, and certain rayons do not have this property. They state that the chemical and physical structure and physical dimensions of the fiber are responsible for different degrees of wrinkle resistance.

Schiefer [33] suggests that in the evaluation of compressibility and the compressional resilience of textiles a pressure range of 0.1 to 2.0 lb/sq in. be used.

Rees [30] developed a sensitive thickness gauge for textile materials. This instrument is also used to measure the volume of a mass of fibers under a desired pressure.

Dillon [14] defined resilience as the ratio of the energy of retraction to the energy of deformation. He also states that this ratio refers only to a given set of conditions for a fiber, bulk fiber sample, or fiber assembly. The value of the ratio will be changed if any of the following factors is varied:

1. Temperature.
2. Moisture content.
3. Rate of strain.
4. Rate of retraction.
5. Number of cycles considered (strain history).
6. Rest period between cycles.

7. Nature of cycles.
   a. Constant rate of strain.
   b. Constant rate of loading.
   c. Constant maximum strain.
   d. Constant maximum stress.
   e. Periodic.
   f. Impact.

Saxl [32] used a gelometer to measure the load compression characteristics of wool. He used a three-arm scale, a cylinder, and a plunger to measure the compressibility of wool and synthetic fibers.

Finch [17] points out that the most important consideration in a test of this kind is the preparation of the test specimen. If the fiber mass consists of partially matted and partially loose fibers, the relaxation rate will be a reflection of both of these conditions. It is necessary to have the fibrous mass as homogenous as possible. This, he states, may be accomplished either by opening the material on a power-driven laboratory-type card or by opening it with hand cards. Either method is satisfactory.

Van Wyk [37] states that wool should be teased out as thoroughly as possible to insure the random orientation of the individual fibers. He found that the presence of lumps raised the coefficient by as much as 32%.

Rees [31] states that well-opened fibers are very sensitive to changes of pressure, so that precautions must be taken in determining the initial volume of the fiber mass under the initial pressure. He prepared his test specimen inside a perspex glass cylinder; he then withdrew the cylinder and placed his prepared sample under the foot of the instrument. By this method, he improved the accuracy of his tests by doing away with the friction between the fibers and the wall of the cylinder.

Dillon [14], in his review of the literature, found a pronounced tendency to employ the ratio of energy of retraction to energy of deformation as a definition of resilience.

$$R' = \frac{\text{Energy of Retraction}}{\text{Energy of Deformation}}$$

Fox and Schwarz [18] also used a method of calculating resilience by utilizing the concept of energy. They state that the resilience is potential energy due to strain. This value is the same in the case of perfectly elastic material where there is no "hysteresis."

Van Wyk [37] found a significant correlation coefficient of 0.55 between the resistance of compression and number of crimps per unit length and a partial correlation coefficient of 0.43 between the resistance to compression and fiber diameter.

Winson [38] found that resilience of a mass of fibers increases as the staple length decreases.

Meredith [27] found that wool was much more elastic than cotton for any given strain.

Rees [31] gives the following values of resilience for various fibers:

Fiber		Mean Value of n Tests	
Name	Source	Resilience (%)	n
Cotton, Bengals	After passing through Shirley analyser	39.1	6
Wool, 70's	Sliver	55.8	3
Kapok, Prime Cava	Bale	44.0	3
Silk, degummed China	1st draft	52.2	4
Nylon waste	Sliver	53.0	3
Cellulose acetate staple	Bale	44.4	3
Hollow viscose staple	Bale	30.7	3

Statement of Problem

This article reports the experiment to determine the relationship between the measurable properties of wool and the bulk compressional resilience of scoured wools from the fine, medium, and long wool types. In the determination of the bulk compressional resilience criterion of these samples, the maximum load values were available and consequently a parallel study was made using this factor as a second criterion.

Plan of Experiment

In the experiment the following quantities were measured: (1) Residual matter tests; (2) mean fiber thickness; (3) mean fiber length; (4) breaking weight; (5) tensile strength; (6) number of crimps per unit stretched staple length; (7) mean crimp depth; (8) mean crimp length; (9) crimp depth to length ratio; (10) contour ratio; (11) major axis minus minor axis of fiber cross section; and (12) medullation tests.

The measurements of these twelve factors or independent variables were considered in relation to resilience. The compressional bulk resilience and maximum load were determined for each sample. It is understood that the maximum load or stiffness

is not simply related to resilience, but the information was readily available and was treated separately as an interesting sidelight on the main problem.

Before starting the analysis between the independent and dependent variables, a preliminary review was made to eliminate some of the independent variables which were closely related and, in some cases, different measures of the same character. Correlations were worked out and those with a correlation coefficient of 0.90 or higher were noted; only one of these closely related measures was used in the final analysis. Those with very low correlations were eliminated. When these preliminary tests were finished and the eliminations made, the solution of the basic problem of resilience was undertaken with the help of the following information: (a) Simple correlations were calculated between the independent variables and the criterion; (b) multiple correlations were calculated between the independent variables and the criterion; and (c) simple and multiple regression equations were computed.

The following 29 wool samples, weighing a pound each, were used in the experiment.

Sample Code Number	Wool Grade	Description
FCF1	Fine	Commercial fleece sample
FBR1	Fine	Rambouillet fleece, Univ. of Wyo. flock
FBR2	Fine	Rambouillet fleece, Univ. of Wyo. flock
FCF2	Fine	Commercial fleece sample
FCA1	Fine	Commercial wool sample, Australian origin
FBR3	Fine	Rambouillet fleece, Univ. of Wyo. flock
FCT1	Fine	Commercial sample, origin Texas
FBM1	Fine	Merino ram fleece, Univ. of Wyo. flock
FBR4	Fine	Rambouillet fleece, Univ. of Wyo. flock
FCF3	Fine	Commercial fleece sample
FCFD	Fine	Commercial fleece sample, origin Delaine flock
FCA2	Fine	Commercial wool sample, Australian origin
FCF4	Fine	Commercial fleece sample
MBE1	Medium	Corriedale fleece, Univ. of Wyo. flock
MDE2	Medium	Corriedale fleece, Univ. of Wyo. flock
MBA1	Medium	Columbia fleece, Univ. of Wyo. flock
MCDT	Medium	Commercial sample, Territory Domestic
MBE3	Medium	Corriedale fleece, Univ. of Wyo. flock
MBA2	Medium	Columbia fleece, Univ. of Wyo. flock
MBE4	Medium	Corriedale fleece, Univ. of Wyo. flock
MBE5	Medium	Corriedale fleece sample, Univ. of Wyo. flock
MBH1	Medium	Hampshire fleece, Univ. of Wyo. flock
MBH2	Medium	Hampshire fleece, Univ. of Wyo. flock
MCF1	Medium	Commercial fleece sample
MCF2	Medium	Commercial fleece sample
MBA3	Medium	Columbia fleece, Univ. of Wyo. flock
LCF1	Long	Commercial fleece sample
LBA2	Long	Columbia fleece sample
LCF2	Long	Commercial fleece sample

Methods and Procedures

Samples were scoured and their residual matter determined according to A.S.T.M. Standards D 584-53T [1]. The standard conditions for residual materials in scoured or clean wool as stated in the standard is 12% moisture, alcohol extractable material 1.5%, and ash content 0.5%. All samples were run through the duster 3 times to ensure thorough opening and mixing. The scouring solution contained 0.3% sodium carbonate and 0.1% textile scouring soap. The samples were scoured in a four-tub train, the first three containing the scouring solution named above and the last one the rinse solution made up with no soap and 0.3% sodium carbonate. The solutions were maintained at $52 \pm 3°C$, and samples were kept in each tub for 3 min. The scoured samples were dried to a constant weight at 105 to 110°C.

The mean *fiber-thickness* measurements were made according to ASTM designation D 419-50T [1]. The number of test specimens and the measurements for each sample are given below:

Fineness Range (μ)	Number of Test Specimens	Total Number of Fibers Measured
18 and under	2	200
18.1 to 21 incl.	2	400
21.1 to 24 incl.	2	600
24.1 to 27 incl.	2	800
27.1 to 30 incl.	2	1200
30.1 and over	2	1600

The mean *fiber-length* measurements were determined by the method outlined in ASTM Designation D 519-49 [1]. The standard condition of the fibers was reached when they were in moisture equilibrium with a standard atmosphere having a relative humidity of 65% at 70°F. A 2% tolerance is allowed for relative humidity and 2 degrees for temperature. All of the length measurements were made on a Suter stapler.

The *number of crimps* per unit length was determined by the method outlined by Burns [8].

The cross-sectional characteristics of the wool samples were determined from cross sections prepared by Hardy's cross-sectioning device by the method described in ASTM Designation D 1444-53T [1]. The contour ratio was obtained by measuring the projected images of the major and minor axis of 100 fibers and calculating the contour ratio and the difference between major and minor axis.

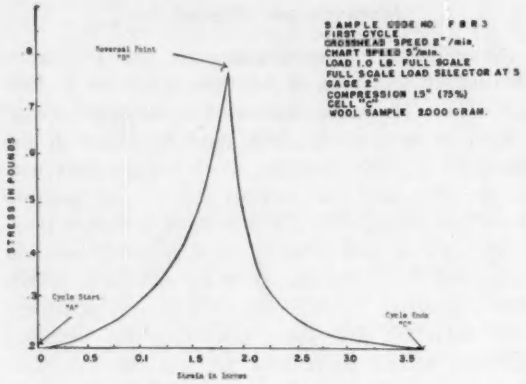

Fig. 1. Load-extension loop of sample FBR3, first cycle.

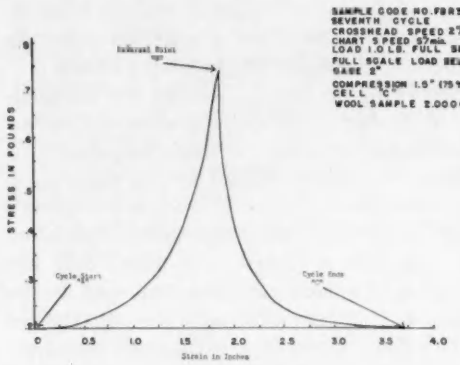

Fig. 2. Load-extension loop of sample FBR3, seventh cycle.

The breaking weight and tensile strength of the samples were tested by the procedure outlined in the ASTM Standards [2], and described as *A Tentative Method for Testing Tensile Strength.*

For each sample, 10 subsamples were analyzed for *crimp length and depth* measurements. The crimp depth and length were measured by taking a strand of about 2–3 mm in thickness from each subsample and projecting its image onto a screen at a magnification of × 10. For this study, a regular 35-mm still-film projector was used which had been modified to adapt it to this study. The lens piece of the projector was removed and between the lens and the light source a staple holder was installed. This staple holder was constructed to hold the sample from the tip and base of the staple and at a fixed distance and perpendicular to the light source. The arms of the staple holder were imbedded in a frame and could be rotated clockwise and counterclockwise, which in turn rotated the sample around its longitudinal axis for 360°. In order to adjust for a × 10 magnification, two parallel lines 10 mm apart were drawn on a semitransparent paper, and this paper was fixed between the arms of the sample holder in the same manner as a wool sample would be fixed, namely, perpendicular to the light source. Two parallel lines 100 mm apart were then drawn and placed on the screen. The parallel lines at the sample holder were then projected onto the screen and the lens piece was moved away from the sample holder until a sharp image of the parallel lines 10 mm apart coincided with those of the parallel lines on the screen which were 100 mm apart. The lens was fixed at this distance from the light source and staple. The subsamples were measured by fixing them onto the clamps on the staple holder and rotating until the crimps were at right angles to the beam of light of the projector or until the largest clear image was obtained. Starting from the base and going over to the tip, 10 crimp length and depth measurements were taken on each subsample and recorded on white paper onto which the images were projected. The apexes of two adjacent crimps were marked on the paper with crosses; the apex of the opposite crest was likewise marked. The three points were joined, forming a triangle, and the shape of the triangle depends on the shape of the crimp. The base of the triangle represents the crimp length while the height shows the crimp depth. Using this method, it was possible to measure the length and depth of crimp with a bidiameter scale very quickly and accurately to the nearest 0.1 mm.

In the short-fiber method of determining the fineness or thickness of the wool samples, it was noted that any amount of *medullation* present in the fiber showed on the screen when projected at 500 magnification as a clear brown spot. This phenomenon was used to determine the amount of medullated fibers present. Using the large cross-sectioning device, fibers of about 400 μ in length were cut off from a representative sample. These fibers were mounted in mineral oil on a glass slide and a cover glass was placed on the sample. These groups of fibers were projected at a 500 magnification on a screen and 1200 fibers were examined at random to determine the medullation present.

Measurements of the compressional bulk resilience and maximum load were made at the Textile Re-

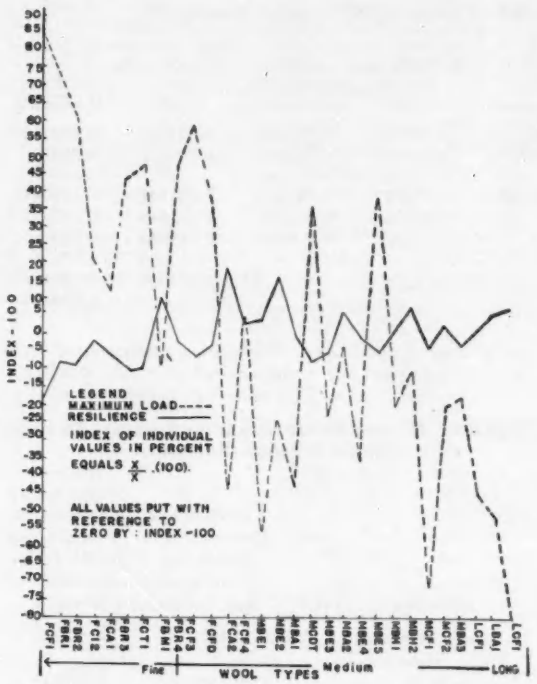

Fig. 3. Results of resilience and maximum-load measurements of the wool samples.

search Institute on the Instron Tensile Tester using the method developed by Dusenbury and deMaCarty [13].

Results in this experiment were concerned with the relationship of the compressional-bulk resilience to the inherent fiber properties. In addition to this main problem, maximum load and its relation to the inherent fiber properties was also studied.

In the preliminary analysis, 12 different inherent fiber properties were used, some of which were very closely related to each other. It was decided to eliminate those factors which described the same fiber property. For example, the crimp factor or property was described by its depth, length, number per unit of stretched staple length, and ratio of length to depth. A simple correlation test was calculated between crimp depth and length which showed a positive correlation of 0.977. Another correlation of 0.958 was found between crimp depth and number of crimps per unit of stretched staple length. These established high correlations made it possible to eliminate two of the four crimp properties, since they will contribute approximately the same degree of effect on the dependent variable, as factors, namely crimps per unit of stretched staple length and crimp length. The same pattern of logic was followed in the elimination of the breaking weight, which had a correlation of 0.999 with the tensile strength. Contour ratio was eliminated because it had a very low correlation, 0.03, with the resilience and a negative correlation of 0.121 with the maximum load. The total per cent of impurities or residuals had low correlations, -0.021 with resilience, and 0.140 with maximum load, and hence was eliminated. Medullation was also eliminated as a factor because only 10 samples had any medullation at all, and of these only 3 had medullation over 1%.

The 6 factors retained out of the original 12 measurable fiber characteristics and used in the study are as follows: (1) Mean fiber thickness; (2) Mean fiber length; (3) Crimp depth; (4) Crimp length to depth ratio; (5) Tensile strength; and (6) Major minus minor axis of fiber cross section.

A negative correlation of -0.667 was found between the resilience and maximum load, and it was significant at the 0.01 level. A graphic presentation of the results, in per cent, of the compressional-bulk resilience and maximum-load measurements of the fine, medium, and long wool types are given in Figure 3.

Simple and multiple correlations between the two criteria, resilience and maximum load, and the six different inherent fiber characters are shown in Tables I–VI.

Simple correlations between resilience and the 6 fiber characteristics ranged from 0.20 to 0.41. Correlations of 0.367 or above were significant at the 0.05 level, and those of 0.470 or above were significant at the 0.01 level.

The tensile strength had the highest correlation ($r = 0.41$) with resilience, followed by fiber length ($r = 0.38$), fiber thickness ($r = 0.32$) and major minus minor axis of fiber cross section ($r = 0.29$), while the two lowest ones were crimp depth to length ratio ($r = 0.27$), and crimp depth ($r = 0.20$).

The multiple relationship of the 6 predictive variables with the compressional-bulk resilience showed a figure of 0.56, which was significant at the 0.01 level. The coefficient of determination, which is the square of the coefficient of correlation, amounted to 0.31. This means that only 31% of the variation in the compressional-bulk resilience could be accounted

TABLE 1. Simple Correlations among the Variables Including the Criterion (Resilience)

		1 Tensile Strength	2 Fiber Length	3 Fiber Thickness	4 Major-Minor Axis of Fiber	5 Crimp Length to Depth Ratio	6 Crimp Depth	7 Resilience
Tensile strength	1.	1.000000	0.721010	0.760138	0.577904	0.119562	0.621152	0.409312
Fiber length	2.		1.000000	0.869611	0.650709	−0.168387	0.760411	0.379726
Fiber thickness	3.			1.000000	0.878191	0.081243	0.754221	0.321605
Major-minor axis of fiber	4.				1.000000	0.215839	0.613543	0.292917
Crimp length to depth	5.					1.000000	−0.349985	0.266055
Crimp depth	6.						1.000000	0.196426
Resilience	7.							1.000000

$N = 29$.

Correlation coefficients of 0.36070 or above are significant at 0.05 level of significance. Correlation coefficients of 0.470 or above are significant at 0.01 level of significance.

TABLE 2. Comparisons of Relative Values of Coefficients of Determination and Corresponding Coefficients of Correlation for Simple Relationships between the Predictive Variables and the Criterion (Resilience)

Variables	Coefficient of Determination	Coefficient of Correlation
1. Tensile strength	0.167536	0.409312
2. Fiber length	0.144191	0.379726
3. Fiber thickness	0.103429	0.321605
4. Major-minor axis of fiber	0.085800	0.292917
5. Crimp length to depth ratio	0.070785	0.266055
6. Crimp depth	0.038583	0.196426

for by the variation in the 6 inherent fiber properties. This would indicate that these 6 measurable fiber properties are only a portion of the cause of variation in compressional-bulk resilience and that other properties are involved. The tensile strength had the highest coefficient of determination, 16%. Major minus minor axis of the fiber cross section added 9% to the coefficient of determination beyond the tensile strength; the crimp length to depth ratio accounted for only 4% beyond the other two; fiber

TABLE 3. Multiple Relationship of Six Predictive Variables with the Criterion (Resilience)

Variables	Coefficient of Determination Measuring Cumulative Relationship	Amount Added to the Coefficient of Determination by the Inclusion of Each Variable
1. Tensile strength (x_1)	0.167536	0.167536
2. Major-minor axis of fiber (x_2)	0.252851	0.085315
3. Crimp length to depth ratio (x_3)	0.291033	0.038182
4. Fiber length (x_4)	0.306382	0.015349
5. Fiber thickness (x_5)	0.310985	0.004603*
6. Crimp depth (x_6)	0.311000	0.000015

* Variables which probably added very little to cumulative relationship.

$r^2 = 0.311000$
$r = 0.557674$
$N = 29$

r is significant at 0.01 level of significance

Regression equation: $Y = 11.1361 - 0.0136\,x_1 + 0.7934\,x_2 - 0.1961\,x_3 + 0.0710\,x_4 - 0.1523\,x_5 + 0.0089\,x_6$

TABLE 4. Simple Correlations among the Variables Including the Criterion (Maximum Load)

		1 Tensile Strength	2 Fiber Length	3 Fiber Thickness	4 Major-Minor Axis of Fiber	5 Crimp Depth	6 Crimp Length to Depth Ratio	7 Maximum Load
Tensile strength	1.	1.000000	0.721010	0.760136	0.577904	0.621152	0.119562	−0.811359
Fiber length	2.		1.000000	0.869611	0.650709	0.760411	−0.168389	−0.755222
Fiber thickness	3.			1.000000	0.878191	0.754221	0.081243	−0.701807
Major-minor axis of fiber	4.				1.000000	0.613543	0.215839	−0.53214
Crimp depth	5.					1.000000	−0.349985	−0.470798
Crimp length to depth	6.						1.000000	−0.179108
Maximum load	7.							1.000000

$N = 29$.

Correlation coefficients of 0.3670 or above are significant at 0.05 level of significance. Correlation coefficients of 0.470 or above are significant at 0.01 level of significance.

TABLE 5. Comparison of Relative Values of Coefficients of Determination and Corresponding Coefficients of Correlation for Simple Relationships between the Predictive Variables and the Criterion (Maximum Load)

Variables	Coefficient of Determination	Coefficient of Correlation*
1. Tensile strength	0.658303	0.811359
2. Fiber length	0.570360	0.755222
3. Fiber thickness	0.492533	0.701807
4. Major-minor axis of fiber	0.283172	0.532140
5. Crimp depth	0.221651	0.470798
6. Crimp length to depth ratio	0.032079	0.179108

* All correlations transferred to positive values.

TABLE 6. Multiple Relationship of Six Predictive Variables with the Criterion (Maximum Load)

Variables	Coefficient of Determination Measuring Cumulative Relationship	Amount Added to the Coefficient of Determination by the Inclusion of Each Variable
1. Tensile strength (x_1)	0.658303	0.658303
2. Fiber length (x_2)	0.718653	0.060350
3. Crimp length to depth ratio (x_3)	0.765486	0.046833
4. Crimp depth (x_4)	0.798639	0.033153
5. Fiber thickness (x_5)	0.822529	0.023890
6. Major-minor axis of fiber (x_6)	0.844854	0.022325

$r^2 = 0.844854$
$r = 0.919159$
$N = 29$

r is significant at 0.01 level of significance

Regression equation: $y = 45.3261 - 0.6739\,x_1 - 0.5600\,x_2 + 0.3380\,x_3 + 0.2842\,x_4 - 0.1265\,x_5 - 0.0809\,x_6$.

length accounted for only 2% of the variation beyond the above 3; and the last 2 variables, fiber thickness and crimp depth, probably added very little to the cumulative relationship.

Simple correlations between the *maximum load* and the variables ranged from − 0.18 to − 0.81 (See Table IV). Correlations of 0.367 or above were significant at the 0.05 level, and those of 0.470 or above were significant at the 0.01 level. The tensile strength had the highest simple correlation (− 0.81) with the maximum load, with the crimp length to depth ratio showing the lowest figure (− 0.47). All of these 6 correlations had negative values showing inverse relationship between the maximum load (stiffness) and the 6 variables. The multiple correlation of the 6 variables with the maximum load showed a figure of 0.92, which was significant at the 0.01 level. The coefficient of determination was 0.85, and consequently 85% of the variation in the maximum load can be accounted for by the variation in 6 fiber properties in the study. The tensile strength was the highest of these and accounted for 66% of the variation in maximum load or stiffness. Fiber length added only 6% to the coefficient of determination beyond that of tensile strength; crimp length to depth ratio added 5% to the total coefficient beyond tensile strength; crimp depth, 3% beyond the above four; and both the fiber thickness and the major minus minor axis of fiber cross section added only 2% each to the total. The relationship of the tensile strength and the compressional-bulk resilience and maximum load (stiffness) are illustrated in Figures 4 and 5.

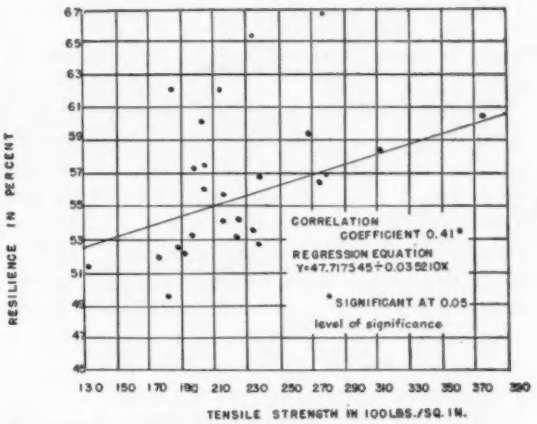

Fig. 4. Compressional bulk resilience vs. tensile strength.

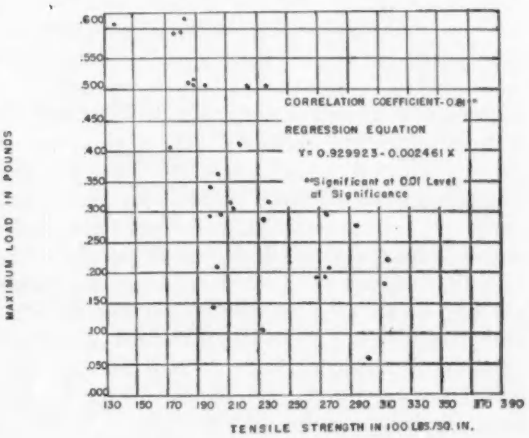
MAXIMUM LOAD IN POUNDS
REGRESSION EQUATION
Y= 0.929923 - 0.002461 X
**Significant at 001 Level of Significance
TENSILE STRENGTH IN 100 LBS./SQ. IN.

Fig. 5. Maximum load vs. tensile strength.

Summary

The relationship of 6 fiber properties to compressional-bulk resilience of wool was determined. As a preliminary study, the relationship of these fiber properties to maximum load or stiffness was also determined. Twelve properties of the wool samples were evaluated, and 6 of these were eliminated by statistics and logical reasoning because they were either measurements of the same character, such as crimp, or were clearly unrelated to the main criterion, as was the case with the residuals. A method of measuring the compressional-bulk resilience and maximum load developed by Dusenbury and deMaCarty [13] at Textile Research Institute was used to obtain the data on these properties used in this paper. The 29 wool samples used in this study represented the fine, medium, and long wool types.

Conclusions

The results of the experiment showed that the 6 measurable fiber properties were responsible for 31% of the variations in the compressional bulk resilience of wool. In the case of maximum load (stiffness), these measurable fiber properties were responsible for 85% of the variations. In both cases, the most important measurable property was tensile strength. It accounted for 18% of the variations in the compressional bulk resilience of wool, and for 66% of the variations in the case of maximum load or stiffness. This study showed that the shape or contour of the fiber and crimp were important measurable qualities affecting the compressional-bulk resilience. In the case of maximum load, the two important factors besides tensile strength were fiber length and crimp. In both resilience and maximum load, fiber thickness or fineness was a less important factor. It is readily seen in Figure 3 that compressional-bulk resilience has a very narrow range within the 3 wool types, and maximum load has over 4 times the range of the compressional bulk resilience. Compressional bulk resilience varies within wool types and is lowest in the fine wool types and highest in the medium wool types, while the long wool type is intermediate between the other two types. Figure 3 also shows that maximum load or stiffness varies within types with the fine wool types showing the highest figures, the long wool types the lowest figures, and the medium wools being in between.

The study indicated clearly that only 31% of the variation in compressional bulk resilience of wool can be accounted for by the variation in the 6 fiber characteristics measured. Therefore, most of the variations in the compressional bulk resilience must be due to physical (molecular) structure and other factors.

Acknowledgment

The writers wish to thank Dr. J. H. Dillon, Director of Textile Research Institute at Princeton, N. J., who made available their laboratory where the resilience measurements were made. Dr. J. H. Dusenbury and Mr. Cormac deMaCarty of that laboratory developed the methods and instruments used. They also thank the Forstmann Woolen Company and the National Wool Marketing Corporation for furnishing some of the wool samples used in the experiment.

Literature Cited

1. Anonymous, "Tentative Methods of Test for Fineness of Wool," *A.S.T.M. Standards on Textile Materials*, A.S.T.M. designation, D 419–50 T, pp. 477–82 (1952).
2. Anonymous, A Tentative Method for Testing Tensile Strength, from a Meeting of Section 1, Subcommittee A-3 on Wool, A.S.T.M. Committee D-13 (Method Adopted from Alexander Smith and Sons Carpet Company, unpublished); later published in *A.S.T.M. Standards of Textile Materials*, "Tentative Method of Test for Tensile Strength of Wool Fiber Bundles," A.S.T.M. Designation: D 1294–53T, pp. 542–544 (October, 1954).
3. Anonymous, *Condensed Operating Data for the Instron Tensile Testing Instrument Model TT-B*, Instron Engineering Corporation, Quincy, Mass., pp. 1–2 (1950).
4. Anonymous, *Operating Instructions for the Instron Tensile Testing Instrument Model TT-B, Model TT-C*, Instron Engineering Corporation, Quincy, Mass., pp. 37–40 (1950).
5. Anonymous, "Crimp Determination," *Text.-Rundschau* **5**, 321–322, SVMT 25, B1018; Abstract, *J. Textile Inst.* **41**: 10, A505 (October, 1950).
6. Beckwith, O. P., and Barach, J. L., "Notes on the Resilience of Pile Floor Coverings," TEXTILE RESEARCH JOURNAL **17**: 6, 305–313 (June, 1947).
7. Buck, George, S., Jr., and McCord, Frank A., "Crease Resistance and Cotton, TEXTILE RESEARCH JOURNAL **19**: 4, 216–247 (April, 1949).
8. Burns, R. H., "Monthly Wool Growth of Rambouillet Ewes," *J. Textile Inst.* **22**: 2, T456–T464 (1931).

9. Burns, R. H., and Johnston, A., "Determination of the Yield of Raw Wool from its Density under Pressure," *J. Textile Inst.* **28**, T13–T20 (1937).
10. Busse, W. F., "Application of High Compression Stresses to Textile Fibres: Cotton," TEXTILE RESEARCH JOURNAL **23**: 2, 77–84 (February, 1953).
11. Cassie, A. B. D., "Characteristics for Warmth in Underwear Fabrics," *J. Textile Inst.* **40**, 444–453 (January, 1949).
12. Cliff, H. S., "A New Autographic Load-Extension Recorder," *J. Textile Inst.* **24**, T351–360 (September, 1933).
13. deMacCarty, P. C., and Dusenbury, J. H., TEXTILE RESEARCH JOURNAL, in press.
14. Dillon, J. H., "Resilience of Fibers and Fabrics," TEXTILE RESEARCH JOURNAL **17**, 207–213 (April, 1947).
15. Edelman, N. B., "Investigation of Methods for Determining the Filling Power of Feathers," TEXTILE RESEARCH JOURNAL **17**: 4, 199–206 (April, 1947).
16. Finch, R. B., "Compressional Behavior of Textile Materials: I. Measurement at a Constant Rate of Deformation, TEXTILE RESEARCH JOURNAL **18**: 3, 165–177 (March, 1948).
17. Finch, R. B., "Compressional Behavior of Textile Materials: II. Measurement of Compressional Stress Relaxation at Constant Deformation, TEXTILE RESEARCH JOURNAL **18**: 4, 237–243 (April, 1948).
18. Fox, K. R., and Schwarz, E. R., "An Instrument for the Study of Compressional and Creep Recovery of Yarns and Fabrics," TEXTILE RESEARCH JOURNAL **11**: 5, 227–237 (March, 1941).
19. Fox, K. R., and Schwarz, E. R., "Determination of Resilience of Textiles by Compression Testing," TEXTILE RESEARCH JOURNAL **12**, 2–7 (August, 1942).
20. Gruntfest, I. J., and Gagliardi, D. D., "Wrinkle Resistance of Fabrics, *Ind. Eng. Chem.* **41**, 760–764 (1949); Abstract, *J. Textile Inst.* **40**, A378 (August, 1949).
21. Hamburger, W. J., "Mechanics of Elastic Performance of Textile Materials," TEXTILE RESEARCH JOURNAL **18**, 102–113 (February, 1948).
22. Hamburger, W. J., "Mechanics of Elastic Performance of Textile Materials," TEXTILE RESEARCH JOURNAL **18**: 12, 705–743 (December, 1948).
23. Hindman, H., and Krook, C. M., "The Electric Strain Gage and its Use in Textile Measurements," TEXTILE RESEARCH JOURNAL **15**: 7, 233–246 (July, 1945).
24. Hoffman, R. M., "A Generalized Concept of Resilience," TEXTILE RESEARCH JOURNAL **18**, 141–148 (1948).
25. Hopkins, G. E., *Wool as an Apparel Fiber.* New York, Rinehart, pp. 31, 35–40, 41 (1953).
26. Mark, H., "Some Remarks about Resilience of Textile Materials," TEXTILE RESEARCH JOURNAL **16**, 361–368 (August, 1946).
27. Meredith, R., "A Comparison of the Tensile Elasticity of Some Textile Fibers," *J. Textile Inst.* **36**, T147 (August, 1945).
28. Morey, D. R., "Design of Devices Used in the Study of Stress-Strain-Time Properties," TEXTILE RESEARCH JOURNAL **15**, 267–273 (August, 1945).
29. Mutschler, H., "Changes in Bulk Elasticity in Processing Fibres," *Textil-Praxis* **4**, 106–108 (1949); Abstract, *J. Textile Inst.* **40**, A376 (September, 1949).
30. Rees, W. H., "Over-All Specific Volume of Kapok," *J. Textile Inst.* **37**, T121–T139 (May, 1946).
31. Rees, W. H., "The Over-All Specific Volume, Compressibility and Resilience of Fibrous Materials," *J. Textile Inst.* **39**, T131 (April, 1948).
32. Saxl, I. J., "Load-Compression-Characteristics in the Textile Industry," ("Last-Kompression-Charakteristiken in der Textil-industrie"), *Melliand Textilber.* **19**, 47 (1938).
33. Schiefer, H. F., "The Compressometer, and Instrument for Evaluating the Thickness, Compressibility and Compressional Resilience of Textiles and Similar Materials," TEXTILE RESEARCH JOURNAL **3**, 505–513 (October, 1933).
34. Schofield, J., "Research on Wool Felting," *J. Textile Inst.* **29**, T239–T252 (September, 1938).
35. Skinkle, J. H., *Textile Testing, Physical, Chemical and Microscopical,* Brooklyn, Chemical Publishing Company, pp. 42–44 (1949).
36. Smith, Harold DeWitt, *Textile Fibers, An Engineering Approach to Their Properties and Utilization,* 19th Edgar Marburg Lecture (1944).
37. van Wyk, C. M., "Notes on the Compressibility of Wool," *J. Textile Inst.* **37**, T285–T292 (November, 1946).
38. Winson, C. G., "Report on a Method, for Measuring the Resilience of Wool," *J. Textile Inst.* **23**, T386–T393 (December, 1932).

Manuscript received April 21, 1955.

Digestibility of Chemically-Modified Wools in Papain-Bisulfite Urea

F. G. Lennox

Biochemistry Unit, Wool Textile Research Laboratory, C.S.I.R.O., Melbourne, Australia

Abstract

The digestibility of wool in papain-bisulfite urea is increased by prior treatment with cold concentrated sulfuric acid, nitrous acid, or iodine but is diminished by 1-fluoro-2,4-dinitrobenzene, formaldehyde, chromium compounds, epichlorhydrin, propylene oxide, methyl iodide at *p*H's above 6, thiocyanate with acetic anhydride at *p*H's below 6, and, if applied to the reduced fiber, by 1,3-dibromopropane, acrolein, and methyl iodide at *p*H's above 7. Treatment with acid solutions of various aliphatic alcohols to esterify the carboxyl groups in wool likewise reduces the digestibility, maximum protection being obtained with methanol.

The rapid method of measuring enzyme resistance used in these studies may be generally suitable for detecting wool damage and for selecting chemical methods of modifying wool for assessment by moth-resistance and soil-burial methods.

Introduction

Enzyme digestion is an essential step in all forms of biological attack on wool, and measurement of the effect of enzymes on processed wool has been recommended to determine its biological resistance. Burgess [6] showed that, whereas chlorination increased the trypsin digestibility, treatment with potassium chromate in sulfuric acid conferred protection. Similarly Geiger et al. [11] increased the resistance of reduced wool to several proteolytic enzymes by inserting hydrocarbon cross-linkages between the peptide chains. Goldschmidt [13] used a proteolytic culture filtrate from a species of *Actinomycete* to demonstrate the superior enzyme resistance of wool in comparison with that of some artificial protein fibers. However, while the digestion of intact wool by unaided proteases is slow and incomplete and does not readily distinguish between chemical treatments which markedly increase the biological resistance, digestion in papain-bisulfite-urea solution is rapid and complete [20]. The present paper describes a method of evaluating the effect of various chemical treatments on wool by the application of this solution, the three components of which are considered to split peptide bonds, disulfide bonds, and hydrogen bonds, respectively. The method probably bears a closer resemblance than does trypsin digestion to wool degradation under the reducing conditions found in the moth larval gut [22].

Materials and Methods

Merino wool of 64's quality was used, from which the weathered tip had been removed prior to Soxhlet extraction with ethanol, repeated washing with distilled water, and drying in a current of warm air.

Table I summarizes the chemical treatments used to modify the wool. The dichromate treatment was typical of that employed in chrome mordanting of wool and the formaldehyde treatment was essentially that used in tanning. Treatments causing discoloration of the wool were picric acid (yellow), 1-fluoro-2,4-dinitrobenzene (orange), nitrous acid (orange-brown), iodine (brown), potassium dichromate (dull green), and epichlorhydrin (pale yellow). The progress of esterification of wool in acid-alcohol solutions was followed by estimation of the free carboxyl groups [1].

Papain digestibility was measured by incubating, for 18 hr at 50° C, 1 g air-dry wool per 30 ml of a solution containing 1% papain, 0.1 *M* sodium bisulphite (fresh analytical reagent), and 3 *M* urea adjusted to *p*H values between 4 and 10 with NaOH or HCl, using a glass-electrode *p*H assembly. The changes in *p*H value during the digestion of untreated wool have already been reported [20]. The changes occurring during digestion of the chemically modified wools differed from these and from one another, and the final *p*H values are therefore given where a variety of chemical treatments are compared, as in Figure 1. The undigested wool was recovered by

TABLE I. Chemical Treatments Used to Modify Wool for Experiments Reported in Figure 1 *

Reagent	Reaction Conditions	Probable Main Effect
Picric acid	1% solution in ethanol acting for 72 hr at 22°C	Forms salts with basic groups, mainly arginine and $-NH_2$
S-Benzyl thiouronium hydrochloride	1% aqueous solution acting for 10 min at 25°C on wool previously treated with excess $NaHCO_3$ solution	Forms salts with COOH groups
Acetic anhydride	0.5 hr at 100°C, excess removed by immersion for 10 min in 2% aniline in dry benzene	$-NH_2 \longrightarrow -NHCOCH_3$ $-OH \longrightarrow -OCOCH_3$
1-fluoro-2,4-dinitrobenzene	2% ethanol solution acting for 48 hr at 21°C	$-NH_2 \longrightarrow -NHC_6H_3(NO_2)_2$ $-OH \longrightarrow -OC_6H_3(NO_2)_2$
Nitrous acid	1.0 *M* $NaNO_2$ adjusted to *p*H 4 for 3 days at 22°C	$-NH_2 \longrightarrow -OH$ and introduces nitroso groups into ring of phenol groups
Methanol in acid solution	95% methanol with 5% 10 *N* HCl acting for 3 days at 22°C	$-COOH \longrightarrow -COOMe$ in terminal and side-chain positions
Thiocyanate with acetic anhydride	2.5 *M* NH_4CNS acting for 4 days; then acetic anhydride for 7 days at 22°C	C terminal amino acids ⟶ thiohydantoins and the reactions listed above for acetic anhydride
Methyl iodide	3% in 0.1 *M* phosphate buffer, *p*H 7.4, acting for 18 hr at 50°C	$-NH_2 \longrightarrow -NHMe$ $-C_6H_4OH \longrightarrow -C_6H_4OMe$
Methyl iodide following thioglycollate reduction	0.2 *M* thioglycollate, *p*H 5.4, acting for 24 hr at 22°C; then methylated as above	$-S-S- \longrightarrow 2-SMe$, in addition to reactions before reduction
Iodoacetate	1.3% Na iodoacetate in 0.1 *M* phosphate buffer, *p*H 7.4, acting for 18 hr at 50°C	$-NH_2 \longrightarrow -NHCH_2COONa$ $-C_6H_4OH \longrightarrow -C_6H_4OCH_2COONa$
Iodoacetate following thioglycollate reduction	0.2 *M* thioglycollate, *p*H 5.4, for 24 hr at 22°C; then treated with iodoacetate as above	$-S-S \longrightarrow 2\ -SCH_2COONa$ in addition to the reactions before reduction
Sulfuric acid	Conc. H_2SO_4 acting for 24 hr at 0°C	$-C_6H_4OH \longrightarrow -C_6H_4OSO_3H$ $-NH_2 \longrightarrow -NHSO_3H$ and loss of some arginine, tyrosine, and tryptophane
Iodine	0.1 *M* I_2 acting for 72 hr at 23°C	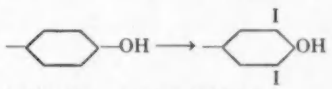 imidazole ⟶ 2-iodoimidazole
Formaldehyde	0.1 *M* HCHO acting for 30 min at 60°C	Cross links between amide, amino, and tyrosine groups
Potassium dichromate	3% $K_2Cr_2O_7$ + 2.5% KH tartrate acting for 1 hr at 100°C	Cross-linking through Cr coordinating =NH and =CO groups of adjacent peptide chains and possibly some destruction through oxidation
Epichlorhydrin	Gas acting for 2 hr at 22°C	Cross-linking reactions between $-NH_2$ and —NH groups
Propylene oxide	2% acting at 100°C for 2 hr	Reacts with $-NH_2$ groups
Dibromopropane	Water for 18 hr at 35°C; then 0.002 *M* 1,3-dibromopropane in 1.0 *M* phosphate buffer, *p*H 8.0, for 20 hr at 35°C	—
Dibromopropane following thioglycollate reduction	0.2 *M* thioglycollate, *p*H 4.5, for 18 hr at 35°C; then dibromopropane treatment as above	$2-SH \longrightarrow -S-CH_2CH_2CH_2-S-$
Acrolein following thioglycollate reduction	0.2 *M* thioglycollate, *p*H 7, for 24 hr at 22°C; then in 3% aqueous acrolein, *p*H 10, for 18 hr at 50°C	Cross-linking between 2SH or between SH and NH_2

* A ratio of 30 ml solution per 1 g wool was used throughout and the samples were washed thoroughly after treatment and dried.

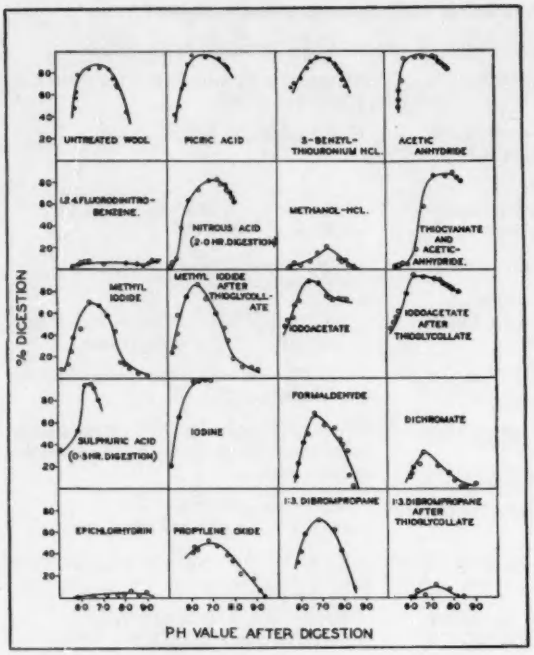

Fig. 1. Digestion of chemically modified wools in 1% papain, 0.1 *M* $NaHSO_3$, and 3 *M* urea at various *p*H values. Digestion period 18 hr at 50° C except for sulfuric acid and nitrous acid treated wools, where the greatly increased susceptibility necessitated short incubation.

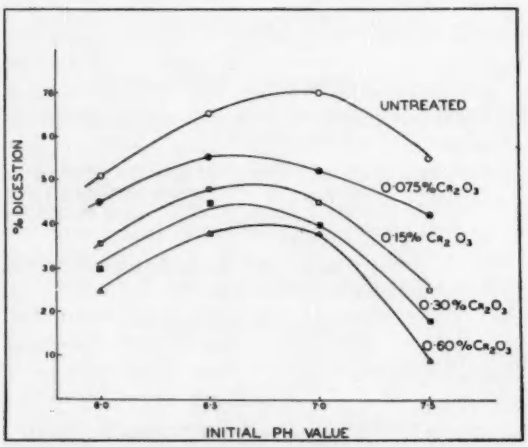

Fig. 3. Digestion of wool in papain-bisulfite urea at different *p*H values following treatment with various concentrations of chromium sulfate. Incubated for 4 hr at 50° C. The 2.8% $Cr_2(SO_4)_3$ solution (equiv. to 0.60% Cr_2O_3) contained also 5% Na_2SO_4, and this was diluted to provide the other chromium solutions tested.

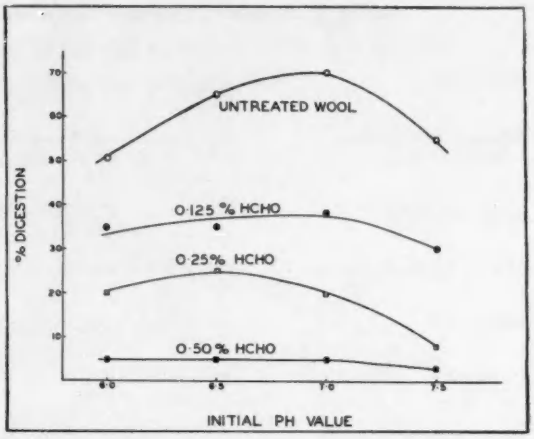

Fig. 2. Digestion of wool in papain-bisulfite urea at different *p*H values following treatment with various concentrations of formaldehyde. Incubated for 4 hr at 50° C. The 0.5% formaldehyde tanning solution contained also 2.5% $MgSO_4$ and 1.5% CH_3COONa, and this was diluted to provide the other formaldehyde concentrations tested.

filtering or centrifuging, washing repeatedly with water, drying at 105° C, and weighing.

Results

Comparison of Various Chemical Treatments

Curves relating the digestion of the modified wools to *p*H are shown in Figure 1.

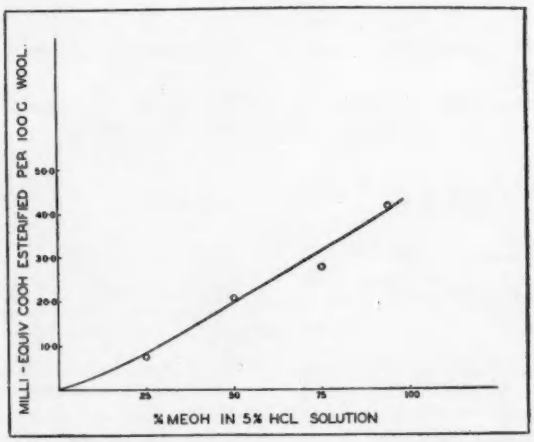

Fig. 4. Effect of methanol concentration on esterification of wool. The digestion of these samples is shown in Figure 6.

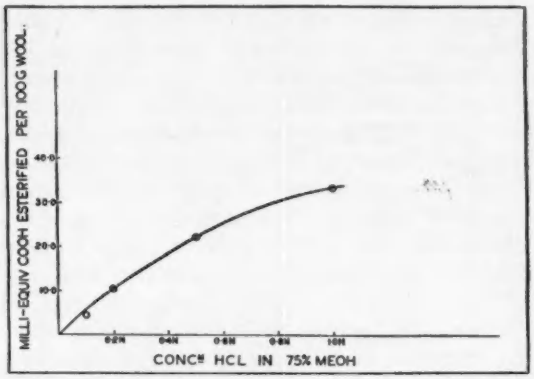

Fig. 5. Effect of concentration of acid in aqueous methanol solution on esterification of wool. The digestion of these samples is shown in Figure 7.

The acrolein-treated wool, when incubated in papain-bisulfite urea in several experiments at *p*H 6.5, was digested to the extent of about 60%. Considerable digestion of the sulfuric acid treated product in bisulfite-urea solutions was observed even in the absence of papain.

It will be noted that the *p*H optima for digestion, being within the *p*H range 6.5 to 7.0, were close to those for untreated wool.

Effect of Concentration of Formaldehyde and Chromium Sulfate

The improved protection conferred on wool by increasing the concentration of the formaldehyde or chromium sulfate solutions is shown in Figures 2 and 3 respectively. Analogous protective effects were previously observed when skin collagen was treated with these solutions [21].

Protection of Wool by Methanol Esterification

Increasing the degree of esterification of wool by raising the methanol concentration in a solution containing methanol, water, and 5% (v/v) of 10 *N* HCl (Figure 4) or the HCl concentration from 0.01 *N* to 1.0 *N* in an aqueous solution containing 75% methanol (Figure 5) lowered the digestibility of the wool in papain-bisulfite-urea solutions at various *p*H values (Figures 6 and 7).

Esterification of wool with a mixture of 5 ml 10 *N* HCl and 95 ml anhydrous methanol conferred almost complete protection after 7 hr treatment at 22° C (Figure 8). It was also shown that up to 50% of the methanol by volume could be replaced by the noninflammable solvent trichlorethylene without reducing the protective effect of the treatment.

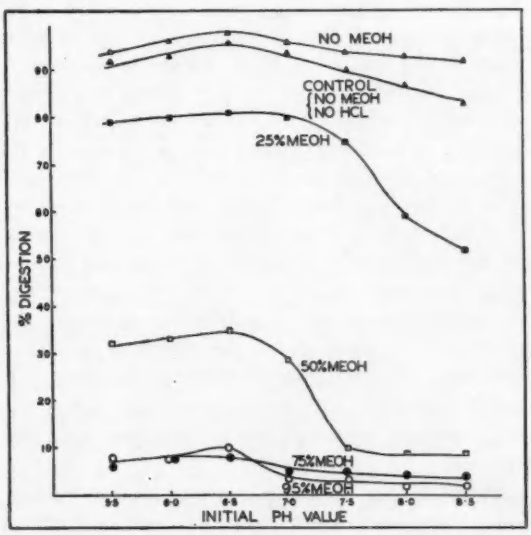

Fig. 6. Digestion of wool during 18 hr at 50° C in papain-bisulfite urea at different *p*H values following esterification for 7 days at 22° C in a methanol-water mixture containing 0.5 *N* HCl.

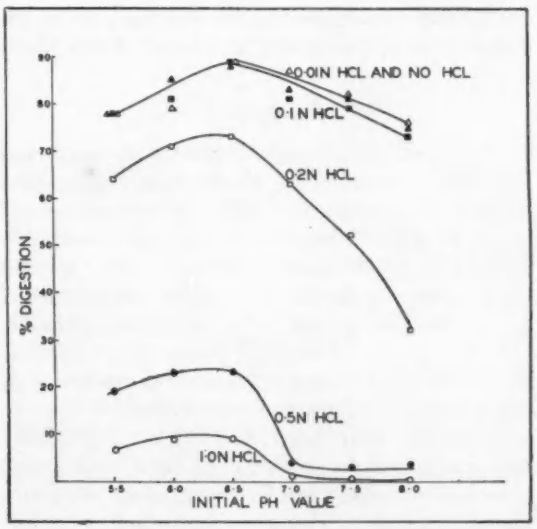

Fig. 7. Digestion of wool during 18 hr at 50° C in papain-bisulfite urea following esterification for 3 days at 22° C in 75% methanol and 25% water (v/v) containing various concentrations of HCl.

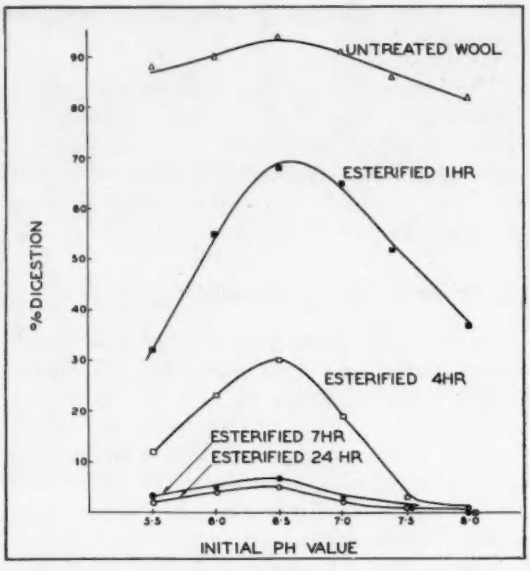

Fig. 8. Digestion of wool during 18 hr at 50° C in papain-bisulfite urea following esterification for various periods in 95% methanol and 0.5 *N* HCl.

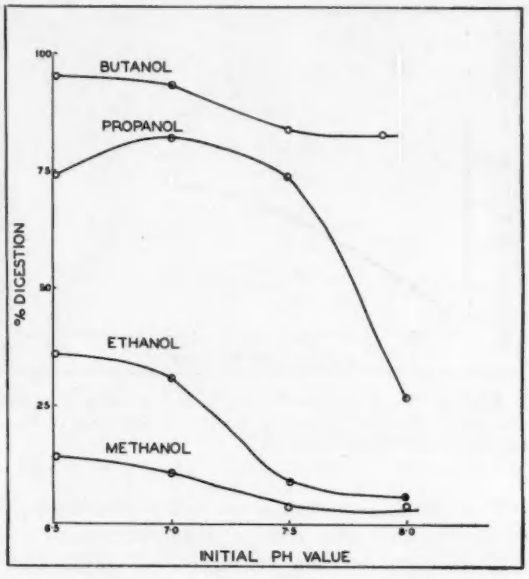

Fig. 9. Digestion of wool during 18 hr at 50° C in papain-bisulfite urea following esterification with different alcohols.

Substitution of other monohydric alcohols for methanol in the esterifying solutions containing 5% (v/v) HCl reduced the protection (Figure 9). This effect corresponded with the previously reported fall in the extent of esterification with increase in the length of the C chain in the aliphatic alcohols [1].

Discussion

Compounds which react with wool are sometimes classified as unifunctional, bifunctional, reactive with cystine, or miscellaneous [28]. The monofunctional group of reagents used in the present investigation includes the monohydric alcohols which, in acid solution, esterify the side-chain and terminal carboxyl groups but are without effect on amino, phenolic, sulfydryl, peptide, and amide groups [9]. Elimination of the terminal carboxyl groups by reaction with ammonium thiocyanate and acetic anhydride in acetic acid solution [26] failed to affect the digestibility appreciably, and the protection by esterification must therefore be ascribed to the covering of the side-chain carboxyl groups. The protective effect of methyl esterification of proteins against digestion by proteolytic enzymes of the intestinal tract has been previously observed [18]. These striking effects could be at least partly accounted for by loss of hydrophilic character and therefore solubility, since ester groups have little affinity for water in comparison with carboxyl groups (for example, [19]). The loss in digestibility is particularly noticeable at alkaline *p*H values (Figure 6) where the amino groups of intact wool would ionize readily. Although resistant to papain, methyl-esterified woolen fabric was readily attacked by larvae of the clothes moth *Tineola bisselliella*. The methyl groups may be removed in the larval gut through the hydrolytic action of esterase. The protective action of 1-fluoro-2,4-dinitrobenzene may have been due to reaction with, and elimination of, the hydrophilic properties of the amino groups. Propylene oxide might also be expected to react with the amino groups and to polymerize on them. An alternative explanation for the effects of esterification and 1-fluoro-2,4-dinitrobenzene and propylene oxide treatments may be the masking of groups in the substrate essential for combination with the enzyme.

When applied to wool, reagents such as picrate, iodoacetate and iodide (in the iodine solution) would compete with the carboxyl groups in the protein for the basic amino and guanidino groups. They would thereby break some of the linkages which

confer stability through their combined electrostatic and hydrogen bond character—the so-called salt linkages of proteins. Destruction of the amino groups by acetylation or by reaction with nitrous acid would be even more drastic in breaking salt links. But unlike the alcohols, these other monofunctional compounds may not reduce the hydrophilic properties of the protein. Reduction of the disulfide bonds and substitution of the sulfydryl hydrogen with acetate groups by treatment with iodoacetic acid increased the digestibility, particularly at *p*H values above 6, where the protein would be expected to carry predominantly negative charges.

The bifunctional compound 1,3-dibromopropane yielded very little protection when applied to intact wool, but its application to the reduced fiber improved the enzyme resistance markedly. Trimethylene bridges would be inserted in the structure by this treatment, as postulated to explain the enhanced resistance to alkali, acid, oxidizing, and reducing compounds and to other biological agents [12].

According to McPhee and Lipson [24], acrolein is also a bifunctional compound, both the carbonyl and olefinic groups reacting with sulfydryl groups in the reduced keratin to eliminate supercontraction in bisulfite, affect the elastic properties, and diminish the swelling in trichloracetic acid. To these effects may now be added protection of the fiber against papain-bisulfite-urea digestion.

With some other compounds the mechanism of the stabilization is even less certain. Some evidence suggests, for example, that formaldehyde forms cross-links in proteins between the amino [8], amide [16], and amino and tyrosine groups [2] and between amide and amino groups [10]. To what extent protection by formaldehyde can be ascribed to reaction of each molecule of formaldehyde with only one amino or amide group with consequent loss of hydrophilic character or elimination of an enzyme combination center, as postulated for the tanning action of formaldehyde [17, 27], is uncertain on the evidence available. Epichlorhydrin may form cross-links [3] even more readily because of the presence of a reactive chlorine atom in addition to the oxygen. By analogy with their accepted action on collagen [14] it may be assumed that chromium compounds also stabilize wool by cross-linking different parts of the keratin structure through the formation of coordination complexes.

Among the miscellaneous reagents are iodine and sulfuric acid. The addition of iodine to the aromatic ring in the tyrosine residues in wool [5] may partly account for the increased digestibility, for a similar increase was reported for the action of pepsin on acetyl-L-phenylalanyl-L-tyrosine following iodination of the tyrosine residue [4]. The cuticle of the wool fiber becomes pitted in the presence of iodine in solution, and this may facilitate penetration of papain-bisulfite urea into the interior.

The severity of the damage to wool by sulfuric acid is reflected in the ready digestibility in papain-bisulfite urea even after incubation for only 0.5 hr at 50° C. Not only does this reagent react with the amino groups to form sulfamic acids [14], but M. S. Grafer has shown that the tyrosine residues are sulfonated [25]. Moreover, the destruction of arginine, tyrosine, and tryptophane residues by sulfuric acid is extensive, and serine and phenylalanine residues are also damaged, although to a lesser extent [23].

It should be appreciated that some of the reagents may not have been used under conditions most favourable to their interaction with keratin. Other conditions of treatment would yield perhaps greater protection with certain reagents and greater susceptibility with others than is reported here. In a more qualitative sense, however, the results are informative and they show clearly the value of papain-bisulfite-urea digestion for distinguishing between the effects of a variety of chemical treatments.

Acknowledgments

The author is indebted to Mrs. H. M. Forss for technical assistance, to Dr. M. Lipson for providing the acrolein-treated samples, and to Dr. M. F. Day of the C.S.I.R.O. Division of Entomology for measurements of moth resistance of methyl esterified woolen fabric.

Literature Cited

1. Alexander, P., Carter, D., Earland, C., and Ford, O. E., *Biochem. J.* **48**, 629 (1951).
2. Alexander, P., Carter, D., and Johnson, K. G., *Biochem. J.* **48**, 435 (1951).
3. Alexander, P., Fox, M., Stacey, K. A., and Smith, L. F., *Biochem. J.* **52**, 177 (1952).
4. Baker, L. E., *J. Biol. Chem.* **193**, 809 (1951).
5. Blackburn, S., and Phillips, H., *J. Soc. Dyers Colourists* **61**, 100 (1945).
6. Burgess, R., *J. Text. Inst.* **25**, T289 (1934).
7. Deleted.

8. Dyachenko, P. F., and Skelpakova, K. F., *J. Int. Soc. Leather Trades' Chemists* **23**, 12 (1939).
9. Fraenkel-Conrat, H., and Olcott, H. S., *J. Biol. Chem.* **161**, 259 (1945).
10. Fraenkel-Conrat, H., Cooper, M., and Olcott, H. S., *J. Am. Chem. Soc.* **67**, 950 (1945).
11. Geiger, W. B., Patterson, W. I., Mizell, L. R., and Harris, M., *J. Research Natl. Bur. Standards* **27**, 459 (1941).
12. Geiger, W. B., Kobayasha, F. F., and Harris, M., *J. Research Natl. Bur. Standards* **29**, 381 (1942).
13. Goldschmidt, M. T., TEXTILE RESEARCH JOURNAL **20**, 613 (1950).
14. Green, R. W., *Biochem. J.* **54**, 187 (1953).
15. Harris, M., Mease, R., and Rutherford, H., *J. Research Natl. Bur. Standards* **18**, 343 (1937).
16. Haworth, R. D., MacGillivray, R., and Peacock, D. H., *J. Chem. Soc.* 2981 (1952).
17. Highberger, J. H., *J. Am. Leather Chemists' Assoc.* **42**, 493 (1947).
18. Hoppe-Seyler-Tierfelder, *Physiologisch und Pathologisch Chemische Analyse*, 9th ed. Schmidt, Berlin (*The Chemistry of the Amino Acids and Proteins*, Charles C Thomas, Springfield, Ill., 1938, p. 298).
19. Katchman, B., and McLaren, A. D., *J. Am. Chem. Soc.* **73**, 2124 (1951).
20. Lennox, F. G., *Australian J. Biol. Sci. Ser. B* **5**, 189 (1952).
21. Lennox, F. G., and Forss, H. M., *J. Soc. Leather Trades' Chemists* **36**, 322 (1952).
22. Linderstrøm-Lang, K., and Duspiva, F., *Compt. rend. trav. lab. Carlberg Sér. chim.* **21**: 4, 53 (1936).
23. Lustig, B., and Kondritzer, A. A., *Arch. Biochem.* **8**, 51 (1945).
24. McPhee, J. R., and Lipson, M., *Australian J. Chem.* **7**, 387 (1954).
25. Speakman, J. B., *J. Text. Inst.* **32**, T83 (1941).
26. Swan, J. M., *Australian J. Sci. Research, Ser. A* **5**, 711 (1952).
27. Weir, C. E., *J. Am. Leather Chemists' Assoc.* **44**, 108 (1949).
28. Zahn, H., and Wilhelm, H., TEXTILE RESEARCH JOURNAL **23**, 604 (1953).

Manuscript received December 23, 1954.

Visual Observations of the Behavior of Soil Particles in Dilute Aqueous Soap Systems

Charles W. Hock

Hercules Experiment Station, Hercules Powder Company
Wilmington, Delaware

Abstract

The nature of one type of detergent action was demonstrated visually upon the addition of graphite to soap solutions of laundry strength. The graphite became coated with elongated soap particles and superficially bore a resemblance to pieces of candy covered with shredded coconut. The soap particles, which may bear some relation to micelles, measured 100 to 150 A wide and from 500 to 1500 A long. This exploratory study involved an electron microscopical examination of specimens from which the water had been removed while in the frozen state.

Introduction

Substantial success has already been achieved in studying a variety of colloidal systems with the electron microscope. This prompted us to use the electron instrument to explore certain phenomena associated with the dilute detergent systems employed in actual laundry practice. The survey, which was completed several years ago, included an examination of various detergents. However, the following report is limited to a discussion of visual observations of 0.15% solutions of a true soap, viz., sodium oleate, in the presence and in the absence of added soil.

The dilute aqueous oleate system is a complicated one owing, on the one hand, to hydrolysis which occurs at extreme dilutions and, on the other, to contamination with atmospheric carbon dioxide, which occurs during manipulation of the solutions. For these reasons, fatty-acid soap systems are difficult to study, especially by the light-scattering technique, and their properties are not so well established as those of cationic systems, for example. There are

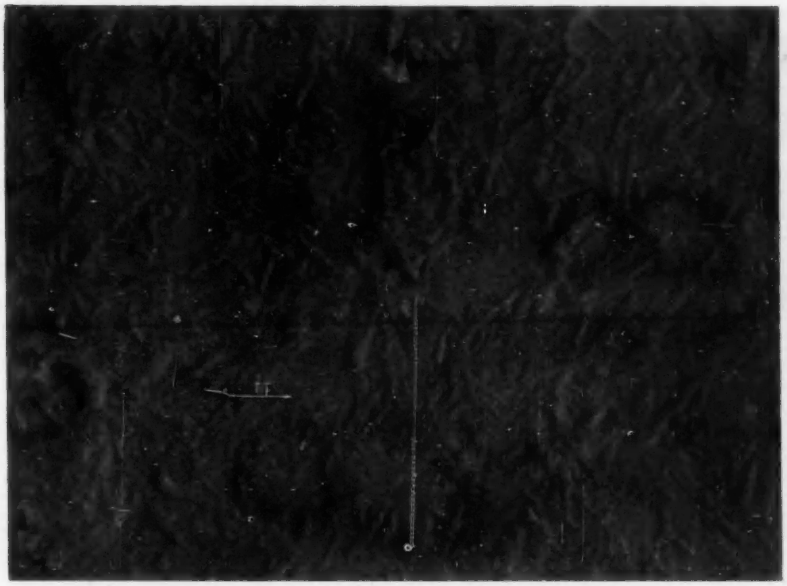

Fig. 1. Particles in sodium oleate system. Electron micrograph of chromium-shadowed specimen. Magnification, ×40,000.

practical reasons, if no other, why one may wish to study these systems anyway.

Since specimens are exposed to a high vacuum when viewed in the electron microscope, direct examination of solutions as such is not possible. In order to carry out the objectives of this investigation, it was necessary therefore to use a technique of specimen preparation which would preserve in dry mounts the character of soap and soil particles as they exist in dilute solutions. To accomplish this, water was removed from specimens in the frozen state.

Interpretation of the observations involves two seemingly unavoidable difficulties. In the first place, the exact nature of the soap particles observed in the system is difficult to establish owing to the propensity of sodium oleate to hydrolyze in dilute solutions. Second, although specimens were prepared in a manner designed to prevent spatial rearrangement of particles from occurring, it must be acknowledged that changes may have occurred during removal of the water. That such rearrangement has not taken place is practically impossible to establish. Despite these limitations, these exploratory observations seemed to be sufficiently interesting to warrant a short publication.

Preparation of Specimens

Sodium oleate solutions were used in only one concentration, viz., 0.15%. The solutions were made up in ordinary distilled water.

The general scheme of specimen preparation was as follows. Specimen screens were first coated with a thin film of nitrocellulose, according to the usual procedure in electron microscopy [2, 14]. A small drop of the soap solution was then placed on the coated screen, which was plunged instantaneously into liquid nitrogen, later withdrawn, and promptly placed on a metal block which had been precooled in dry ice. The cold metal block, with the specimen screens on it, was covered (but not touched) with another precooled metal plate and placed in an evacuation chamber (actually a metal shadow-casting unit) where the moisture was removed from the frozen specimens (and, of course, from the surface of the metal blocks also). Measurements of the vapor pressure in the vacuum jar during evacuation and also direct readings on a mercury bulb thermometer revealed that during this operation the temperature did not rise above $-40°C$. After the moisture was withdrawn the dry specimens were shadowed with chromium by the method now commonly employed to increase contrast in electron microscopical images.

Results and Discussion

Particles were visible in specimens obtained from both the liquid and foam phases of the dilute soap systems (Figure 1). The particles were elongated, rod-shaped, or cylindrical bodies whose width lay between 100 and 150 A and whose length ranged from 500 to 1500 A. Occasionally the pictures

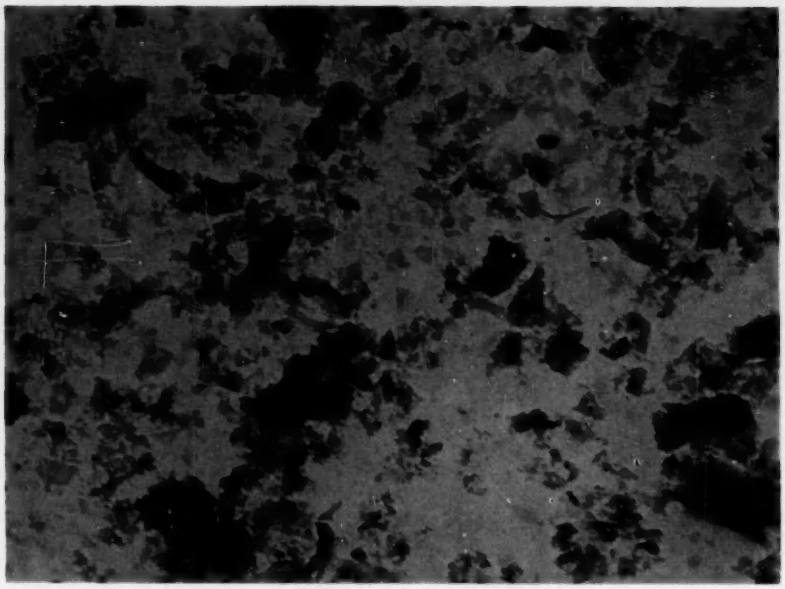

Fig. 2. Graphite. Electron micrograph of unshadowed specimen. Magnification, ×40,000.

showed a faint suggestion of a finer structure within the elongated bodies themselves, but more refined techniques of specimen preparation would be required to clarify this point.

In order to observe the behavior of these particles in the presence of soil, approximately 0.1 g of graphite (Aquadag) was added to a half liter of 0.15% solution of sodium oleate. Specimens taken from the resulting turbid system showed small pieces of graphite surrounded by particles from the soap solution. Whereas pieces of graphite ordinarily have smooth angular profiles (Figure 2), those from the soap system resembled pieces of candy covered with shredded coconut (Figure 3). In the systems containing only soap the particles of soap were distributed evenly, but in the systems which also contained soil the soap particles were distributed unevenly, owing to their aggregation around the soil particles. This behavior throws some light on the mechanism of detergent action. It does not indicate how the soap, with the aid of mechanical work, accomplishes removal of soil in the first place, but it does suggest that by surrounding the soil the soap particles prevent its redeposition on cloth, for example. This may be brought about by equivalence of charges between the soil-soap complex and the substrate-soap complex, thereby leading to repulsion.

The principal outcome of this work was the direct visual demonstration of at least one mode of detergent action. At the same time, the speculation seems warranted that the particles seen in the soap solutions may be related to micelles. As a result of conductivity, light scattering, surface tension, osmotic pressure, and other measurements, it is generally accepted that within the range of concentrations extending from about 0.1 to 0.3% solutions of soaps and detergents undergo rather marked changes which are believed to indicate the formation of molecular aggregates or micelles [8, 9, 11, 12]. Spherical, lamellar, ellipsoidal, cylindrical, and rodlike [3] micelles have been postulated, but it is not yet possible to assign definite sizes and shapes to them [5, 6]. They are, however, generally thought to be smaller than the rodlike soap particles seen here by means of electron microscopy. On the other hand, the 100 to 150 by 500 to 1500 A particles delineated in the electron microscope should not be confused with larger fibrous crystalline forms of soaps and greases which are present in concentrated systems and which have been observed by means of both light and electron microscopy [1, 4, 7, 9, 10, 13]. However, the results of the present exploratory study do point up the potential usefulness of electron microscopy in arriving at a clearer understanding of micellar configurations and the mechanism of detergent action.

Fig. 3. Graphite coated with particles of sodium oleate. Electron micrograph of chromium-shadowed specimen. Magnification, ×40,000.

Acknowledgment

It is a pleasure to acknowledge the able assistance of Mr. A. N. Abbott in carrying out the electron microscopical examinations.

References

1. Ellis, S. G., *Can. J. Research* **25**, 119 (1947).
2. Hall, C. E., *Introduction to Electron Microscopy*, New York, McGraw-Hill (1953).
3. Halsey, G. D., *J. Phys. Chem.* **57**, 87 (1953).
4. Hattiangdi, G. S., and Swerdlow, M., *J. Research Nat. Bur. Standards* **42**, 343 (1949).
5. Klevens, H. B., *J. Am. Oil Chemists' Soc.* **30**, 74 (1953).
6. Kushner, L. M., *Soap and Chem. Specialties* **30**, 50 (1954).
7. Marton, L., McBain, J. W., and Vold, R. D., *J. Am. Chem. Soc.* **63**, 1990 (1941).
8. McBain, J. W., in *Colloid Science*, Vol. V, edited by J. Alexander, New York, Reinhold (1944).
9. McBain, J. W., in *Frontiers in Colloid Chemistry*, Vol. VIII, edited by R. E. Burk and O. Grummitt, New York, Interscience (1950).
10. Mottlau, A. Y., *J. Appl. Phys.* **20**, 1055 (1949).
11. Niven, W. W., *Fundamentals of Detergency*, New York, Reinhold (1950).
12. Preston, W. C., *J. Phys. & Colloid Chem.* **52**, 84 (1948).
13. Thiessen, P. A., and Erdmann, H., *Z. physik. Chem.* **193**, 367 (1944).
14. Wyckoff, R. W. G., *Electron Microscopy*, New York, Interscience (1949).

Manuscript received March 4, 1955.

An Evaluation and Comparison of Evenness Testers[1]

William T. Waters

Research Assistant Professor, Textile Research Department, School of Textiles, North Carolina State College, Raleigh, North Carolina

Introduction

In recent years, due to a highly competitive textile market, the rapid and reliable detection, location, and analysis of unevenness occurring in sliver, roving, and yarn have become problems of increasing importance. The older method of examining yarn on a seriplane board has two serious drawbacks: it is more qualitative than quantitative and it is not very informative in regard to periodic faults. The cut-length method was one of the most accurate methods of obtaining unevenness figures and graphs, but if short lengths are desired this method becomes very tedious and time-consuming.

Recently various evenness testers which overcome the above shortcomings have been introduced to the textile trade. Many mills are contemplating the purchase of these instruments but frequently are unacquainted with the various testers available and, therefore, are incapable of judging the merits of each. Also, each tester presents its evenness data differently from the others, and many mill men who already have an evenness tester have expressed a desire for constants to convert the results of one tester to another for comparison of results. With these thoughts in mind, a series of experiments were undertaken to systematically evaluate and compare results of the following evenness testers:

ITT-Brush Uniformity Analyzer—graph recorder and Automatic Evaluator;
Uster Evenness Tester, Model A—graph recorder, Linear Integrator, and Quadratic Integrator;
Fielden-Walker Evenness Tester—graph recorder and Deviation Integrator;
Pacific Evenness Tester—graph recorder only;
Saco-Lowell Graphic Sliver Tester—graph recorder only.

From this work it is expected to determine which tester is superior in operating performance, which tester is best suited for a specific job, what correlation, if any, exists between the measurements of the various testers, and what relationship exists between yarn evenness and fabric appearance.

Several limitations of this investigation should be noted:

1. The conclusions to be drawn from this work apply only to the testers listed in the introduction. Several newer model testers are now available on the market.
2. All tests were made on cotton and do not necessarily apply to other fibers or blends.
3. The samples available for testing were limited in size range, and the conclusions drawn should apply only to the range of samples tested.
4. In general, the tests have been arranged to compare and evaluate the measurements rather than the physical or electrical properties of each instrument.

Testing Conditions

All tests with the exception of the ones using the Uster Quadratic Integrator were carried out in the testing laboratory of the Physics Division at the Institute of Textile Technology, in which the various evenness testers are located. This laboratory is not air-conditioned; therefore, standard testing conditions could not be met. However, it is equipped with an automatic humidifier and a constant relative humidity of 65% was maintained during all tests. The windows and doors were kept closed in order to help maintain constant relative humidity and to prevent air drafts from affecting the heat stabilization of the evenness testers. The temperature ranged from 70° to 90°F during the course of this work. Since the Uster Quadratic Integrator is very sensitive to temperature and since the manufacturer recommends that it be used only in an air-conditioned laboratory, it was necessary to move this

[1] This paper is taken from a thesis submitted by William T. Waters in partial fulfillment of the requirements for the degree of Master of Science at the Institute of Textile Technology, Charlottesville, Virginia, June 1954.

TABLE I. Per Cent CV between Readings of 10 Successive Runs of a 30's Carded Yarn Sample

Testers	Per Cent Coefficient of Variation (% CV)	Yarn Speed (yd/min)	Sample Length (ft)
Uniformity Analyzer Graph	0.8	100	1000
Uniformity Analyzer Automatic Evaluator	0.8	100	1000
Uster Graph	0.8	8	90
Uster Linear Integrator	1.5	100	750
Uster Quadratic Integrator	1.8	100	750
Fielden-Walker Graph	1.8	2	39
Pacific Graph	2.0	12	75
Fielden-Walker Integrator	2.4	2	39

equipment to the Standards Testing Laboratory at the Institute for the running of its tests. The conditions maintained in this laboratory are 72°F ± 2° and 62% R.H. ± 2%.

All instruments were given a warm-up time of at least 1 hr to stabilize drift before taking data. The samples to be tested were allowed to condition at least overnight in the laboratory. Throughout the tests, the manufacturer's recommended operating procedures, sampling techniques, and yarn and chart speeds were used wherever possible.

Reproducibility of Yarn Measurements

A series of tests were made to determine the precision or reproducibility of each tester. An evenness tester should be able to reproduce the unevenness of a sample at any time, place, or under any common atmospheric conditions. The samples used were taken from a bobbin of 30's carded cotton yarn. Ten successive runs of the same sample were made on each tester, and the coefficient of variation (CV) of the results was calculated. A new sample from the same bobbin was used for each tester because of wear on the yarn. Different sample lengths were used on the various testers because of the differences in material speeds of each.

Numerous attempts were made to rerun the same sample on the Pacific Tester, but in each case the yarn was chewed up by the tongue and groove rolls on the first run and could not be rerun. Because of this, it was decided to run 10 consecutive samples from the same bobbin and compute the CV of the results. Because of intrabobbin variation, it was expected that this CV would be greater than if the same sample could be rerun. The coefficient of variation obtained for each tester is shown in Table I.

TABLE II. Per Cent CV of Data Obtained in Yarn Characterization Test

Testers	Yarn Speed (yd/min)	Sample Length (ft)	CV (%)
Uniformity Analyzer Automatic Evaluator	100	1000	0.82
Fielden-Walker Integrator	20	540	0.98
Uster Linear Integrator	8	168	1.01
Uster Linear Integrator	100	750	1.17
Uster Quadratic Integrator	100	750	1.19
Pacific Graph	12	75	3.55

Yarn Characterization

The precision with which the average uniformity of a large number of bobbins can be determined depends for the most part upon the sampling technique employed. Sampling technique as used here refers to the number of bobbins tested and the sample length used from each bobbin. A test was run to determine how good an average the various testers gave from a group of randomly picked samples using the recommended or commonly used sampling technique for each tester. A recommended sample length was given for each tester, but in all cases except the Uniformity Analyzer no recommendation could be found in the various instruction manuals as to the number of bobbins to be tested. Therefore, from a lot or group of 25 bobbins of 31's carded cotton yarn, 10 bobbins were picked at random and run on each tester using the recommended or commonly used methods, speeds, sensitive lengths, and sample lengths for each tester. The per cent coefficient of variation of the results for each tester is shown in Table II.

Each per cent CV listed in Table II is the per cent coefficient of variation of the mean and not of the individual bobbins. In this table, it can be seen that the value for the Pacific tester is out of line. The reason for this high per cent CV in respect to the others is that the recommended sample length per bobbin of only 75 ft is considered entirely too short.

Comparison and Correlation of Yarn Measurements

A group of 25 yarn samples representing many different types and degrees of unevennesses and covering a range in count from 13's to 50's were run on the various testers for a comparison and correlation of yarn measurements. For the majority of cases, the identical sample was used; one exception being the Pacific where only part of the sample was used

TABLE III. Correlation Coefficients Obtained in the Comparison and Correlation of Yarn Measurements

Instruments	Correlation Coefficient (r)
Uniformity Analyzer Graph—Uniformity Analyzer Automatic Evaluator	0.996
Uniformity Analyzer Graph—Fielden-Walker Integrator	0.974
Uniformity Analyzer Automatic Evaluator—Fielden-Walker Integrator	0.985
Uniformity Analyzer Graph—Uster Quadratic Integrator	0.978
Uniformity Analyzer Automatic Evaluator—Uster Quadratic Integrator	0.985
Fielden-Walker Integrator—Uster Quadratic Integrator	0.970
Fielden-Walker Integrator—Uster Linear Integrator	0.963
Uniformity Analyzer Graph—Uster Linear Integrator	0.962
Uniformity Analyzer Automatic Evaluator—Uster Linear Integrator	0.974
Pacific Evenness Graph—Uniformity Analyzer Graph	0.844
Pacific Evenness Graph—Uniformity Analyzer Automatic Evaluator	0.863
Pacific Evenness Graph—Uster Linear Integrator	0.832
Pacific Evenness Graph—Uster Quadratic Integrator	0.876
Pacific Evenness Graph—Fielden-Walker Integrator	0.876
Uster Linear Integrator—Uster Quadratic Integrator	0.986
Uster Graph—Uster Linear Integrator	0.996

because of the slower speed. In a comparison of the Uster Graph and Linear Integrator, new samples were used and a yarn speed of 4 yd/min employed because of the low frequency response of the Uster recorder. A sensitive length of 10 ft was used on the Uniformity Analyzer and a sensitive length of 1 yd on the Pacific and Uster graphs.

From the results obtained in this comparison, correlation coefficients, prediction equations, and average multipliers were calculated between the various instruments. The coefficients of correlation computed are shown in Table III, and for a visual comparison typical correlation plots are shown in Figures 1 and 2. The yarn speeds and sample lengths used with each instrument and the prediction equations and average multipliers calculated are listed in Appendix I.

From the correlation coefficients calculated, it is seen that the correlation between yarn measurements on the Pacific Evenness Tester (mechanical type) and the capacitance type testers is not as high as was obtained between the measurements of the capacitance type testers alone. The coefficients of correlation found between the results of the capacitance type testers ranged from 0.962 to 0.996, while a range of 0.832 to 0.876 was obtained on the results between the Pacific and the capacitance type testers. One possible explanation of this difference in degree of correlation could be that the two different type testers are not measuring the same property of yarn. Another explanation could be that a 1-yd sensitive length, which is normally used in calculating the Pacific charts, was used here; and that if some other sensitive length is used, better correlation may exist. However, it should be pointed out that in correlating the Uster graph and Uster Linear Integrator a 1-yd sensitive length was used, and a correlation coeffi-

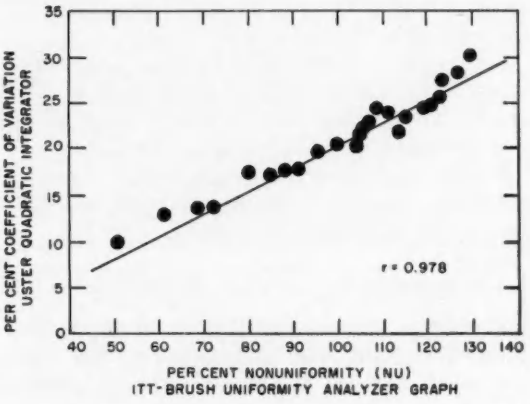

Fig. 1.

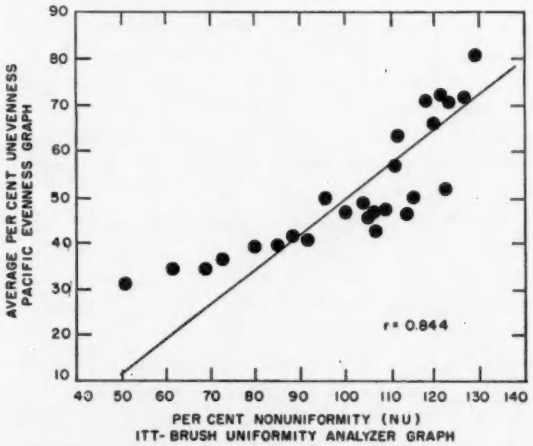

Fig. 2.

cient of 0.996 was obtained. Also, in both the work by Bernet and Waters and ASTM Committee D-13, Subcommittee B-1 [1], all charts were calculated in the same manner, and the yarn measurements on the Pacific testers were always lower. In view of these points, it is believed that the Pacific tester is not measuring the same property of yarn as are the capacitance type testers.

Effect of Gain Setting on Precision of Yarn Measurements

The purpose of this test was to determine if the position of the trace or fluctuations on the evenness chart of the various testers had any effect on the precision of the measurement being made. The positioning of the diagram on the chart is controlled by the gain setting on all the yarn evenness testers except the Pacific, where positioning of the chart is controlled by the gage micrometer setting. Because of the inherent material variability, it is practically impossible to center these fluctuations on the evenness chart around the zero line or center of the chart, depending on the specific tester being used. Displacement of the diagram or trace above the center of the chart results in an increase in amplitude of the chart fluctuations; displacement below results in a corresponding decrease in amplitude. When the charts are calculated by the range method and with the zero (no material in measuring head) located at the bottom of the chart, no correction factor is needed. If zero is taken in the center of the chart as on the Uster, displacement of the mean weight or average height of diagram above or below zero must be corrected by the proper factor determined from the average value reading taken. When the various integrators or Automatic Evaluator are used instead of the chart, correction factors are supplied by such meters as the Fiducial Mean on the Uniformity Analyzer, Average Value on the Uster, and Mean Level on the Fielden-Walker.

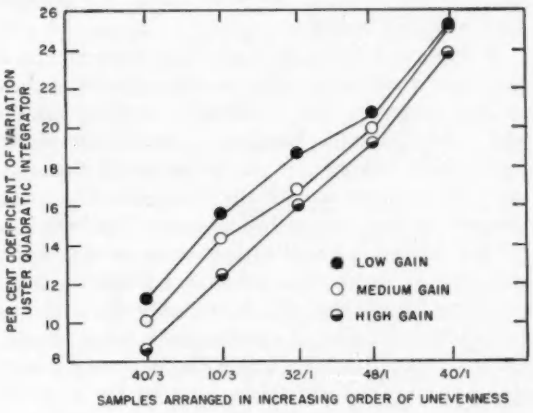

Fig. 3.

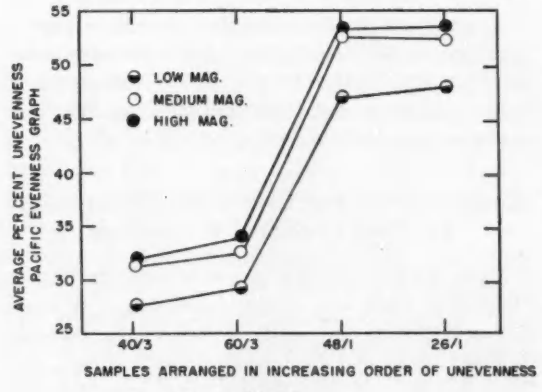

Fig. 4.

A group of yarn samples representing various types of unevenness was run on the testers at high, medium, and low gain. The same sample was used for each of these gain settings. For this test, high gain placed the diagram approximately three-fourths the way up the chart from the bottom; medium gain, approximately midscale; and low gain, approximately one-fourth the way from the bottom.

The results obtained for each tester were plotted, and typical plots are shown in Figures 3 and 4. Due to the nature of these plots, the individual points would tend to fall on each other if the gain setting had no effect on the precision of measurement. From the results it was found that the gain setting does not have any significant effect on the various testers except in the case of the Uster Quadratic Integrator (Figure 3). Here it is noted that the results appear to be significantly different and that there is a common trend for each sample to give an increasing per cent CV from high to low gain. The high gain corresponds to a positive average value reading, and the low gain corresponds to a negative average value reading.

Since the chart diagram on the Pacific tester is positioned by the gage micrometer setting and not a gain setting, it was decided to investigate the ef-

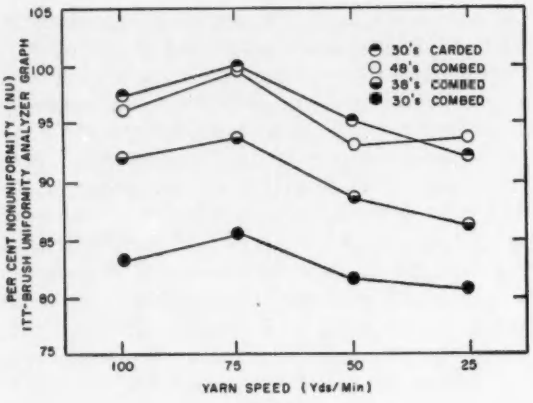

Fig. 5.

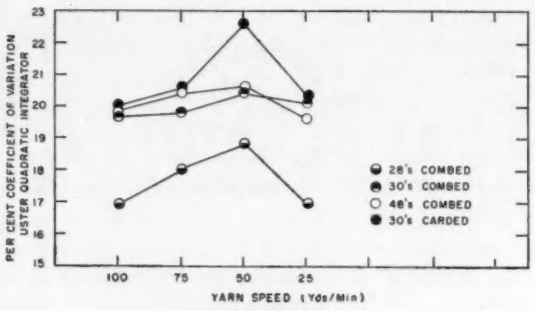

Fig. 6.

fect of gage micrometer setting and magnification setting on the precision of yarn measurements. Due to the chewing of the yarn by the Pacific tester, successive samples from the same bobbin were used for the different magnification and gage micrometer settings. It should be realized that this could possibly introduce an error due to variations within the bobbin. From the results obtained, it was found that the gage micrometer setting did not appear to have any effect on the precision of measurement. In the case of the effect of the magnification setting (Figure 4), it was found that for each sample the low magnification setting (E) was incorrect. Since some Pacific testers have different magnification values and are set and calibrated by different service men, this conclusion applies only to this specific tester. The significance of this test, however, is that the various magnification values should be checked for each tester to be sure they are correct.

Effect of Yarn Speed on Precision of Yarn Measurements

A test was run on the various testers to determine if the material (yarn) speed had any effect on the precision of yarn measurements. A group of yarn samples representing various types of unevenness were run at yarn speeds of 100, 75, 50, and 25 yd/min. These speeds were obtained by means of a variable speed drive and are not commonly used by all testers but were chosen for comparison purposes. The same sample was run at the various speeds keeping the gain and other settings constant. Zero adjustments were checked before and after each run. The Pacific tester was excluded because its speed could not be varied. The effect of yarn speed on the results of the Fielden-Walker graph was investigated in Research Report 60 [2], and it was found that the frequency response of the recorder was too low, even for the slow speed of 2 yd/min used with this recorder.

In Figures 5 and 6, it is seen that material speed does have a significant effect on the precision of yarn measurements on the Uniformity Analyzer graph and Uster Quadratic Integrator. In the case of the Uniformity Analyzer, it should be noted that this unit, in conjunction with the Brush recorder, was designed to test yarn at 100 yd/min. The high frequency response of the Brush recorder necessary for this speed is obtained by means of a frequency compensating circuit, and this is probably the explanation of the variation of results at the lower speeds. On the Uster Quadratic Integrator, it is noticed that the measurements are fairly constant for most of the speeds, but that at 50 yd/min there is a significant difference in results and a common trend in all cases to give higher results. The explanation for this is not known, but this effect should be kept in mind when using this speed. From the results obtained on the other testers, it appears that material speed does not have a significant effect on their precision of yarn measurements.

Comparison of Per Cent Nonuniformity and Per Cent Coefficient of Variation

Many textile men have become interested in the "Degree of Perfection" formula used by Dr. Martindale of England. By means of this formula, yarns of different count and fiber quality can be compared. Since this formula uses the statistical term per cent

CV, a number of mills have inquired about the relation between per cent nonuniformity (per cent NU) as obtained with the Uniformity Analyzer and per cent coefficient of variation (per cent CV) as obtained using the Uster tester with the Quadratic Integrator. Preliminary investigations [2] indicated good correlation between per cent NU and per cent CV and that per cent NU was approximately 5 times per cent CV. In view of this fact, it was decided to investigate the statistical relationship existing between these two measurements, employing a larger group of samples.

In many books on statistics, mention is made of a relationship existing between the standard deviation and the range in an unbiased sample whereby the average range can be divided by a factor from Tippett's tables [6] to give the standard deviation. Since per cent NU is actually an average range divided by the mean, the above relationship should exist; the problem is to determine the number of subdivisions to select the proper divisor constant.

On the Brush graph recording, there are 100 groups of 10-ft lengths (1000-ft sample length) in which the difference between the high and low peak in each 10-ft length can be designated the specimen range. The numerical difference between the average high and average low therefore gives the average specimen range. It has been established in the literature [3] by a number of writers that the length of the drafting wave is approximately twice the staple length, and this relationship was used in determining the number of subdivisions or peaks and dips in 10 ft of yarn, which is the standard sensitive length used with the Uniformity Analyzer. It was found that there are approximately 54 drafting waves on the average in 10 ft of cotton yarn made from $1\frac{1}{4}$ in. staple, and since each drafting wave has a peak and a dip, there are approximately 108 peaks and dips in 10 ft of yarn. From Tippett's tables, a divisor constant of 5.02 is found for 100 subdivisions, and this figure can be used to convert per cent NU to per cent CV. This figure is in very close agreement with the average divisor of 5 found in Research Report 60 [2].

To investigate further this statistical relationship between per cent NU and per cent CV, a group of 150 yarn samples was run on the Uniformity Analyzer graph, Uniformity Analyzer Automatic Evaluator, and Uster Quadratic Integrator. One-third of these samples were 30's warp yarn; another third were 40's filling yarn; and the remaining third were different count samples ranging from 13's to 150's and including carded, combed, plied, and double-carded yarn. The 30's and 40's yarns were spun from $1\frac{1}{32}$ in. SLM and $1\frac{1}{16}$ in. M cotton respectively, while the various staple lengths of the mixed-count samples are unknown. A sample length of 1000 ft and a yarn speed of 100 yd/min were used. These results were summarized and the average divisor existing between per cent NU and per cent CV results is shown in Table IV.

TABLE IV. Summary of the Relationship Between Per Cent NU as Obtained on Uniformity Analyzer and Per cent CV as Obtained by Uster Quadratic Integrator

Sample Group	Divisor (Graph)*	Divisor (Automatic Evaluator)*
30's warp	4.81	4.86
40's filling	4.57	4.73
Mixed count	5.02	5.03

* This divisor represents the figure obtained when per cent NU is divided by per cent CV.

From the results of this test, it is seen that the relationship between per cent NU and per cent CV is slightly less than 5 except in the case of the mixed-count samples. It should be noted that the warp and filling samples [2] were trashy and neppy. It is believed that the Uster tester is sensitive to neps and trash, and this could be a possible explanation of the difference in average divisors obtained between these samples and the mixed-count samples. Also, the staple length of all samples was not known, and the divisor constant will change slightly with a change in staple length. From this test, it is concluded that to a first approximation per cent NU as measured on the Uniformity Analyzer can be divided by 4.8 to obtain per cent CV as observed on the Uster Quadratic Integrator.

Comparison of Filling Per Cent Nonuniformity and Fabric Appearance

A question frequently asked is "What relationship or correlation exists between evenness of yarn and fabric appearance?" Since it is believed that one of the prime objectives of an evenness tester is to help improve fabric appearance, an investigation was made of this question. This investigation includes a comparison of fabric filling per cent nonuniformity with fabric appearance of both a dyed chambray fab-

[2] These samples were surplus yarn from a 17 mill test.

ric and a grey printcloth (80 × 80). Both types of fabrics were included because a dyed chambray increases the contrast, which tends to make small differences more apparent.

Sixteen dyed chambray fabric samples, of which the per cent nonuniformity of the filling was known, were sent to member mills for ranking in order of appearance by cloth graders. These samples were woven on the same loom, and it was impressed upon the graders that the warp uniformity should not enter into their judgment since interest was only in the filling nonuniformity. Although such things as neps, twist, color, bulkiness, hairiness, etc. enter into fabric appearance, these samples were graded only on the basis of filling yarn uniformity or variations in weight per unit length. The fabric samples were ranked from best to poorest and the rankings given by the various graders are shown in Appendix II. The ranking correlation coefficients (p) were determined from Spearman's rank correlation formula and appear in Appendix II. These coefficients represent the ranking correlation between each grader and the per cent NU of the filling.

Several of the samples were very close in filling per cent NU, and this difference in per cent NU was not considered to be significant. Graders ranking these samples might easily rank them either way, in which case this would affect the ranking correlation whereas the samples were not significantly different in filling per cent NU. Because of this, 10 of the samples which were most evenly spaced as regards to filling per cent NU were chosen and new ranking correlation coefficients were determined. These figures appear in Appendix III, and it is noticed that a much higher degree of rank correlation is obtained.

In Spearman's Table of Critical Values of Rank-Correlation, the following significant rank correlation coefficients for the 99% confidence level are listed:

Sample Size (N)	99% Confidence Level
10	0.746
16	0.601

From this table, it is seen that all rank correlation coefficients obtained were significant and that there appears to be a definite correlation between fabric appearance and filling nonuniformity in the case of the blue chambray samples.

The comparison of filling nonuniformity and fabric appearance was further extended to include grey goods. Various carded and combed 30's yarns were analyzed for per cent NU and 10 samples covering a range of per cent NU from 70 to 123 in steps of approximately 5% NU were chosen. These samples were then woven into cloth and distributed to various mills for grading as before. The results obtained are shown in Appendix IV.

Spearman's Table of Critical Values of Rank Correlation lists 0.746 to be significant on the 99% confidence level for a sample size of 10 (N). Three of the 4 graders appear to be fairly high in significance, while the fourth one (Grader 1) is a borderline case. From the results of both the dyed chambray samples and gray goods samples, there appears to be a relationship between fabric appearance and per cent NU of the filling. On the average, approximately 3% NU difference could be noted in the dyed chambray samples and 5% NU difference in the gray goods samples.

Roving Characterization

A test similar to the yarn characterization test was run on roving to determine how precise an average the various testers gave from a group of randomly picked samples. From a group of 25 bobbins of 3.00 hank roving, 10 bobbins were chosen and run on each tester, using the recommended or commonly used sample length. A material speed of 20 yd/min was used on all testers except the Pacific, where 12 yd/min was used. A sensitive length of 10 ft was used in calculating the Uniformity Analyzer graphs and a 1-yd sensitive length was used for the Pacific.

The per cent coefficient of variation of the mean for each tester is shown in Table V. In this table, it can be seen that the Uster Linear Integrator with a sample length of 300 ft had the smallest per cent CV, or less spread in data. A reason for the higher per cent CV of the Pacific is probably that the recommended sample length per bobbin of only 75 ft is not sufficient.

TABLE V. Per Cent CV of Data Obtained in Roving Characterization Test

Tester	Sample Length (ft)	CV (%)
Uster Linear Integrator	300	0.67
Uniformity Analyzer Graph	500	0.87
Uster Quadratic Integrator	500	0.97
Fielden-Walker Integrator	500	1.14
Pacific Graph	75	1.47

TABLE VI. Correlation Coefficients Obtained in the Comparison and Correlation of Roving Measurements

Instrument	Correlation Coefficient (r)
Uster Graph—Uster Linear Integrator	0.859
Uniformity Analyzer Graph—Pacific Graph	0.768
Pacific Graph—Uster Linear Integrator	0.776
Fielden-Walker Graph—Pacific Graph	0.809
Uster Linear Integrator—Fielden-Walker Integrator	0.734
Pacific Graph—Uster Quadratic Integrator	0.764
Uster Quadratic Integrator—Fielden-Walker Integrator	0.656
Uster Linear Integrator—Uster Quadratic Integrator	0.570
Uniformity Analyzer Graph—Uster Linear Integrator	0.653
Pacific Graph—Uniformity Analyzer Graph	0.830
Uniformity Analyzer Graph—Uster Quadratic Integrator	0.858
Fielden-Walker Integrator—Uniformity Analyzer Graph	0.717

Comparison and Correlation of Roving Measurements

A group of roving samples representing various amounts and types of unevenness and covering a range of hank-roving size from 1.30 to 5.00 were run on the various testers for a comparison and correlation of roving measurements. The identical roving samples could not be run on each tester as was done in the case of yarn because of the handling and inevitable stretching of the roving; therefore, successive samples were taken from the same bobbin to be run on the different testers. Due to the intra-bobbin variations which occur within the bobbin, adequate sample lengths were run to keep these variations to a minimum. In the comparison of the Uster Linear Integrator and graph, both measurements were taken on the identical sample.

From the results obtained in this comparison correlation coefficients, prediction equations, and average multipliers were calculated between the various instruments. The coefficients of correlation computed are shown in Table VI and for a visual comparison typical correlation plots are shown in Figures 7 and 8. The various material speeds and sample lengths used with each instrument and the prediction equations and average multipliers calculated are listed in Appendix V.

From the correlation coefficients calculated (ranging from 0.656 to 0.859), it is seen that the roving measurements do not correlate as well as did the yarn measurements. Some possible explanations of this could be the different size roving slots (measuring heads) on the various testers, the form and fill factors of roving in the slots, and the twisting of roving while moving through the slot. Since a correlation coefficient of only 0.86 was found between the Uster Linear Integrator and graph using identical samples, it is believed that the same relationship that existed between peak to peak measurements and integrator measurements in yarn does not exist in roving measurements. An average multiplier of 5.57 was found to exist between the Uniformity Analyzer and Uster Quadratic Integrator roving measurements, whereas an average multiplier of 4.80 was found for the yarn measurements. Also, it was noticed that the correlation between the Pacific measurements and the other units was higher than in the

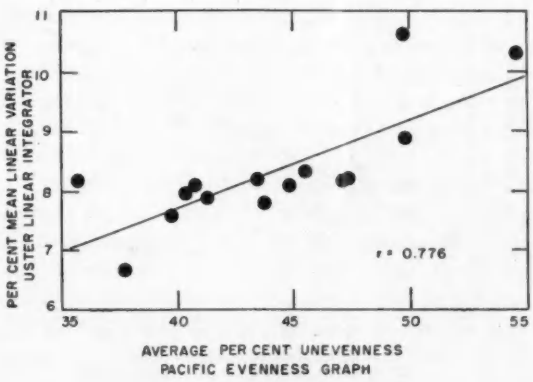

Fig. 7.

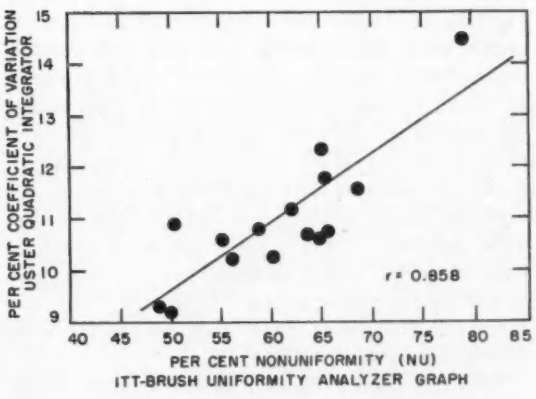

Fig. 8.

TABLE VII. Correlation Coefficients Obtained in the Comparison and Correlation of Sliver Measurements

Instrument	Correlation Coefficient (r)
Uniformity Analyzer Graph—Uster Quadratic Integrator	0.890
Uster Linear Integrator—Saco-Lowell Graph	0.037
Uster Linear Integrator—Uster Graph	0.643
Uster Linear Integrator—Fielden-Walker Integrator	0.072
Pacific Graph—Fielden-Walker Integrator	0.927
Pacific Graph—Uniformity Analyzer Graph (3′ S.L.)	0.960
Pacific Graph—Uniformity Analyzer Graph (10′ S.L.)	0.974
Uster Linear Integrator—Uniformity Analyzer Graph	0.033
Uniformity Analyzer Graph—Fielden-Walker Integrator	0.930
Uniformity Analyzer Graph—Saco-Lowell Graph	0.918
Uster Linear Integrator—Pacific Graph	0.203
Pacific Graph—Saco-Lowell Graph	0.973
Saco-Lowell Graph—Fielden-Walker Integrator	0.928

yarn comparison. The roving samples were not chewed up by the Pacific tester as were the yarn samples, and possibly there is insufficient mass in the finer cotton yarns on the Pacific for the high compressive forces used. From these results it appears that the Pacific tester is making the same type of measurement on roving as the capacitance testers.

Comparison and Correlation of Sliver Measurements

Ten sliver samples, of which 6 were card sliver, 2 breaker drawing sliver, and 2 finisher drawing sliver, were processed at the Institute and run on the various testers for a comparison of measurements. Experience in analyzing sliver at the Institute has shown that the nonuniformity of the sliver sample varies from the top of the can to the bottom due to "coiler head nonuniformity" which is caused by the sliver already in the can pressing up against the under side of the tube gear with sufficient force to draft the new sliver as it emerges from the tube gear. The samples were processed from partial laps from the 20-mill cleaning test and, in order to eliminate variations of the samples due to "coiler head nonuniformity," 300-ft samples were run from each partial lap for testing on each instrument. By only running a 300-ft sample into each can the sliver did not rise up to the tube gear.

From the results obtained in this comparison correlation coefficients, prediction equations and average multipliers were computed between the various testers. The correlation coefficients are shown in Table VII, and for a visual comparison typical correlation plots are shown in Figures 9 and 10. The various material speeds and sample lengths used with each instrument and the prediction equations and average multipliers calculated are listed in Appendix VI.

It was noticed from the results obtained that the highest correlation was found between the measurements of the Uniformity Analyzer and Pacific, Fielden-Walker, and Saco-Lowell testers. The measurements on the Uster Linear Integrator had very little spread and practically no correlation with the measurements made by the other instruments. Since sliver is very uniform in comparison with rov-

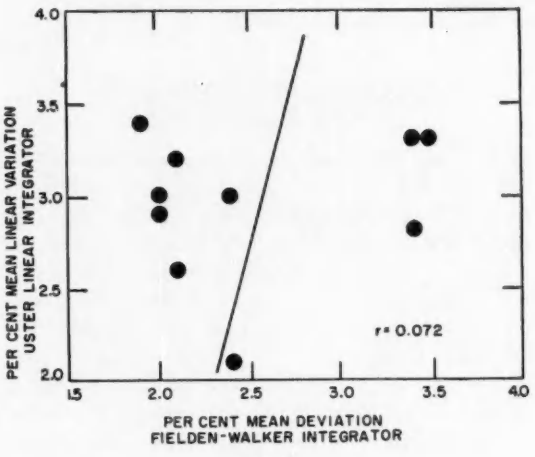

Fig. 9.

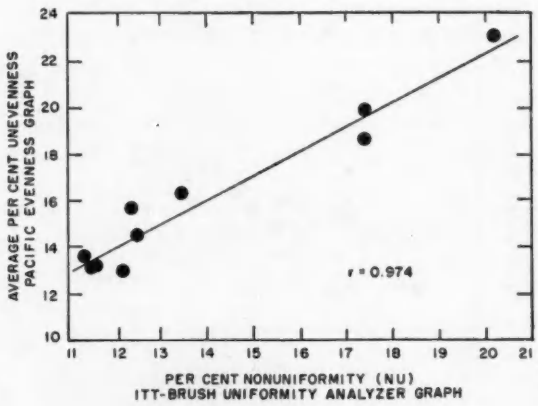

Fig. 10.

ing and yarn, it could be possible that the integrating instruments tend to average out the unevenness and show only small changes in sliver measurements, while the peak to peak type instruments are more sensitive in sliver measurement. This was also borne out previously in the roving comparison. From the results obtained in both the roving and sliver comparison of measurements, it appears that the peak to peak measuring instruments (Uniformity Analyzer, Pacific, and Saco-Lowell) are more sensitive to unevenness and correlate better than the integrating instruments in measuring roving and sliver unevenness.

Recorder Linearity Check

The electrical device which records the fluctuations of unevenness should be able to do so in a linear manner; i.e., all record fluctuations should be directly proportional to the corresponding sample unevenness. This feature is essential for accurate results and precision of reproducibility of measurements.

A series of tests was run on the various instruments to compare the recorder linearity and where applicable to compare the linearity of the meter scale which indicates average weight (such as Fiducial Mean of the Uniformity Analyzer and Average Value of the Uster) and is used as a correction factor in obtaining the corrected measurement. The relation between instrument output and both recorder chart divisions and the average weight scale was made on the Uniformity Analyzer, Uster, and Fielden-Walker testers. A typical plot of these values is shown in Figure 11. The recorder linearity of the Pacific tester was checked by varying the gage micrometer setting and noting the recorder chart displacement from center for each setting. In order to minimize errors in making the micrometer gage setting, 3 settings were made at each position and the average of these taken. This was performed at 3 magnification settings, and the family of curves obtained is shown in Figure 12.

The linear relationships of the instruments can be seen in Figures 11 and 12, a straight line indicating a linear relationship between the instrument output and its recorder or mean weight scale. From the results of this experiment it appears that the various recorders are absolutely linear with one or two points a little off at the extreme edges of the recorder on the Uniformity Analyzer and on the Pacific at 60 magnification.

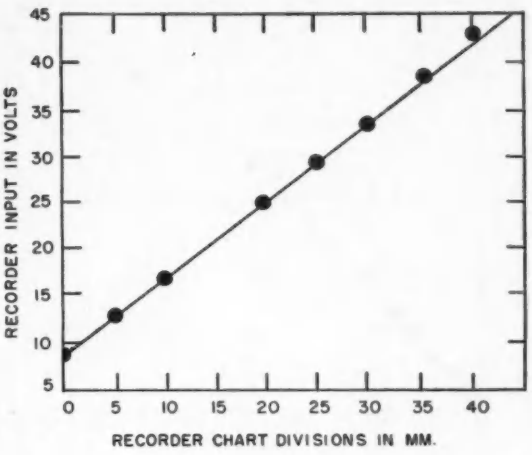

Fig. 11.

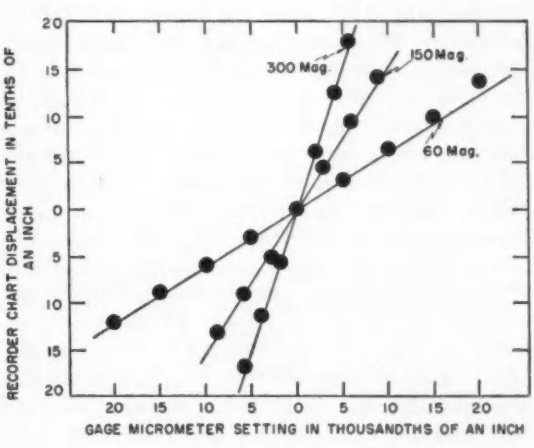

Fig. 12.

Zero Warm-Up Drift

To obtain accurate and reproducible results on an electronic tester, a warm-up period is generally needed to allow the tubes to become heat stable, at which time there would be no further drifting of the tester if it is not sensitive to temperature fluctuations. Some mills who use their testers daily make it a habit to leave the units on continuously, thereby eliminating this possibility of error being introduced.

A 4-hr zero warm-up drift check was run on all the applicable testers simultaneously to compare the minimum warm-up time for each tester to reach a stable operating condition. In order for all testers to have a comparable set-up in regard to gain or

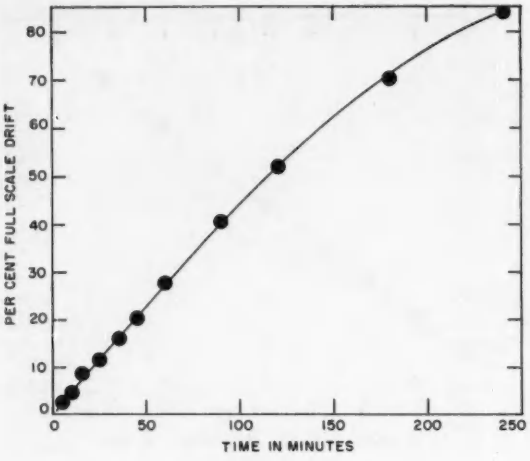

Fig. 13.

amplification, a 30's yarn was run on each the day before, and the various settings for midscale noted. All testers were turned on and allowed a 5-min warm-up in order that the tubes might stabilize enough to make an accurate zero setting. After 5 min the zeroes were set on each instrument and periodically the recorder was turned on and the time noted. The test was run in a closed room at a constant humidity of 60% R.H. No means were available to control the temperature and the temperature change was noted throughout the test. The results obtained are shown in Figures 13 through 17 in which per cent full scale deflection is plotted against time. After running the test, it was observed that a temperature rise of 15°F had occurred over the 4-hr period. This rise was attributed to a warm spring day, closed room, and 4 testers on at the same time.

From the graphs plotted it is seen that the Fielden-Walker and Pacific testers had practically no zero drift (1.2% full scale in both cases) while the Uniformity Analyzer and Uster testers did not stabilize over the entire 4-hr period. After analyzing these results, it was concluded that the Uniformity Analyzer and Uster Tester are both sensitive to temperature changes. In view of this, another test was run in the air-conditioned laboratory in which a Uniformity Analyzer was available. The results obtained are shown in Figure 17, and it is seen that a different situation exists. From the graph in Figure 17 it is noticed that an increase in per cent full-scale drift occurred at 60 min and then

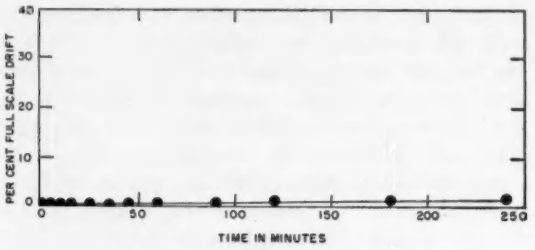

Fig. 14.

came back down and remained fairly constant. Temperature recordings were taken during the test, and at the 60-min time the temperature rose from 72°F to 74°F and then came back down to the constant temperature of 72°F for the remainder of the test.

In analyzing these results, it should be kept in mind that the amount of drift is not nearly as important as the time required to reach a stable operating point at which no further drifting occurs. From the results obtained, it appears that a 15-min warm-up period is adequate for the Fielden-Walker and Pacific testers. In the case of the Uniformity Analyzer and Uster tester, it is believed that a warm-up period of 1 hr is required for the tester to reach stability. This time was arrived at for the Uster tester by noting that in Figure 15 the curve flattened off at approximately 45 min. It also began dropping after 60 min, but this is believed to be due to the tester being sensitive to temperature changes in the room. The above times recommended may vary between testers, depending on the tube characteristics. From this test it is seen that both the Uniformity Analyzer and Uster tester are sensitive to temperature changes, and in view of this frequent zero checks should be made to obtain accurate results.

Summary and Conclusions

1. The precision of reproducibility of 10 successive runs of a 30's carded yarn sample on the various testers was found to be in the following order, with the highest precision first: Uniformity Analyzer graph, Uniformity Analyzer Automatic Evaluator, Uster graph, Uster Linear Integrator, Uster Quadratic Integrator, Fielden-Walker graph, Pacific graph, and Fielden-Walker Integrator.

2. The precision with which each tester could characterize the average unevenness of a number of

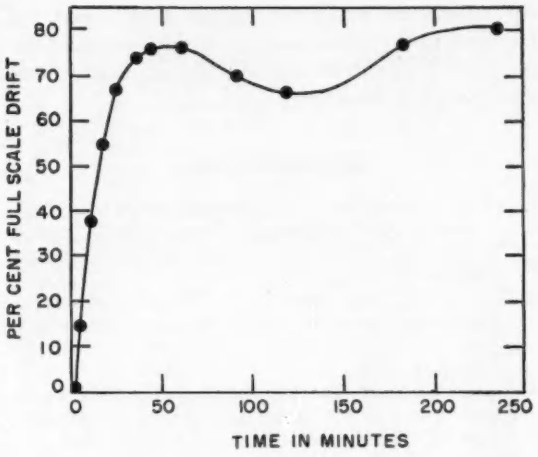

Fig. 15.

random bobbins from a large group of yarn bobbins was found to be in the following order, with the most precise instrument first: Uniformity Analyzer Automatic Evaluator, Fielden-Walker Integrator, Uster-Linear Integrator, Uster Quadratic Integrator, and Pacific graph.

3. In a test of a group of different yarn samples covering a wide range of uniformities, it was found that the results obtained from the various electronic testers showed almost perfect relationship between their measurements, while the results obtained on the Pacific tester showed the same general trends in uniformity measurements but to a lesser degree than the other.

4. The gain setting was found to have no significant effect on the precision of results of the various electronic testers except in the case of the Uster Quadratic Integrator where lower gains (negative average value) tended to give a higher per cent CV. The effect of gage micrometer and magnification setting on yarn measurements was investigated on the Pacific tester, and it was found that gage setting had no significant effect but that the *E*-magnification setting gave a lower result in every case.

5. Yarn speed was found to have an effect on the precision of yarn measurements on the Fielden-Walker graph, Uniformity Analyzer graph, and Uster Quadratic Integrator. No effect was found on the remaining instruments.

6. It was found that, to a first approximation, the yarn per cent CV as obtained on the Uster Quadratic

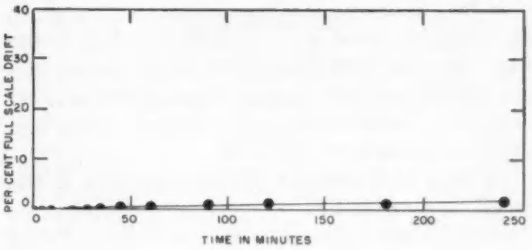

Fig. 16.

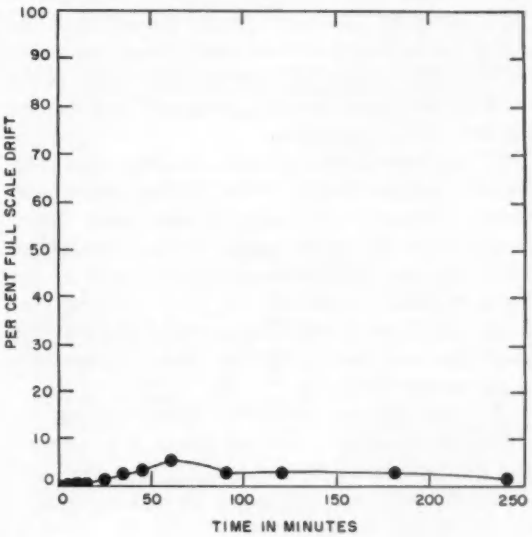

Fig. 17.

Integrator can be multiplied by 4.8 to obtain yarn per cent NU.

7. In a comparison of filling per cent NU and fabric appearance on both dyed chambray and gray goods samples, there appeared to be a correlation or relationship between these two qualities. On the average, approximately 3% NU difference could be noted in the dyed chambray samples and 5% NU difference in the gray goods samples.

8. The precision with which each tester could characterize the average unevenness of a number of random bobbins from a large group of roving bobbins was found to be in the following order, with the most precise instrument first: Uster Linear Integrator, Uniformity Analyzer graph, Uster Quadratic Integrator, Fielden-Walker Integrator, and Pacific graph.

9. In a comparison of measurements of a group of roving samples of varying uniformity, it was found that the results obtained from the various testers showed the same general trends; however, the degree of correlation was not as high as obtained in the yarn comparison.

10. In a comparison of 10 sliver samples, it was found that the results obtained on the Uniformity Analyzer, Pacific, Saco-Lowell, and Fielden-Walker showed a high degree of correlation, while the results of the Uster Linear Integrator showed almost no correlation with the results of the other testers.

11. Recorder Linearity checks showed that the various instruments are absolutely linear with one or two points a little off at the extreme edges of the recorder on the Uniformity Analyzer and on the Pacific at 60 magnification.

12. In a test to determine the minimum warm-up time for precise results on the various testers containing electronic equipment, it was found that a 15-min warm-up period appears to be adequate for the Pacific and Fielden-Walker testers while a 1-hr warm-up period is necessary for the Uniformity Analyzer and Uster testers. It was found that both the Uniformity Analyzer and Uster testers are sensitive to temperature changes.

13. From the results of this thesis and the experience in running the various testers, it is believed that the capacitance type testers (Uniformity Analyzer and Uster) are best suited for measuring yarn unevenness and the compression type tester (Pacific) is best suited for measuring roving and sliver unevenness. These conclusions were based on the following points:

a. The capacitance type testers are superior for yarn testing because of their precision, speed, ease of running, and nondamaging effect on yarn being run.

b. The compression type tester is superior for testing roving and sliver because of its ease of operation, nonloading of measuring head, negligible effect of uneven regain, and control limit pens available for quality control of evenness and size variation.

Acknowledgment

The author wishes to express his appreciation to Dr. Edwin J. Bernet for his interest and assistance in carrying out this investigation. Thanks are also expressed to Brush Electronics Company and member mills from which the various testers were on loan and to the manufacturers of the evenness testers used for contributing instruction manuals and other pertinent literature.

Literature Cited

1. ASTM Committee D-13, Subcommittee B-1, Task Group for the Evaluation of Yarn Evenness Testers, *Report No. 1, Preliminary Study of Yarn Evenness Testers,* October, 1952.
2. Fiori, L. A., and Oser, L. F., "The Importance of Correcting Range Values on the Uster Uniformity Tester," *Textile Industries* **116**, 149, 151, 153, 169 (January, 1952).
3. Foster, G. A. R., and Martindale, J. G., "The Form and Length of the Drafting Wave in Cotton Rovings," *J. Textile Inst.* **37**, T1–12 (1946).
4. Mullen, P. W., "The Current Story on Evenness Testing," *Textile Industries* **117**, 118–135 (July, 1953).
5. Sanborn, M. A., "Irregularity in Textile Yarns and Strands, a Literature Survey," TEXTILE RESEARCH JOURNAL **24**, 86–96 (January, 1954).
6. Tippett, L. H. C., *The Methods of Statistics,* 3rd ed., London, Williams and Norgate, 1941.
7. West, A. E., "Instrumentation in Quality Control," *Proceedings of the Spring Meeting of Textile Quality Control Association,* 80–93 (April, 1952).

Appendix I: Prediction Equations and Average Multipliers Calculated in the Comparison and Correlation of Yarn Measurements

Prediction Equation	Average Multiplier*
$A = 0.95B + 4.6$	0.99
$B = 1.05A - 4.6$	1.01
$A = 4.15C + 13.6$	4.80
$C = 0.23A - 2.2$	0.21
$B = 4.40C + 8.8$	4.82
$C = 0.22B - 1.3$	0.21
$C = 1.22D + 1.0$	1.28
$D = 0.80C - 0.3$	0.78
$B = 5.39C + 12.8$	6.17
$C = 0.18B - 1.4$	0.16
$A = 5.05D + 17.9$	6.15
$D = 0.18A - 2.0$	0.16
$A = 5.55E + 19.3$	6.87
$E = 0.17A - 2.6$	0.14
$B = 5.91E + 14.4$	6.90
$E = 0.16B - 1.9$	0.14
$C = 1.30E + 1.9$	1.43
$E = 0.72C - 0.5$	0.70
$D = 1.04E + 1.1$	1.12
$E = 0.89D$	0.89
$A = 1.34F + 33.2$	2.00
$F = 0.53A - 3.4$	0.50
$B = 1.44F + 28.7$	2.01
$F = 0.52B - 6.2$	0.50
$C = 0.33F + 4.5$	0.42

Appendix I (Cont.)

Prediction Equation	Average Multiplier*
$F = 2.35C + 1.0$	2.40
$D = 0.25F + 3.8$	0.32
$F = 2.76D + 5.1$	3.07
$E = 0.24F + 2.4$	0.29
$F = 3.15E + 4.1$	3.43
$G = 7.36D - 5.9$	6.90
$D = 0.13G + 0.8$	0.14

* Results from tester on right side of equation times average multiplier equals results to be expected on tester in left side of equation.

Code	Sample Length (ft)	Yarn Speed (yd/min)
A = Uniformity Analyzer Graph.	1000	100
B = U. A. Automatic Evaluator.	1000	100
C = Uster Quadratic Integrator.	1000	100
D = Uster Linear Integrator.	1000	100
E = Fielden-Walker Integrator.	1000	20
F = Pacific Graph.	300	12
G = Uster Graph.	90	4

Appendix II: Ranking Correlation Data between Fabric Appearance and Per Cent Nonuniformity of Filling (Blue Chambray, 80 × 80, 30's Filling)

Filling (% NU)	Rankings			
	Grader 1	Grader 2	Grader 3	Grader 4
81.6	1	1	1	1
84.0	2	2	2	2
96.7	3	3	3	3
101.4	11	7	8	4
104.2	6	6	4	6
105.4	4	13	6	7
105.8	5	4	5	8
108.0	10	11	11	5
108.4	7	8	7	10
110.3	8	14	13	9
113.6	13	10	12	11
114.5	14	5	14	14
115.1	12	9	10	12
117.8	9	12	9	13
121.1	15	15	15	15
127.9	16	16	16	16
Spearman's Ranking Coefficient (p)	0.85	0.76	0.88	0.97

Appendix III: Ranking Correlation Data between Fabric Appearance and Per Cent Nonuniformity of Filling (Blue Chambray, 80 × 80, 30's Filling)

Filling (% NU)	Rankings			
	Grader 1	Grader 2	Grader 3	Grader 4
81.6	1	1	1	1
84.0	2	2	2	2
96.7	3	3	3	3
101.4	7	5	4	4

Appendix III (Cont.)

Filling (% NU)	Rankings			
	Grader 1	Grader 2	Grader 3	Grader 4
105.8	5	4	5	5
108.4	4	7	7	6
113.6	8	8	8	7
117.8	6	6	6	8
121.1	9	9	9	9
127.9	10	10	10	10
Spearman's Ranking Correlation Coefficient (p)	0.89	0.95	0.96	1.00

Appendix IV: Ranking Correlation Data between Fabric Appearance and Per Cent Nonuniformity of Filling (Grey Printcloth, 80 × 60)

Filling (% NU)	Ranking			
	Grader 1	Grader 2	Grader 3	Grader 4
70.6	4	1	1	1
80.6	2	2	2	2
85.7	1	4	5	3
94.9	3	3	3	4
101.3	8	6	6	5
105.5	5	8	4	6
111.9	9	7	9	10
116.3	6	5	7	8
121.9	10	9	10	7
123.3	7	10	8	9
Spearman's Ranking Correlation Coefficient (p)	0.745	0.903	0.879	0.915

Appendix V: Prediction Equations and Average Multipliers Calculated in the Comparison and Correlation of Roving Measurements

Prediction Equation	Average Multiplier*
$C = 0.22F + 1.46$	0.25
$F = 2.69C + 14.44$	4.00
$C = 0.15A + 1.96$	0.18
$A = 4.99C + 6.35$	5.57
$H = 0.57A + 23.74$	0.96
$A = 1.03H + 0.88$	1.04
$D = 0.39C + 4.08$	0.76
$C = 0.84D + 4.02$	1.32
$E = 0.20F + 0.88$	0.22
$F = 3.25E + 12.43$	4.53
$A = 1.37F + 0.99$	1.39
$F = 0.50A + 13.38$	0.72
$E = 0.11A + 3.11$	0.16
$A = 4.76E + 15.03$	6.31
$G = 7.92D - 13.00$	6.32
$D = 0.09G + 3.35$	0.16
$D = 0.08A + 3.68$	0.14
$A = 5.60D + 14.64$	7.36
$D = 0.15F + 1.73$	0.19
$F = 4.02D + 10.52$	5.28
$E = 0.58C + 3.39$	0.88

Appendix V (Cont.)

Prediction Equation	Average Multiplier*
$C = 0.75E + 3.74$	1.13
$D = 0.57E + 2.80$	0.86
$E = 0.95D + 1.83$	1.17

* Results from tester on right side of equation times average multiplier equals result to be expected on tester in left side of equation.

Code	Sample Length (ft)	Material Speed (yd/min)
A = Uniformity Analyzer Graph.	500	20
C = Uster Quadratic Integrator.	500	20
D = Uster Linear Integrator.	500	20
E = Fielden-Walker Integrator.	500	20
F = Pacific Graph (1 yd S.L.).	300	12
G = Uster Graph.	90	4
H = Pacific Graph (10′ S.L.).	300	12

Appendix VI: Prediction Equations and Average Multipliers Calculated in the Comparison and Correlation of Sliver Measurements

Prediction Equation	Average Multiplier*
$D = 0.01A + 2.78$	0.21
$A = 0.27D + 13.14$	4.71
$E = 0.19A - 0.13$	0.18
$A = 4.53E + 2.52$	5.53
$F = 1.18A - 5.71$	0.77
$A = 0.78F + 5.57$	1.30
$H = 1.03A + 1.71$	1.15
$A = 0.92H - 0.84$	0.88
$F = 0.64I + 1.42$	0.74
$I = 1.48F - 1.34$	1.36

Appendix VI (Cont.)

Prediction Equation	Average Multiplier*
$E = 0.10I + 1.04$	0.17
$I = 8.47E - 6.78$	5.87
$D = 0.002I + 2.92$	0.20
$I = 0.57D + 12.87$	4.92
$G = 5.44D - 1.32$	4.84
$D = 0.086G + 1.39$	0.21
$E = 0.12D + 2.16$	0.85
$D = 0.42E + 2.85$	1.17
$H = 5.56E - 3.27$	4.26
$E = 0.15H + 0.87$	0.24
$A = 0.49I + 6.81$	0.96
$I = 1.72A - 9.42$	1.04
$H = 2.04D + 4.70$	3.63
$D = 0.02H + 2.74$	0.28
$A = 8.74C - 13.65$	5.66
$C = 0.09A + 2.14$	0.18

* Results from tester on right side of equation times average multiplier equals results to be expected on tester in left side of equation.

Code	Sample Length (ft)	Material Speed (yd/min)
A = Uniformity Analyzer Graph.	250	20
C = Uster Quadratic Integrator.	250	10
D = Uster Linear Integrator.	250	20
E = Fielden-Walker Integrator.	250	20
F = Pacific Graph (1 yd S.L.).	250	12
G = Uster Graph.	90	4
H = Pacific Graph (10′ S.L.).	250	12
I = Saco-Lowell Graphic Sliver Tester.	90	1

Manuscript received October 22, 1954.

Stress-Strain Relationships in Yarns Subjected to Rapid Impact Loading

Part III. Effect of Wave Propagation [1,2]

Jack C. Smith, Frank L. McCrackin, and Herbert F. Schiefer

Textiles Section, National Bureau of Standards

Abstract

The tensile behavior of a Hookean material elongated by rapid impact at one end has been calculated, using a theory in which wave propagation is considered. As a result of these calculations, limits have been established on the applicability of a simpler theory, discussed in a preceding publication, in which wave propagation was neglected.

I. Introduction

When a filament of uniform cross section is clamped at each end and rapidly elongated, data for a stress-strain curve can be obtained by measuring the force at one end and the elongation of the whole filament, both as functions of the time. In this case the assumption is made that stresses and strains in the filament are uniform along the length and can be represented by the stresses measured at an end and by the average elongations. This assumption is no longer valid when the rate at which the filament is lengthened approaches in order of magnitude the velocity of propagation of a tension wave along the filament.

In previous work [1] this effect of wave propagation was disregarded. It is the purpose here to determine how previously obtained results must be reinterpreted as a result of the wave-propagation effect.

II. Wave Theory

Consider a filament lying along the negative x-axis, with one end at the origin and the other end fixed at the point $x = -L$. At time $t = 0$ and subsequently, the end at $x = 0$ is constrained to move with velocity v_0 in the positive direction. Assume that the tensile behavior is in accordance with Hooke's law. Then, after impact, a strain pulse of magnitude $\epsilon_0 = v_0/c$ is propagated down the filament with a velocity c. When the pulse is reflected at the fixed end, the strain is increased to $2\epsilon_0$. A similar increase takes place at each reflection.

This behavior is shown in Figure 1, in which the strains at several points along the filament are plotted as functions of the time. The strains are thus seen to vary discontinuously with time. These discontinuous increases in the strain become more pronounced as v_0 is increased. If we require that ϵ_0 be less than 1% in order that wave-propaga-

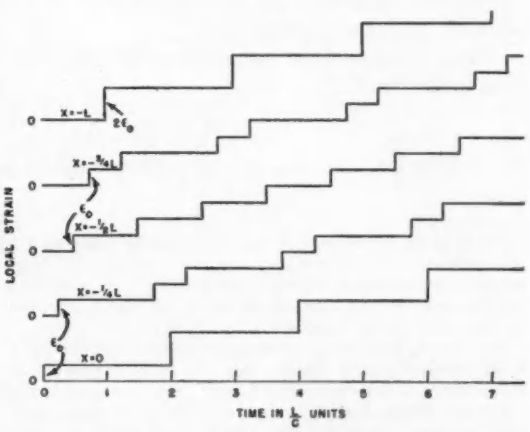

Fig. 1. Local strain vs. time for a filament clamped at $x = -L$ and rapidly elongated at $x = 0$ at velocity v_0.

[1] Presented in part at the November 1954 meeting of the Society of Rheology. Parts I and II of this article appeared in the June 1955 issue of the TEXTILE RESEARCH JOURNAL.

[2] Permission to publish this paper has been granted by the Office of the Quartermaster General, Department of the Army, which has sponsored and supported this work as a part of a broad and long-term fundamental program of research on textile materials.

tion effects in most textile fibers may be safely disregarded, we must limit v_0 to values less than $0.01c$, which in the case of high-tenacity nylon is approximately 25 m/sec.

In the present experimental method a filament is terminated at $x = -L$ by a mass nw where n is a number and w is the mass of the filament. At $x = 0$ the filament is terminated by a mass so large that its momentum will be practically unchanged by reaction forces from the filament and attached mass. At time $t = 0$ the head mass is given a velocity v_0. The behavior of the system is recorded photographically [2]. The data of interest are the elongation of the filament and the reaction force applied to the filament at the tail mass, both as functions of time. From these data the experimental stress-strain curve is constructed.

The theoretical behavior of this system, when Hooke's law applies,[3] is most easily calculated by finding suitable solutions of the wave equation:

$$\partial^2 u/\partial t^2 = c^2(\partial^2 u/\partial x^2) \qquad (1)$$

In this equation, t is the time variable and x denotes the position of a cross section of the filament relative to fixed coordinates when the filament is in the unstrained state; $u\,(x,t)$ denotes the distance the cross section has moved from its original position at x; and c is the velocity of propagation of an elastic tension wave along the filament.

$$c = \sqrt{E/\rho}$$

where E = Young's modulus of elasticity for the unstrained filament, and ρ = the density of the unstrained filament material.

These solutions must satisfy the boundary condition at the head:

$$u(0,t) = v_0 t \qquad (2)$$

A suitable solution (for the unreflected wave) is given by:

$$\begin{aligned} u\,(x,t) &= 0 && \left(t + \frac{x}{c} \leqslant 0\right) \\ &= v_0\left(t + \frac{x}{c}\right) && \left(t + \frac{x}{c} > 0\right) \\ \epsilon\,(x,t) &= \frac{\partial u}{\partial x} = 0 && \left(t + \frac{x}{c} \leqslant 0\right) \\ &= \frac{v_0}{c} && \left(t + \frac{x}{c} > 0\right) \end{aligned} \qquad (3)$$

where u represents a wave of velocity c travelling along the filament in the minus x direction, and ϵ is the local strain or increase in length per unit length set up in the filament in the wake of the wave. It should be noted that both u and ϵ are equal to zero for values of $t < |x|/c$; i.e., no strain or displacement is present at a point in advance of the wave.

When the wave arrives at the end of the filament it is reflected and travels back in the positive direction. The strain between the reflected wave front and the tail mass is represented as the sum of the strains caused by the incident and reflected waves. If the tail end of the filament were fixed, this strain would be $2\epsilon_0$. However, since the tail mass can move, this strain, initially $2\epsilon_0$ at reflection, will decrease with time. The rate of decrease depends upon the tail mass and upon the order of the reflection, i.e., whether it is the first or a subsequent reflection. Reflections also occur at the head mass. A different solution of the wave equation is required to describe the state of the filament after each reflection. The first 10 of these solutions are tabulated in Appendix I.

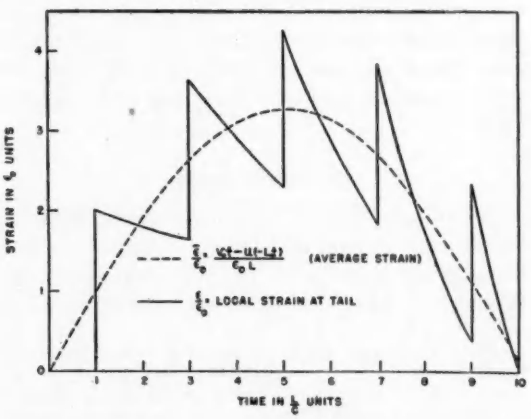

Fig. 2. Strain-time curves for a filament loaded at the tail with a mass $10w$ and rapidly elongated at the head at velocity v_0.

[3] The stress-strain behavior of most textile fibers may be described by Hooke's law only for small strains. At larger strains, the solutions derived here provide only rough approximations to the behavior of an actual textile fiber but are adequate for the purposes of this theory.

In order to take into account the significant reduction in cross-sectional area of the filament for the finite strains considered here, it is assumed that Hooke's law is obeyed in such a way that the product of Young's modulus and cross-sectional area remains constant. The small effect of mass motion associated with the lateral contraction has been neglected.

Using these solutions it is possible to calculate curves of average strain vs. time, and local strain vs. time. These curves are given in Figure 2 for the case where the tail has a mass of $10w$ ($n = 10$). The curve of local strain, $\epsilon(-L,t)$, vs. time is jagged, the decrease in ϵ between successive reflections becoming greater with each reflection.

Since the force at the tail, which is found experimentally from the acceleration of the tail mass, is proportional to the strain at the tail, it is possible to construct a theoretical stress-strain curve of local tail stress (strain) vs. average strain. Such a curve is given in Figure 3. Experimental curves are similar to this curve in that they show dips in the vicinity of maximum stress. There is also a delay in the initial rise of stress by the time it takes for the tension wave to be propagated to the tail mass.

III. Theory, Neglecting Wave Propagation[4]

A solution, applicable at low testing speeds, can be obtained by disregarding wave propagation along the filament and assuming the mass of the filament to be concentrated partly at the tail and partly at the head. The resulting solution, derived in Appendix II, is:

$$u = \epsilon_0 L[\theta - \sqrt{n'}\sin(\theta/\sqrt{n'})] \quad (4)$$

$$[\epsilon/\epsilon_0] = \sqrt{n'}\sin(\theta/\sqrt{n'}) \quad (5)$$

[4] For convenience we shall frequently refer to this theory as the nonwave theory.

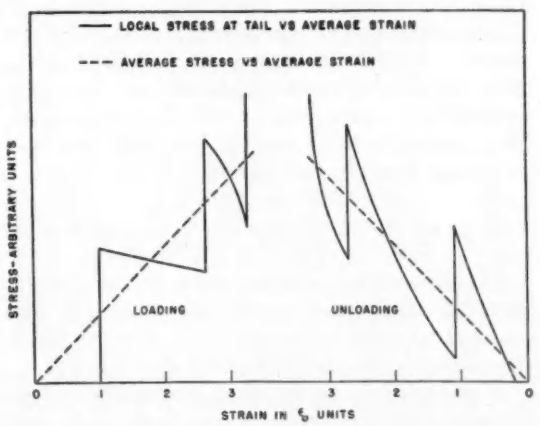
LOCAL STRESS AT TAIL VS AVERAGE STRAIN
AVERAGE STRESS VS AVERAGE STRAIN
STRESS-ARBITRARY UNITS
LOADING
UNLOADING
0 1 2 3 3 2 1 0
STRAIN IN ϵ_0 UNITS

Fig. 3. Stress-strain curves for a filament loaded with tail mass $10w$ and rapidly elongated at the head at velocity v_0.

where

$$\theta = (c/L)t$$
$$\epsilon_0 = v_0/c$$

and

$$n' = n + f$$

f is the fraction of the filament mass assumed concentrated at the tail.

It is helpful to think of θ as time expressed in L/c units. Likewise, one can think of $[\epsilon/\epsilon_0]$ as strain expressed in ϵ_0 units. ϵ_0 and c here have only formal significance in order to put the solution in a form analogous to that obtained when wave propagation is considered.

IV. Comparison of Wave Theory with Theory Neglecting Wave Propagation

Plots of $[\epsilon/\epsilon_0]$ vs. θ for values of $n' = 10$, 10 1/2, and 11 are shown in Figure 4. Values of $\bar{\epsilon}/\epsilon_0$ have also been computed from the wave theory for the case $n = 10$, using the formula:

$$\bar{\epsilon}/\epsilon_0 = v_0 t - u(-L,t)/\epsilon_0 L$$
$$= \theta - (c/Lv_0)u(-L,t) \quad (6)$$

These points are plotted as circles and are seen to fit best to the curve drawn for $n' = 10\ 1/2$. This indicates that for a mass ratio of 10, the nonwave theory results agree most closely with those for the wave theory when half the mass of the filament is assumed concentrated at each end ($f = 1/2$).

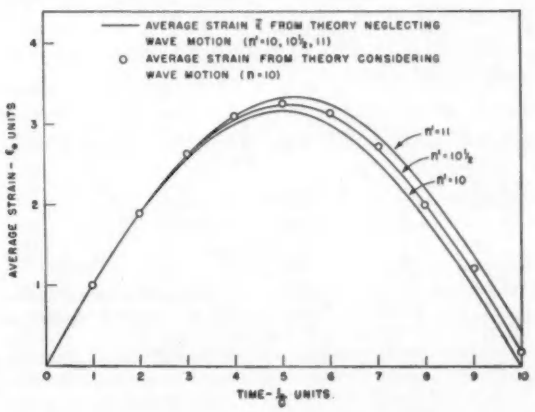
AVERAGE STRAIN $\bar{\epsilon}$ FROM THEORY NEGLECTING WAVE MOTION (n'=10, 10½, 11)
AVERAGE STRAIN FROM THEORY CONSIDERING WAVE MOTION (n=10)
n'=11
n'=10½
n'=10
AVERAGE STRAIN - ϵ_0 UNITS
0 1 2 3 4 5 6 7 8 9 10
TIME - $\frac{L}{c}$ UNITS

Fig. 4. Strain-time curve for filament loaded with tail mass $10w$, according to the wave theory, and according to the theory neglecting wave propagatives.

According to the nonwave theory, the maximum average strain which can be obtained in a filament is given by:

$$[\epsilon/\epsilon_0]_{max} = \sqrt{n+f} = \sqrt{n+1/2} \qquad (7)$$

and this strain is obtained when

$$\theta_m = (c/L)t = (\pi/2)\sqrt{n+1/2}$$

or

$$t_m = (\pi/2)(L/c)\sqrt{n+1/2} \qquad (8)$$

This suggests that the maximum average strain $\bar{\epsilon}/\epsilon_0$ as computed by the wave theory is approximately equal to $\sqrt{n+1/2}$ and occurs for a value of θ_m approximately equal to $(\pi/2)\sqrt{n+1/2}$. That this is a good approximation is demonstrated in Table I.

According to the nonwave theory (Appendix II):

$$\log v_n = -1/2 \log (n+1/2) + \log \sqrt{\frac{2}{\rho}\int_0^{\epsilon_r} \sigma d\epsilon} \qquad (9)$$

where v_n is the lowest impact velocity to cause rupture in a filament to which a tail mass nw is attached. σ is the tensile stress expressed as force divided by the cross-sectional area of the unstrained filament, and ϵ_r is the strain at which rupture occurs.

If the values of ϵ_r and σ are independent of the rate of elongation, then $\log \sqrt{\frac{2}{\rho}\int_0^{\epsilon_r} \sigma d\epsilon}$ will be a constant and the plot of $\log v_n$ vs. $\log (n+1/2)$ will be a straight line of slope $-1/2$.[5]

When $\log (n+1/2)$ is zero we have the extrapolated velocity:

$$v_b = \sqrt{\frac{2}{\rho}\int_0^{\epsilon_r} \sigma d\epsilon} \qquad (10)$$

When Hooke's law applies, we have

$$v_b = \sqrt{(E/\rho)\epsilon_r^2} \qquad (11)$$

[5] At high rates of straining, the value of ϵ_r for an actual textile fiber is less than that obtained at conventional testing rates. Also, the slope of the stress-strain curve is greater at higher rates of straining. However, for rates of straining of the same order of magnitude, these changes are small and tend to cancel each other out. Consequently, the area under the stress-strain curve, or rupture energy density in the filament, should be essentially constant for rates of straining corresponding to impact velocities near the limiting breaking velocity.

TABLE I. Values of Maximum Average Strain and Position of Maximum Average Strain as Computed by the Wave Theory and by the Nonwave Theory

	Maximum Average Strain		Position	
	Wave Theory	Nonwave Theory	Wave Theory	Nonwave Theory
n	$\frac{\bar{\epsilon}}{\epsilon_0}$	$\sqrt{n+1/2}$	θ_m	$\frac{\pi}{2}\sqrt{n+1/2}$
2	1.61	1.58	2.39	2.48
5	2.39	2.34	3.59	3.68
10	3.26	3.24	5.10	5.08
25	5.13	5.05	7.90	7.93

According to the wave theory $\sqrt{E/\rho}$ is the velocity of propagation c of an elastic tension wave along the filament and thus:

$$v_b = c\epsilon_r \qquad (12)$$

the velocity just sufficient to cause immediate rupture at $x = 0$.

We call this velocity, defined by equation (10), the limiting breaking velocity. The concept of a limiting breaking velocity has been discussed previously [1].

As an example, consider a Hookean material for which $\epsilon_r = 0.12$, and $c = 2500$ m/sec. From equation (7) for the case of rupture we have

$$\epsilon_r = \epsilon_0\sqrt{n+1/2} = (v_n/c)\sqrt{n+1/2}$$

or

$$v_n = c\epsilon_r/\sqrt{n+1/2} \qquad (13)$$

In Figure 5 are plotted values of v_n computed from these assumed values of ϵ_r and c. The result is a straight line giving an extrapolated value of 300 m/sec as the limiting breaking velocity.

The breaking velocities have also been calculated on the basis of the more exact theory in which wave motion is considered and Hooke's law is assumed. Average strains are calculated from equation (6), and the breaking velocities are then computed from the formula:

$$v_n = \frac{c\epsilon_r}{[\bar{\epsilon}(n)/\epsilon_0]_{max}} \qquad (14)$$

These results are also plotted in Figure 5. It is seen that these breaking velocities for a Hookean material of constant ϵ_r are lower (for small n's) than those predicted by the nonwave theory.

In actuality the strain at a given point along the filament does not change continuously with time but increases suddenly by an amount ϵ_0 when one of the strain pulses passes through the point.

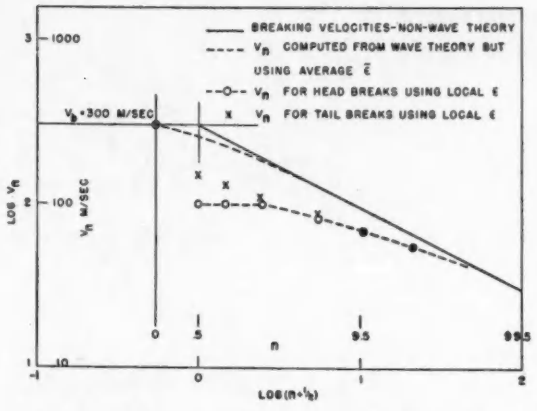
BREAKING VELOCITIES-NON-WAVE THEORY
V_n COMPUTED FROM WAVE THEORY BUT USING AVERAGE $\bar{\epsilon}$
V_n FOR HEAD BREAKS USING LOCAL ϵ
V_n FOR TAIL BREAKS USING LOCAL ϵ
V_b = 300 M/SEC
LOG V_n
V_n M/SEC
n
LOG(n+½)

Fig. 5. Breaking velocities for a hypothetical specimen, as computed by the wave theory, and by the theory neglecting wave propagation.

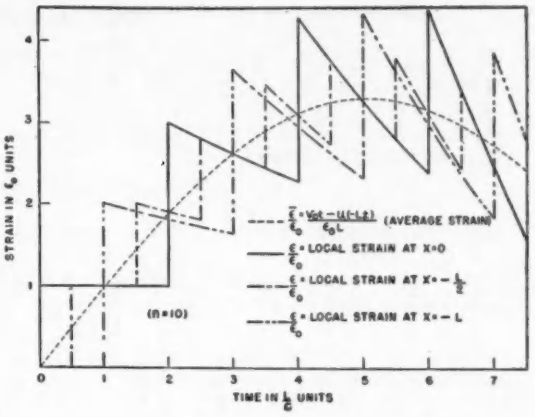

Fig. 6. Local strain-time curves for a filament loaded with a tail mass $10w$.

Rupture then occurs whenever the local strain exceeds the rupture strain.

In Figure 6 are plotted local strains at the head, tail, and midpoint for a filament loaded with a tail mass $10w$ ($n = 10$). Note here that maximum strain occurs at the head on the third reflection ($\theta = 6$). This corresponds to a lowest breaking velocity of 68.6 m/sec.

Increases in the local strain always occur first upon reflection at either the head or the tail. Increases in the local strain at an intervening point occur later, but these strains never exceed the head or tail strains in magnitude. For this reason it is to be expected that a uniformly strong filament will break only at the ends.

If the maximum values of local strains $[\epsilon/\epsilon_0]_{max}$ are substituted into equation (14), the lowest breaking velocities, v_n, for head and tail breaks can be computed. These breaking velocities, also plotted in Figure 5, are seen to be the lowest of all.

The curves of local strains vs. time for an actual material having approximately the properties chosen for this example would not be as jagged as those shown in Figure 6 for an ideal Hookean material. Thus the velocities found experimentally for this actual material could be expected to lie between the bounds established in Figure 5 by the curve of the velocities computed from average strains in the filament and the curve of velocities computed from the extreme local strains at the head or tail of the filament. The breaking velocities computed by any of the methods considered are the same when n is greater than 50. It is thus possible, in this example, to determine a limiting breaking velocity by extrapolation of experimental data taken with n greater than 50, provided ϵ_r remains constant and Hooke's law applies. This criterion also applies provided the energy density at rupture for the material remains nearly constant at the impact velocities used for determination of the limiting breaking velocity.

In the example just considered, the breaking velocity for $n = 50$ is 42 m/sec. A tensile impact at this velocity produces a strain pulse of $\epsilon_0 = 1.6\%$. This suggests a criterion applicable to any textile fiber for which the energy density at rupture remains nearly constant at high strain rates. For such a fiber a limiting breaking velocity may be found by extrapolation of experimental data taken such that all v_n's used are less than $0.02c$, where c is the velocity of propagation of the tensile strain pulse along the sample for the material tested.

V. Summary and Conclusions

When the stress-strain characteristics of a textile fiber are measured at longitudinal impact rates exceeding 10 m/sec the effects of tension-wave propagation along the fiber must be considered. These initial and reflected waves cause the local strains to vary with time in a stepwise fashion. The average strain in the filament, which is the quantity measured experimentally, does not adequately represent the state of strain under these

TABLE II. Displacement Function

$$u = u_0 + u_1 + u_2 + u_3 + \cdots$$

$$\tau = n\frac{L}{c}$$

u	z
$u_0 = v_0 z_0$	$z_0 = t + \frac{x}{c}$
$u_1 = v_0 z_1 - 2v_0\tau[1 - e^{-(z_1/\tau)}]$	$z_1 = t - \frac{2L}{c} - \frac{x}{c}$
$u_2 = -v_0 z_2 + 2v_0\tau[1 - e^{-(z_2/\tau)}]$	$z_2 = t - \frac{2L}{c} + \frac{x}{c}$
$u_3 = -v_0 z_3 + 4v_0\tau\left[1 - \left(1 + \frac{z_3}{\tau}\right)e^{-(z_3/\tau)}\right]$	$z_3 = t - \frac{4L}{c} - \frac{x}{c}$
$u_4 = v_0 z_4 - 4v_0\tau\left[1 - \left(1 + \frac{z_4}{\tau}\right)e^{-(z_4/\tau)}\right]$	$z_4 = t - \frac{4L}{c} + \frac{x}{c}$
$u_5 = v_0 z_5 - 6v_0\tau\left[1 - \left(1 + \frac{2}{3}\frac{z_5}{\tau} + \frac{2}{3}\frac{z_5^2}{\tau^2}\right)e^{-(z_5/\tau)}\right]$	$z_5 = t - \frac{6L}{c} - \frac{x}{c}$
$u_6 = -v_0 z_6 + 6v_0\tau\left[1 - \left(1 + \frac{2}{3}\frac{z_6}{\tau} + \frac{2}{3}\frac{z_6^2}{\tau^2}\right)e^{-(z_6/\tau)}\right]$	$z_6 = t - \frac{6L}{c} + \frac{x}{c}$
$u_7 = -v_0 z_7 + 8v_0\tau\left[1 - \left(1 + \frac{z_7}{\tau} + \frac{1}{3}\frac{z_7^3}{\tau^3}\right)e^{-(z_7/\tau)}\right]$	$z_7 = t - \frac{8L}{c} - \frac{x}{c}$
$u_8 = v_0 z_8 - 8v_0\tau\left[1 - \left(1 + \frac{z_8}{\tau} + \frac{1}{3}\frac{z_8^3}{\tau^3}\right)e^{-(z_7/\tau)}\right]$	$z_8 = t - \frac{8L}{c} + \frac{x}{c}$
$u_9 = v_0 z_9 - 10v_0\tau\left[1 - \left(1 + \frac{4}{5}\frac{z_9}{\tau} + \frac{4}{5}\frac{z_9^2}{\tau^2} - \frac{4}{15}\frac{z_9^3}{\tau^3} + \frac{2}{15}\frac{z_9^4}{\tau^4}\right)e^{-(z_9/\tau)}\right]$	$z_9 = t - \frac{10L}{c} - \frac{x}{c}$
$u_{10} = -v_0 z_{10} + 10v_0\tau\left[1 - \left(1 + \frac{4}{5}\frac{z_{10}}{\tau} + \frac{4}{5}\frac{z_{10}^2}{\tau^2} - \frac{4}{15}\frac{z_{10}^3}{\tau^3} + \frac{2}{15}\frac{z_{10}^4}{\tau^4}\right)e^{-(z_{10}/\tau)}\right]$	$z_{10} = t - \frac{10L}{c} + \frac{x}{c}$

conditions. Since stress measured is roughly proportional to the local strain at an end, experimental stress-time curves also vary in a stepwise fashion. The stress-strain curves likewise exhibit fluctuations.

The tensile behavior of a Hookean material having a breaking elongation independent of testing speed has been calculated using a theory in which wave propagation is considered. The results of these calculations have been used to modify the predictions of a simpler theory that neglects wave propagation. Thus, it has been shown that a filament weighted at the tail and pulled rapidly at the head at constant speed will attain a maximum average elongation proportional to $\sqrt{n + 1/2}$ after the tension wave has been reflected $(\pi/2)\sqrt{n + 1/2}$ times, where n is the ratio of the tail mass to the mass of the specimen.

If logarithms of the lowest breaking velocities for each n are plotted vs. log $(n + 1/2)$, the theory neglecting wave propagation predicts that a straight line of slope $-1/2$ is obtained, provided that the rupture-energy density is nearly constant at high testing speeds. An extrapolated velocity [for log $(n + 1/2)$ equals zero] is thus obtained which is termed the limiting breaking velocity of the material, i.e., the velocity above which the sample will always rupture at the head immediately upon impact. Both theories predict the same breaking velocities, provided extrapolation is made from data taken at impact speeds less than 2% of the velocity of propagation of a tension wave pulse along the material. If this limitation is observed, the theory neglecting wave propagation is valid and extrapolation to the limiting breaking velocity may be made.

TABLE III. Velocity Function

$$v = \frac{\partial u}{\partial t} = \frac{\partial u_0}{\partial t} + \frac{\partial u_1}{\partial t} + \frac{\partial u_2}{\partial t} + \cdots = v_0 + v_1 + v_2 + \cdots$$

$$v_0 = v_0 \text{ (for } z_0 > 0)$$

$$v_1 = v_0 - 2v_0 e^{-(z_1/\tau)}$$

$$v_2 = -v_0 + 2v_0 e^{-(z_2/\tau)}$$

$$v_3 = -v_0 + 4v_0 \frac{z_3}{\tau} e^{-(z_3/\tau)}$$

$$v_4 = v_0 - 4v_0 \frac{z_4}{\tau} e^{-(z_4/\tau)}$$

$$v_5 = v_0 - 6v_0 \left(\frac{1}{3} - \frac{2}{3}\frac{z_5}{\tau} + \frac{2}{3}\frac{z_5^2}{\tau^2} \right) e^{-(z_5/\tau)}$$

$$v_6 = -v_0 + 6v_0 \left(\frac{1}{3} - \frac{2}{3}\frac{z_6}{\tau} + \frac{2}{3}\frac{z_6^2}{\tau^2} \right) e^{-(z_6/\tau)}$$

$$v_7 = -v_0 + 8v_0 \left(\frac{z_7}{\tau} - \frac{z_7^2}{\tau^2} + \frac{1}{3}\frac{z_7^3}{\tau^3} \right) e^{-(z_7/\tau)}$$

$$v_8 = v_0 - 8v_0 \left(\frac{z_8}{\tau} - \frac{z_8^2}{\tau^2} + \frac{1}{3}\frac{z_8^3}{\tau^3} \right) e^{-(z_8/\tau)}$$

$$v_9 = v_0 - 10v_0 \left(\frac{1}{5} - \frac{4}{5}\frac{z_9}{\tau} + \frac{8}{5}\frac{z_9^2}{\tau^2} - \frac{4}{5}\frac{z_9^3}{\tau^3} + \frac{2}{15}\frac{z_9^4}{\tau^4} \right) e^{-(z_9/\tau)}$$

$$v_{10} = -v_0 + 10v_0 \left(\frac{1}{5} - \frac{4}{5}\frac{z_{10}}{\tau} + \frac{8}{5}\frac{z_{10}^2}{\tau^2} - \frac{4}{5}\frac{z_{10}^3}{\tau^3} + \frac{2}{15}\frac{z_{10}^4}{\tau^4} \right) e^{-(z_{10}/\tau)}$$

Acknowledgment

Support for this work and permission to publish, by the Office of the Quartermaster General, Department of the Army, is gratefully acknowledged.

Appendix I: Wave Theory Solutions

In Table II, u_0 gives the displacement due to the original incident wave proceeding towards the tail mass. After reflection at the tail, the displacement, u, is computed from the sum of u_0 and u_1, the displacement of the reflected wave. Similarly, after the first head reflection, displacement is computed from the sum of u_0, u_1, and u_2. Displacement due to each reflected wave is a function of a z-parameter which in turn is a function of x and t. Only positive values of these z-parameters are allowed. Negative values represent position-time events in advance of the wave, where $u = 0$.

TABLE IV. Local Strain Functions

$$\epsilon = \frac{\partial u}{\partial x} = \frac{\partial u_0}{\partial x} + \frac{\partial u_1}{\partial x} + \cdots = \epsilon_0 + \epsilon_1 + \cdots$$

$$\epsilon_0 = \frac{v_0}{c} \text{ (for } z_0 > 0)$$

$$\epsilon_1 = -\epsilon_0 + 2\epsilon_0 e^{-(z_1/\tau)}$$

$$\epsilon_2 = -\epsilon_0 + 2\epsilon_0 e^{-(z_2/\tau)}$$

$$\epsilon_3 = \epsilon_0 - 4\epsilon_0 \frac{z_3}{\tau} e^{-(z_3/\tau)}$$

$$\epsilon_4 = \epsilon_0 - 4\epsilon_0 \frac{z_4}{\tau} e^{-(z_4/\tau)}$$

$$\epsilon_5 = -\epsilon_0 + 6\epsilon_0 \left(\frac{1}{3} - \frac{2}{3}\frac{z_5}{\tau} + \frac{2}{3}\frac{z_5^2}{\tau^2} \right) e^{-(z_5/\tau)}$$

$$\epsilon_6 = -\epsilon_0 + 6\epsilon_0 \left(\frac{1}{3} - \frac{2}{3}\frac{z_6}{\tau} + \frac{2}{3}\frac{z_6^2}{\tau^2} \right) e^{-(z_6/\tau)}$$

$$\epsilon_7 = \epsilon_0 - 8\epsilon_0 \left(\frac{z_7}{\tau} - \frac{z_7^2}{\tau^2} + \frac{1}{3}\frac{z_7^3}{\tau^3} \right) e^{-(z_7/\tau)}$$

$$\epsilon_8 = \epsilon_0 - 8\epsilon_0 \left(\frac{z_8}{\tau} - \frac{z_8^2}{\tau^2} + \frac{1}{3}\frac{z_8^3}{\tau^3} \right) e^{-(z_8/\tau)}$$

$$\epsilon_9 = -\epsilon_0 + 10\epsilon_0 \left(\frac{1}{5} - \frac{4}{5}\frac{z_9}{\tau} + \frac{8}{5}\frac{z_9^2}{\tau^2} - \frac{4}{5}\frac{z_9^3}{\tau^3} + \frac{2}{15}\frac{z_9^4}{\tau^4} \right) e^{-(z_9/\tau)}$$

$$\epsilon_{10} = -\epsilon_0 + 10\epsilon_0 \left(\frac{1}{5} - \frac{4}{5}\frac{z_{10}}{\tau} + \frac{8}{5}\frac{z_{10}^2}{\tau^2} - \frac{4}{5}\frac{z_{10}^3}{\tau^3} + \frac{2}{15}\frac{z_{10}^4}{\tau^4} \right) e^{-(z_{10}/\tau)}$$

Velocity functions obtained by differentiating the displacement functions with respect to time are tabulated in Table III. Local strain functions, obtained by differentiating the displacement functions with respect to the position coordinate along the filament, are given in Table IV.

The method of obtaining these solutions is demonstrated in the following derivation for u_1.

The initial conditions that must be satisfied for the first reflection at the tail are:

$$\text{At } x = -L, \quad t = L/c, \quad z_0 = 0, \quad \text{and } z_1 = 0$$

Displacement at the tail just before reflection = displacement at the tail just after reflection, or:

$$u_0(0) = u_0(0) + u_1(0)$$

Hence $u_1(0) = 0$

Velocity at the tail just before reflection = velocity at the tail just after reflection, or:

$0 = v_0(0) + v_1(0)$

Hence $v_1(0) = -v_0(0) = -v_0$.

In addition, we have the boundary condition at $x = -L$:

$$nw(\partial^2/\partial t^2)[u_0(z_0) + u_1(z_1)]_{x=-L} = EA(\partial/\partial x)[u_0(z_0) + u_1(z_1)]_{x=-L}$$

or

$$nw(\partial^2/\partial t^2)u_1(z_1) = EA(v_0/c) + EA[(\partial/\partial x)u_1(z_1)]_{x=-L}$$

or

$$nw(d^2/dz^2)u_1 = EA(v_0/c) - (EA/c)(d/dz)u_1$$

where $z = t - (L/c)$ and A is the cross-sectional area of the unstrained filament. If we let $\tau = nwc/EA = n\rho Lc/E = n(L/c)$ we obtain:

$$d^2u_1/dz^2 + (1/\tau)(du_1/dz) = v_0/\tau$$

The solution of this equation that satisfies the initial conditions is:

$$u_1 = v_0(t - L/c) - 2v_0\tau[1 - e^{-(1/\tau)(t-L/c)}]$$

If we replace $(t - L/c)$ by $z_1 = t - (2L/c) - (x/c)$ we obtain the required solution for u_1.

Appendix II: Theory, Neglecting Wave Propagation

Consider a filament of length L, cross section A, and density ρ having a mass $n'\rho AL$ attached at the tail, where n' is equal to $n + f$; n is the ratio of the tail mass to the mass of the filament; and f is the fraction of the mass of the filament assumed concentrated at the tail. It is shown in the body of this paper that the best value for f is 1/2.

At zero time and subsequently, let the head end of the filament be constrained to move with velocity v_0. The equation of motion is:

$$n'\rho AL(d^2u/dt^2) = F \qquad (1)$$

where u is the displacement of the tail mass, and F is the accelerating force transmitted through the filament to the tail mass.

The strain in the filament ϵ is given by:

$$\epsilon = (v_0t - u)/L \qquad (2)$$

When Hooke's law applies:

$$F = AE\epsilon \qquad (3)$$

where E is Young's Modulus for the filament material. Substituting (2) and (3) into (1) we obtain:

$$(d^2u/dt^2) + \omega_0^2u = \omega_0^2v_0t \qquad (4)$$

where

$$\omega_0 = (c/L)(1/n') \qquad (5)$$

and

$$c = \sqrt{E/\rho} \qquad (6)$$

A solution of (4) satisfying the boundary conditions

$$\left.\begin{aligned} u &= 0 \\ du/dt &= 0 \end{aligned}\right\} \quad \text{At } t = 0$$

is:

$$u = v_0[t - (1/\omega_0)\sin\omega_0t] \qquad (7)$$

If we let $t = (L/c)\theta$, and $\epsilon_0 = v_0/c$, we obtain:

$$u = \epsilon_0L[\theta - \sqrt{n'}\sin(\theta/\sqrt{n'}) \qquad (8)$$

$$= \epsilon_0\sqrt{n'}\sin(\theta/\sqrt{n'}) \qquad (9)$$

In a previous paper [1] the following equation was derived.

$$\log v_n = -1/2\log\frac{(n + 1/2)(m + 1/2)}{n + m + 1} + \log\sqrt{\frac{2}{\rho}\int_0^{\epsilon_r}\sigma d\epsilon} \qquad (10)$$

where v_n is the lowest impact velocity sufficient to cause rupture in a filament to which a tail mass n times that of the filament and a head mass m times that of the filament are attached. For comparison with the work discussed here, we let $m \to \infty$, obtaining:

$$\log v_n = -1/2\log(n + 1/2) + \log\sqrt{\frac{2}{\rho}\int_0^{\epsilon_r}\sigma d\epsilon} \qquad (11)$$

Literature Cited

1. McCrackin, Frank L., Schiefer, Herbert F., Smith, Jack C., and Stone, Walter K., "Stress-Strain Relationships in Yarns Subjected to Rapid Impact Loading: II. Breaking Velocities, Strain Energies, and Theory, Neglecting Wave Propagation," TEXTILE RESEARCH JOURNAL **15**, 529 (1955).
2. Stone, Walter K., Schiefer, Herbert F., and Fox, George, "Stress-Strain Relationships in Yarns Subjected to Rapid Impact Loading: I. Equipment, Testing Procedure, and Typical Results," TEXTILE RESEARCH JOURNAL **15**, 520 (1955).

Manuscript received January 28, 1955.

Applications of Thermodynamics to the Stretching of Cellulose Fibers[1]

W. E. Roseveare[2] and Louise Poore

Rayon Research Division, Textile Fibers Department, E. I. du Pont de Nemours and Company, Richmond, Virginia

Abstract

Mechanical deformations of cellulose are recognized to take place primarily in the amorphous regions whose nature has not been well defined. Since these regions do not have a regular type of order, attention has been turned to entropy of stretching as a statistical measure of the changes in structure on stretching.

Data are presented giving the retractive force, coefficient of thermal expansion, and modulus under a wide variety of conditions. Thermodynamic treatment of the data shows that moisture content and temperature control the bonding between chains in the amorphous regions. These cross links to a large extent determine the mechanical properties, which vary from an elastic glass in the dry state to those of a partially rubbery material in the wet state at high temperatures. At low temperatures in the wet state, the amorphous parts of the chains "precipitate" out of the swelling water and thereby form cross links between chains, which makes the modulus tend to approach infinity at the cellulose-water eutectic point.

This work provides a better understanding of the relationship between molecular and fiber properties.

Introduction

The equation of state for a material under a tensile stress equal to the reversible retractive force, f, is given by the equation [1, 2, 7]:

$$f = (\partial E/\partial l)_T - T(\partial S/\partial l)_T \qquad (1)$$

where E, l, S, and T are the internal energy, length, entropy, and temperature, respectively. In its most general form equation (1) should be written with the enthalpy, H or $E + PV$, in place of the internal energy, E, as has been pointed out by Katz [2]. However, the change in the product of the pressure and the volume, PV, with length is so small for fibers at atmospheric pressure that it is ordinarily neglected, and E is generally used in place of H. The two right-hand terms in equation (1) cannot be determined directly for fibers, but the entropy term can be obtained readily with the aid of the following equation [1, 7, 8]:

$$(\partial S/\partial l)_T = -(\partial f/\partial T)_l \qquad (2)$$

The energy term is then determined as the difference between the total force and the entropy term. Equation (1) resolves the retractive force into energy and entropy components, as follows:

$$f = f_E + f_S \qquad (3)$$

These two components of the force have been reported for nylon and some protein fibers by Woods [8] and for cellulose fibers by Wakeham and Gerrow [6]. In the case of rubber, the energy component of the force is quite small because the interaction between the chains is largely of the van der Waals type. However, in cellulose very strong hydrogen bonding is present, making the energy component a very large part of the force under most conditions.

It follows from the property of differentials that the reversible force, length, and temperature are related also in the following way:

$$(\partial f/\partial T)_l = -l(\partial f/\partial l)_T \frac{1}{l}(\partial l/\partial T)_f \qquad (4)$$

[1] Presented at the American Chemical Society Meeting, New York City, September 16, 1954.

[2] Present address, E. I. du Pont de Nemours and Co., Kinston, N. C.

Substituting equation (3) in this one gives:

$$(\partial S/\partial l)_T = \frac{1}{l}(\partial l/\partial T)_f \, l(\partial f/\partial l)_T \qquad (5)$$

or

Entropy of Stretching
= Coefficient of Expansion × Modulus (6)

The above equations have been derived on the assumption that the variables f, l, and T fully define the state of the material at all times; i.e., the system is elastic so that the thermodynamics of reversible processes apply. However, it is well known that polymers show viscous as well as elastic effects. In order to eliminate or reduce time effects, thermodynamic measurements have been made on samples stabilized by a stress-relaxing treatment at high temperatures. During this stress relaxation the force decreases rapidly at first (Figure 1), but after some time the force becomes constant within the experimental error for any selected period, t_1 to t_2. After this treatment, lowering and again raising the temperature in most cases gives retractive forces independent of time and direction of change in temperature, provided the time of observation is less than the period of time between t_1 and t_2 and the temperature of stress relaxation is not exceeded. In the present work, a high degree of reversibility of the modulus measurement was obtained for most conditions by the very low extension of 0.07% used in the modulus determination.

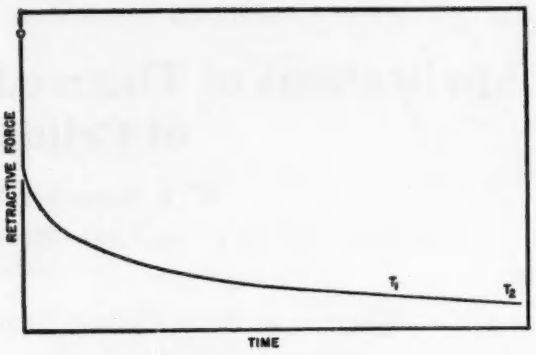

Fig. 1. Typical behavior of retractive force during stress relaxation.

Discussion

Dry Rayons

Experimental determinations of the retractive force, length, and modulus at various temperatures in dry air were made on a single filament of stress-relaxed tire-cord rayon by the methods previously described by the authors [4]. Special precautions were used to insure very dry air by passing it first over Drierite and then over a large fresh surface of phosphoric anhydride on glass wool. A low rate of air flow of 5 ml per minute was used to prevent cooling of the lower end of the sample by the incoming air. Counterdiffusion of moisture from the atmosphere was made insignificant by attaching to the upper end of the apparatus a 2-in. length of 5-mm rubber tubing through which the dry air escaped. Rapid cooling caused the air in the apparatus to contract and to draw some moist air in through the tube. To avoid this effect the rubber tube was pinched off on the suspension wire and a positive pressure of the dry air was maintained in the apparatus during cooling.

The values of the modulus were determined by extending the sample 0.07% and determining the resulting change in retractive force after 15 sec and again after 5 min. The retractive forces and lengths were practically the same on raising the temperature as on lowering it and were time independent for periods of 5 min to 1 hr. The moduli obtained on shortening the sample were found to be within experimental error of those obtained on stretching the sample for the 15-sec period. This system was practically elastic for this period of observation, but for longer periods of time the modulus was more time dependent. In a 5-min determination, the observed modulus on stretching was less than the reversible value by 3% at 75°C and 10% at 125°C.

Since this system is nearly elastic, the application of all of the above thermodynamic equations is justified. The three terms of equation (4) are given by the three sets of experimental data plotted in Figure 2. The retractive force is given in grams per denier and the modulus in grams per denier per 100% extension; denier is the linear density or weight of 9000 m of dry fiber. According to equation (3), the negative of the slope of the retractive force plotted against temperature in Figure 2*a* is the value of the entropy of stretching, while the slope of the length-temperature curve, Figure 2*b*, is the value of the coefficient of thermal expansion. The moduli for a 15-sec deformation, observed over a range of temperatures, are plotted in Figure 2*c*. The moduli at two temperatures were calculated

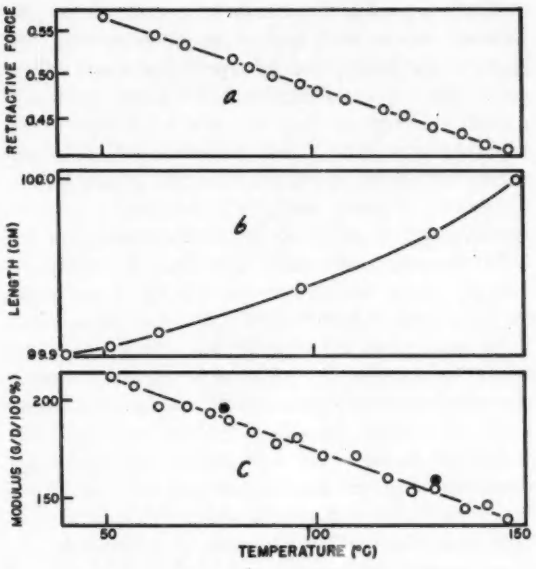

Fig. 2. Thermodynamic properties of a dry tire-cord rayon stretched 1% and stress-relaxed for 4 hr at 150°C.

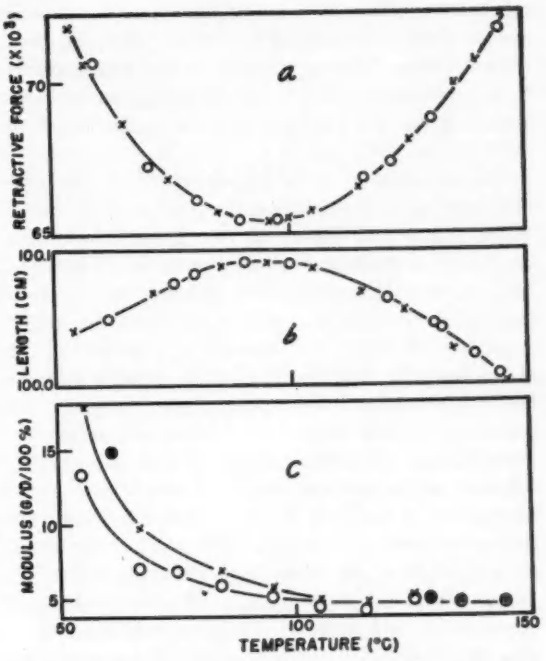

Fig. 3. Thermodynamic properties of a wet tire-cord rayon stretched 5% and stress-relaxed 16 hr at 95°C.

from the slopes of the curves in Figures 2*a* and 2*b*. These values are shown by the two solid circles in Figure 2*c*. The agreement with the directly determined values shows that equation (4) holds within the error of reading the slopes from the length curve for this system for high and low temperatures.

Substituting the retractive force and the entropy of stretching obtained from Figure 2*a* at 100°C into equation (1) gives f, f_E, and f_S equal to 0.49, 1.12, and -0.63 g/den, respectively. The energy component of the force is much larger than the force, and the entropy component is negative, indicating that the latter actually tends to elongate the sample. This disordering entropy of stretching is essentially the same as that occurring in the normal thermal expansion of most solids, namely, an increase in the number of vibrational states activated. For dry rayon, whose retractive force is a linear function of the temperature, the energy component of the force is independent of the temperature. In a previous work, the authors [4] have shown that there is no significant reversible slippage of chains over each other in completely dry rayon because the entropy of stretching is independent of the supermolecular structure. Both this conclusion, the time independence of the modulus, and the low breaking elongation of about 4% support the view that short-period reversible deformations in dry rayons involve almost entirely the very elastic deformations of valence bonds and angles.

Wet Rayons

A considerably different behavior is exhibited by wet tire-cord rayons. Figure 3 presents data giving the values of the three terms in equation (4) for a single filament of such a rayon in water after stretching 5% and stress relaxing at 95°C for 16 hr. Under these conditions, the time the sample is at a given temperature in the range of 5 to 60 min has no apparent effect on the retractive force at constant length, but has a slight effect on the length at constant force. There is little effect of time on the modulus of the wet rayon above 50°C for a 0.07% extension, but below this temperature retarded effects occur, giving considerably lower moduli for the longer period of deformation. Calculations of the modulus from equation (4), using the slopes of the curves in Figure 3*a* and *b*, give the values shown by the solid circles in Figure 3*c*. Above 50°C where the wet rayon is moderately elastic, the equation holds quite well, but below this temperature the

calculated modulus is considerably above the experimental value. This is in agreement with the poor work recovery of a wet rayon at low temperatures from a 3% stretch in a cycle involving over a minute duration; the reported [4] recoveries are 95% at 92°C and 35% at 3°C.

The ordering on stretching, indicated by the positive slope of the force-temperature curve above 50°C, suggests a rubberlike elasticity. However, in this range the modulus decreases slightly with temperature and is not proportional to the absolute temperature, as is the case for rubber; therefore, the mechanism of stretching cannot be entirely rubberlike. It seems probable that the entropy of stretching above 50°C arises to a considerable degree from an increase in the amount of bound water on stretching.

Additional information about the low-temperature behavior of the modulus can be obtained by plotting the reciprocal of the modulus, or compliance, against the temperature. This treatment reduces the plots to sets of straight lines, as shown in Figure 4. Above 50°C, the modulus is nearly independent of temperature and time, as shown above, but below this temperature it drops sharply, giving straight-line relationships of $1/M$ against T. The temperature at which the drop starts depends on the duration of deformation; a twentyfold increase in time lowers the temperature of the break in the curve about 8°C. Extrapolating these two straight lines down to $1/M$ equal to zero gives the temperature at which the modulus would be infinite if the behavior giving straight-line segments continued at the lower temperatures. Since the two curves extrapolate to roughly the same temperature of -19°C, this point is nearly time independent and therefore a thermodynamic property. This approximate convergence at low temperatures of the $1/M$ values for different times of observation was found also for several other tire-cord rayons in the range of -12 to -19°C. The extrapolated point is the temperature where a degree of freedom is frozen out, not because of a slow rate but because the degree of freedom does not exist thermodynamically below this temperature. Additional evidence for the thermodynamic nature of this point is the observation of Preston and Nimkar [3], who found about the same temperature, -19°C, for the eutectic point of a rayon-water system. This eutectic point was determined from the freezing point of the water in rayons at various moisture contents.

Mechanistically, the change of modulus with temperature can be explained in the following way. At high temperatures, the amorphous sections of the chains are highly solvated or "dissolved" in the water of swelling and have to a considerable extent rubberlike properties. This solvation of amorphous chains is to be expected since glucose is very soluble in water. Cooling partially desolvates the amorphous material, resulting in the formation of cross links between the chains through the hydroxyl groups, either directly or through water molecules as a hydrate. Above 50°C, some of these cross links are present, but their life is too short to greatly affect the modulus in a 15-sec deformation; lowering the temperature increases their life, and at about 50°C they begin to affect the observed modulus. Below the break in the $1/M$ plots, the modulus depends on both the equilibrium number and life of the cross links; thus the modulus is dependent on both time and a thermodynamic property. As the temperature is further lowered, more and more cross links are formed (more amorphous material is precipitated out) until the eutectic point is reached. Below this temperature only the pure dry cellulose or possibly a dry hydrate and ice phases exist. This dry amorphous cellulose is essentially a highly cross-linked polymer which is glassy in showing no re-

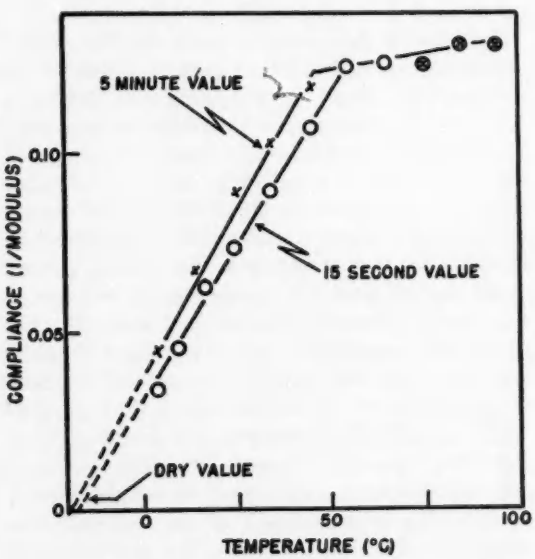

Fig. 4. Effect of temperature on reciprocal of modulus or compliance of wet rayon.

versible slippage of chains. Thus the degree of freedom frozen out on cooling down to the eutectic point is the freedom of the amorphous portions of the chains to slip over each other. Actually, the modulus does not become infinite at the eutectic point since both glassy cellulose and ice must have finite moduli. The $1/M$ value for dry cellulose at low temperatures, shown by the arrow in Figure 4, is so low that extrapolating to this $1/M$ value gives, within experimental error, the same point as extrapolating to $1/M$ equal to zero.

In the case of highly crystalline, highly oriented rayons, such as Lilienfeld and Fiber G types, the compliance-temperature straight lines are parallel in the low-temperature range, and hence their extensions do not converge at $1/M$ equal to zero, as is the case for the tire-cord rayons. Thus the extrapolated temperatures of infinite modulus for the brittle rayons are time dependent, and therefore these temperatures cannot be interpreted thermodynamically. Possibly data taken on a widely different time scale would give values near enough to equilibrium to have thermodynamic significance.

Behavior of Rayon in Air

A still different behavior is shown by rayon in air having a constant absolute-moisture content. The upper curve, Figure 5, illustrates the variation of retractive force with temperature for a filament of rayon after stretching 1% and stress relaxing in air having a relative humidity of 50% at 25°C. At very high temperatures, the force-temperature curve is a straight line with the same slope as that shown for dry rayons at all temperatures. On cooling below 120°C, moisture begins to be adsorbed, and the deviation from the dry behavior gets larger as the temperature is further lowered. At temperatures below 120°C, time effects become significant, and a longer time is required to obtain a steady force. The retractive-force data in Figure 5 were obtained by allowing the sample to stand for ½ hr at each temperature before reading the force. However, the curve obtained on cooling to low temperatures is not retraceable on raising the temperature. The hysteresis below 120°C appears to arise from a lag in the change of structure associated with the adsorption of water. Although the behavior is poorly reversible when the rayon contains moisture, the large positive slope indicates qualitatively a negative entropy or ordering on stretching.

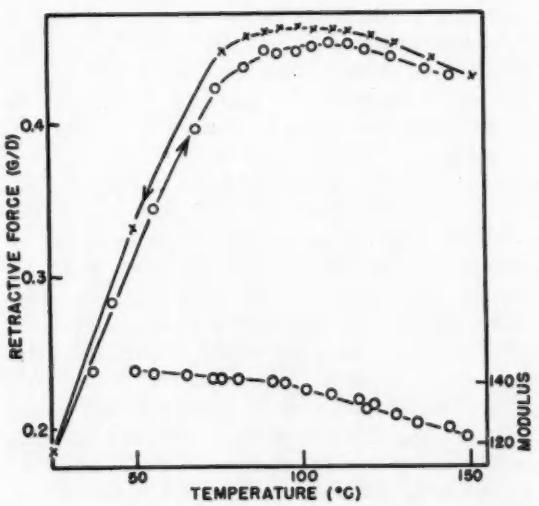

Fig. 5. Effect of temperature on retractive force and modulus of rayon in air having 50% R.H. at 25°C.

The change in modulus with temperature for a 0.07% extension under the above conditions in air is given by the lower curve in Figure 5. The modulus decreases with increase in temperature over the whole range, but at a lower rate below 95°C. The increased plasticization by the higher moisture contents accounts for the lower slope at the lower temperatures. Since modulus in air at constant absolute-moisture content has the opposite temperature coefficient from that of rubber, the ordering, as measured by the entropy of stretching, must be largely of a type different from the ordering of the chains on stretching rubber. Treloar [5] has reported that an increase in moisture content occurs in rayon on stretching. This adsorption of moisture decreases the freedom of the water molecules and will represent an entropy decrease which should be large compared to any entropy effects arising from ordering of the chains. Therefore, it appears probable that the decrease in entropy on stretching a rayon in air is due primarily to the adsorption of water following a disordering of the chains. The increase in length of rayon with increasing moisture content is also in agreement with this observation.

A rayon in atmospheric air between 0 and 100°C is similar to a wet rayon in that chain slippage occurs, but this slippage is small compared to that in the wet state, as indicated by a comparison of the

modulus at 50°C for the dry, room-air, and wet states of 208, 144, and 18 g per dry denier per 100% extension, respectively. These large differences relative to the effects of temperature show that the water content is more important than the temperature in determining the properties of a regenerated cellulose.

Literature Cited

1. Elliot, D. R., and Lippmann, S. A., *J. Appl. Phys.* **16**, 50 (1945).
2. Katz, S. M., TEXTILE RESEARCH JOURNAL **20**, 16 (1950).
3. Preston, J. M., and Nimkar, M. V., TEXTILE RESEARCH JOURNAL **23**, 119 (1953).
4. Roseveare, W. E., and Poore, L., *J. Polymer. Sci.* **14**, 341 (1954).
5. Treloar, L. R. G., *Trans. Faraday Soc.* **49**, 816 (1953).
6. Wakeham, H., and Gerrow, W. F., TEXTILE RESEARCH JOURNAL **23**, 593 (1953).
7. Wiegert, W. B., and Snyder, J. W., *Trans. Rubber Ind.* **10**, 234 (1934).
8. Woods, H. J., *J. Colloid Sci.* **1**, 407 (1946)

Manuscript received February 3, 1955

The Mechanism of Supercontraction in Keratin

G. M. Jeffrey, J. Sikorski, and H. J. Woods

Textile Physics Laboratory, Department of Textile Industries, The University, Leeds, England

DETAILED studies of the group of phenomena usually referred to as "supercontraction" in keratin fibers [3] have led to the accumulation of a vast body of data in which there are many unexplained anomalies. The term supercontraction is commonly used to describe any shortening of the fiber to less than its original length; it is usually tacitly assumed that all such effects have a common molecular origin, although this is by no means evident on *a priori* grounds. In fact, it could reasonably be argued that the lack of correlation between the physicochemical conditions used for producing the effect, the extent of the contraction, and the crystallographic changes points to a diversity, if not in the fundamental causes, then in their secondary manifestations, at least. We shall here adopt the viewpoint that the contraction is due, in the end, to folding or disorientation of the chain molecules which originally had an oriented, but not crystalline, configuration [3]. The question with which we shall be chiefly concerned is whether the histological heterogeneity of the fiber structure has any influence on the contraction; as far as the grosser details of the structure are concerned it is fairly certain that the cellular texture itself has no profound effect, for it has always been found that the behavior of the isolated cortical cells is similar to that of the whole fiber in respect to their response to supercontracting treatments [20]. We are thus led to consider the possibility that the intracellular texture, on a scale coarser than the crystallographic, may influence the contraction.

The cortical cells of keratin fibers may, by appropriate treatments, be disintegrated to give fibrillar sheets [7] and ultimately microfibrils [5, 7]; the former, and possibly the latter, are cemented together by an interfibrillar material whose properties are at present unknown [7]. The proportion of fibrillar material appears to be so high, however, that it is reasonable to assume that it is there that the crystallographic changes studied by X-rays have their origin. Whether this is so or not, it is relevant to enquire whether any observable changes in the fibrils themselves are brought about by contractions of the kind in question. Recently Mercer [11] has observed an effect in which bundles of twisted fibrils appear after fibers treated in a suitable reagent have been disintegrated to a fine enough condition for electron microscopy. On account of the twist, the fibrillar bundle must be shorter than it was originally, and Mercer suggests this as a possible mechanism of supercontraction capable of explaining also the loss of crystallite orientation and the decrease in birefringence which often accompany the contraction. Although the proposed mechanism has such very attractive features, there are obvious arguments which can be advanced against it as a means of producing the observed contraction in intact fibers. However, the idea that fibrillar distortion of some

kind (e.g. flexure, such as has been suggested in connection with muscular contraction [6]) may accompany contraction is one worthy of close examination.

We have, therefore, reexamined our electron-microscope results for the effects of various supercontraction techniques. Although our experiments are not comprehensive, we have included examples of most of the various crystallographic effects associated with supercontraction.

Experimental

The experiments were done with nonmedullated root ends of Australian merino, Cotswold, and Lincoln wool fibers and with horsehair. These were cleaned by extraction in petroleum ether at room temperature for about a week, followed by Soxhlet extraction first in benzene and then in ethyl alcohol for 24 hr. The fibers were washed in repeated changes of distilled water to remove water-soluble impurities and then dried at room temperature.

There are a number of methods by which supercontracted material suitable for electron-microscope examination can be prepared, each having its own advantages and disadvantages. For example, when fibers are subjected to a supercontracting treatment they are often so modified that enzymatic digestion is difficult to control [11, 20]; in such circumstances it might be desirable to start with the cortical cells instead of intact fibers. On the other hand, certain treatments (e.g. relaxation of stretched material) are clearly impossible with the isolated cells. We have therefore done experiments of three types: (1) cortical cells were isolated from untreated fibers and were then subjected to the supercontraction treatment before being finally disintegrated; (2) the fibers were treated in such a way as to render them potentially contractile and were disintegrated into cells which were then made to contract by suitable treatment before being finally reduced to a fine enough state for examination in the electron microscope; and (3) the fibers themselves were subjected to the supercontraction treatment and were subsequently disintegrated in various ways.

In some cases the final disintegration could be brought about by grinding the material between microscope slides in the presence of a swelling agent (formic acid); more usually, however, the material was subjected to ultrasonic vibrations (23 kc/s and 15 w/cm^2) in water or solutions of urea or lithium bromide. When ultrasonics were used the time of irradiation ranged from 15 min to 2 hr.

1. Experiments with Cortical Cells from Virgin Wool

a. The effect of cuprammonium hydroxide. Cotswold wool fibers were treated in a 0.5% solution of trypsin (buffered to *p*H 8.6) at 40°C for 1 wk; the wool:liquor ratio was 1:100. The cortical cells

Fig. 1. Cotswold wool (cortical cell) supercontracted by 36% in cuprammonium hydroxide solution. Magnification, ×25,000.

thus isolated were washed by sedimentation and were then treated in a solution of cuprammonium hydroxide containing 15 g of copper and 200 cc of ammonia per liter; after 3 hr they had contracted by about 36%. The contraction was estimated by comparing the mean lengths of the cells before and after treatment; about 100 cells were measured in each case. The contracted cells, after having been washed in water, were ground between a microscope slide and a cover slip in water; this was found to be effective in reducing them to layered sheets of microfibrils. No evidence was found of any serious deformation of the microfibrils, which appeared to lie more or less parallel to each other in the sheets (Figure 1). The X-ray photograph of a control sample of fibers subjected to the above treatment without disintegration by grinding showed the features (disappearance of the α-photograph and appearance of a heavy central scattering) already reported elsewhere [19].

b. The effect of sodium bisulfite. Cortical cells isolated from Lincoln wool by tryptic digestion were treated for 1 hr in a boiling aqueous solution of sodium bisulfite. The mean contraction of the cells was 24%; this is less than the 38% obtained with single fibers which were used as controls, but it is doubtful whether the discrepancy has any real significance. The X-ray photograph of the control fibers showed the presence of completely disoriented β-crystallites. The supercontracted cells were opaque to the electron beam at 75 kv and proved to be very difficult to disintegrate into fibrillar fragments. Negligible fragmentation was achieved even when the cells were subjected to ultrasonic vibrations in 100% lithium bromide solution. The negative result of this experiment serves to emphasize the fact that reduction of the disulfide sulfur by sodium bisulfite solutions at high temperatures is followed by recombination, which leaves the structure effectively crosslinked [17].

c. The effect of peracetic acid. The cells used for this experiment were isolated from Lincoln wool which had been treated for 5 min in 2% peracetic acid; the effect of this treatment was, however, very slight, either in modifying the properties of the fibers or in reducing the lengths of the cells. The retting was done in 0.05% pepsin solution (pH 1.42) at 40°C for 3 mo. The cells thus isolated were transferred to a 2% solution of peracetic acid and treated therein for times ranging up to 24 hr at room temperature; they were then washed in distilled water. The X-ray photographs of control samples of oxidized wool fibers showed that there was a progres-

Fig. 2. Lincoln wool (cortical cell) treated in peracetic acid and exposed to ultrasonic vibrations in lithium bromide solution; contraction, 10%. Magnification, ×4,700.

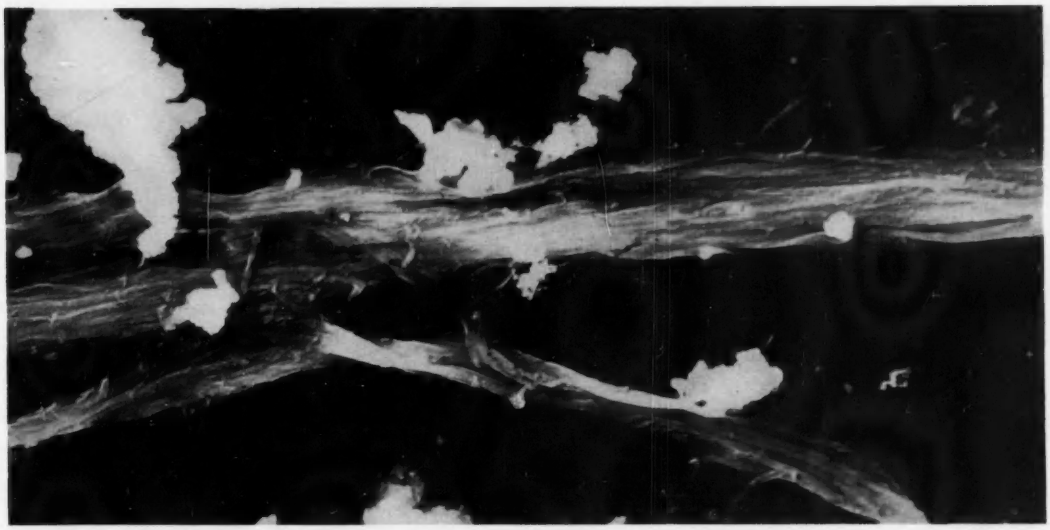

Fig. 3. Lincoln wool (cortical cell), treated similarly to the sample of Figure 2; contraction, 40%. Magnification, ×16,000.

sive disorientation of the crystallites, which, however, remained in the α-form even after treatment for 24 hr. When the duration of the oxidation treatment was longer than 1 hr the subsequent effect of lithium bromide solution was to produce an almost completely disoriented α-structure.

Preparations of cortical cells were examined after treatment in the peracetic acid for 30 min and 2 hr, these leading respectively to oxidations of about 45% and 75% of the disulfide linkages [1]. The milder treatment produced a supercontraction of about 10% and was ineffective in giving much fibrillation. After ultrasonic irradiation in lithium bromide solution the cells had disintegrated into flat ribbons of parallel microfibrils; the thickness corresponded to the diameter of the individual microfibril. The subdivision of the major portion of a single cortical cell is shown in Figure 2. Although this picture is not typical of this particular preparation, it serves to show clearly that the microfibrils on the whole remain untwisted.

The cells which had been oxidized for 2 hr contracted by about 40% when subjected to ultrasonic vibrations in lithium bromide solution. Figure 3, which is a typical electron micrograph of this preparation, shows that the microfibrils remain nearly straight and parallel. The cleancut and smooth appearance of the microfibrils resulting from these treatments is noteworthy; in contrast, fibers treated for 3 wk in peracetic acid can be broken down [16] to show a remarkable fibrillar structure, but, as can be seen from Figure 4, the microfibrils thus made evident are markedly "globular" in appearance. In this preparation several groups of regularly arranged isolated globules, possibly originating in the interfibrillar matrix, can also be seen.

2. *Experiments with Cells from Pretreated Wool*

a. Relaxation in sodium hydroxide solution. Lincoln wool fibers were stretched to an extension of 60% in water and relaxed for 15 min in a 1% aqueous solution of sodium hydroxide at room temperature. After washing in water they were retted in trypsin for 3 days to release the cortical cells [20]. The washed cells were then made to contract by putting them in boiling water for 1 hr; their mean contraction was about 42%. The X-ray photograph of fibers supercontracted by this method shows the presence of rather highly disoriented parallel-β crystallites [19].[1]

The cells were examined in the electron microscope before and after contraction. The former (which, by inference from the results for fibers,

[1] The term "parallel-β" is used here to refer to the normal β-configuration to distinguish it from the cross-β configuration (See, for example, Rudall [15]).

Fig. 4. Cotswold wool treated in peracetic acid for 3 wk. Magnification, ×55,000.

should give an X-ray photograph of the α-type, with slight disorientation [19]) showed signs of incipient disintegration of straight microfibrils into a very fine debris but otherwise showed little internal structure, even after ultrasonic treatment in lithium bromide. The contracted cells showed little evidence of fibrillation although some were somewhat frayed at the ends and some fibrous fragments of cells were also present (Figure 5). Such details as could be seen clearly point to a straight and parallel configuration of the component fibrils. The effect of ultrasonic irradiation in lithium bromide solution on these supercontracted cells was dramatic, leading, as it did, to preparations similar to that shown in Figure 6, with sheets and ribbons of remarkably straight and parallel microfibrils.

b. Reduction and ethylation. An attempt was made to repeat Mercer's experiment [11], using, as nearly as possible, the same conditions. Some Lincoln wool fibers (2 g) were chopped into 5-mm lengths and treated at 40°C in 400 cc of a 5% solution of sodium bisulfite to which was added 3 ml of

TABLE I.

Preparation	Sample	Time of Digestion (days)	Length of the Cells (μ)			
			In Pepsin	In Water	Dry	After Boiling
	1	3	111	115	116	—
	2	4	112	—	113	—
1	3	5	111	—	112	—
	4	5	—	—	—	106
	5	6	—	110	—	—
	6	19	105	107	110	109
2	1	3	110	112	—	97

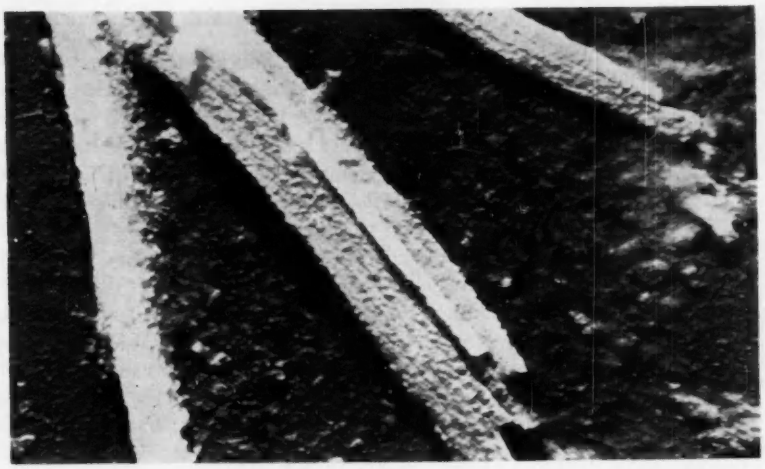

Fig. 5. Lincoln wool (cortical cell from fiber relaxed in sodium hydroxide solution) contracted by 42% in boiling water. Magnification, ×27,000.

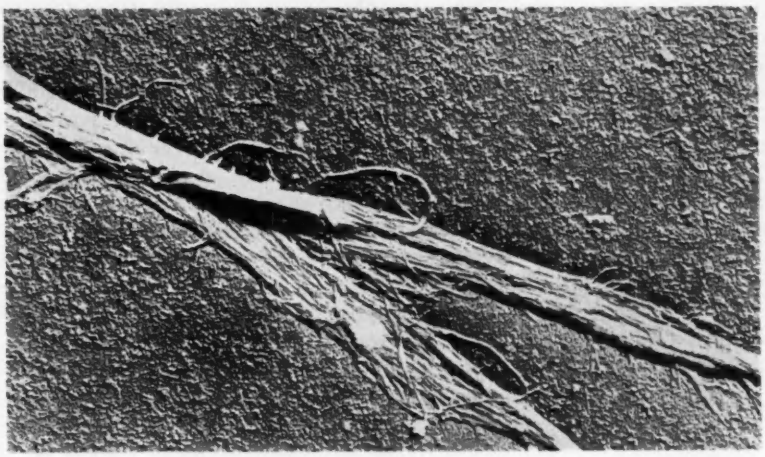

Fig. 6. Lincoln wool, preparation of Figure 5 subjected to ultrasonic vibrations in lithium bromide solution. Magnification, ×27,000.

ethyl bromide and sufficient sodium carbonate to bring the *p*H to 7. The treatment was carried out in a tightly stoppered flask. The treated wool gave a negative response to the nitroprusside test, in contrast to the strong positive response given by wool which had been reduced under similar conditions but without ethylation. The X-ray photograph of the reduced and ethylated fibers was of the oriented α-type, but traces of the β-pattern were also evident.

The treated wool was digested in pepsin solution to give cells of about the same length as those from untreated fibers (ca 110 μ). Little success resulted from attempts to induce contraction by boiling the cells in water; details of the observations are recorded in Table I, where each length is the mean of 50 observations, the standard deviation being about 6 μ in each case. As might be expected under these conditions, the electron micrographs showed no widespread twisting of the microfibrils; when any was apparent it occurred in isolated fibrils only. The negative results of this experiment might have been due to the use of Lincoln wool, for which the conditions might not have been the best for obtaining the effects searched for. We therefore repeated the experiment using Australian merino wool, but obtained results of the same general character as those described above. The fact that Mercer observed that the treated cells had contracted in length,

whereas ours did not, can only mean that there is a considerable variation in the response of different samples of wool to the reduction and ethylation treatment. This is supported by Mercer himself, who has told us (privately) that in cases where the initial treatment described by him is ineffective, he has been successful in producing both supercontraction and twisted fibrils by increasing the time and temperature of the treatment. There is a faint possibility, which we do not regard very seriously, that the discrepancy may be associated with the bilateral asymmetry of merino wool fibers [8, 12], his attention being confined to the less resistant fraction and ours to the other. The only other way in which our experiments differed from his was in his use of a Waring Blendor for disintegrating the cells; this could have had a contributory effect in producing the twisted fibrils.

3. Experiments with Supercontracted Fibers

a. Contraction in urea bisulfite. Lincoln wool fibers were immersed in a saturated solution of urea with 5% sodium bisulfite, adjusted to *p*H 7 with solid sodium carbonate. After remaining in the solution at 40°C for 24 hr the fibers were washed and dried and were found to have contracted by about 35% of their initial length. The X-ray photograph of fibers thus treated is of the disoriented β-type [9], with orientation to the cross-β configuration on stretching [10]. The treated fibers could be disintegrated by gentle grinding in 98–100% formic acid and when then examined in the electron microscope showed that the microfibrils remained, on the whole, straight and parallel.

b. Contraction in boiling formic acid. Horsehair fibers were treated in boiling 98–100% formic acid under reflux. After 3 hr they were washed, and it was found that they could be broken down by grinding in fresh formic acid to give preparations suitable for examination in the electron microscope. The fibrillar structure was quite clearly shown, and the microfibrils remained straight. The degree of contraction realized in fibers subjected to this treatment was not very high, being of the order of 15% of the initial length [18]; the X-ray photograph was of the disoriented β-type, with rather diffuse reflections.

Discussion

Our results clearly indicate that in general we must reject the idea that any important deformation, apart from shortening, takes place in the microfibrils when the fibers are made to contract. Although the possibility of some moderate degree of bending of the microfibrils cannot be excluded, this cannot be large enough to account for contractions of the order of 40%, such as were obtained in some of our experiments. It is, of course, possible that when a group of microfibrils have become detached from the main bulk of the cortical cell internal stresses (possibly associated with drying) may cause a twisting of the kind observed by Mercer [11]; and, in fact, whenever such an effect has been observed in these experiments the group of microfibrils had at least one free end.

Since the fibrillar manifestation of supercontraction is a shortening in length, it might be expected that corresponding changes would occur in fibrillar width and in any periodic structure apparent along the fibrils. Any examination of these possibilities will, however, necessitate much more detailed and precise experiments than those described here. In the absence of such data we can only speculate about the course of events inside the fibrils which lead to contraction. The ambiguous results of X-ray investigations, which show that the crystallites in fibers supercontracted by various techniques may be in the α-, β-, or cross-β forms, with varying degrees of imperfection ranging down to that which results in no crystalline reflections at all and with varying degrees of crystallite disorientation, are usually taken to mean that the prime contractile agency resides in the material which is too poorly organized in the normal fiber to give discrete X-ray reflections. There is no difficulty in accepting the idea that such material does occur in the microfibrils. What may be a difficulty is their restricted width, which does not allow overmuch room for an arrangement of crystalline and noncrystalline material in parallel—a type of structure which appears to be necessary if the phenomena of crystallite disorientation are to be explained.

This difficulty, if difficulty it is, could be overcome by invoking the idea that the interfibrillar matrix is itself contractile, in this respect constituting part of the "parallel" material and reducing the degree of contractibility which it would be necessary to ascribe

to the microfibrils. It should be noted, however, that the idea of a contractile matrix implies some degree of molecular orientation in its constitution, so that it would not have the completely amorphous character suggested by Mercer and Rees [13]. At the same time, there is no necessity to suppose that it is as well oriented as the fibrillar material, and we may, perhaps, reconcile the ideas put forward here with those of Mercer and Rees by supposing that the matrix is only imperfectly oriented molecularly and therefore of somewhat limited potential contractibility. It would then be possible to ascribe contractions of the order of 20%, when unaccompanied by any profound changes in crystalline configuration, as being due to the matrix, whose contraction would tend to be restricted by the fibrils by virtue of intercomponent interactions. On the other hand, circumstances could arise in which the microfibrils have been so severely modified by the treatment that they become contractile themselves to an even greater extent than is the matrix. In these circumstances the latter, having contracted to its maximum extent by chain disorientation, would tend to exert a restrictive action on any further fibrillar contraction.

In a scheme of this sort it seems clear that supercontraction effects might depend to an important extent on linkages between the microfibrils and the interfibrillar material and that if such linkages exist contraction might be facilitated if they are broken. In this connection it is relevant to note that in our experience treatments which are effective in leaving the fibers in a condition where well-marked fibrillation can be brought about are very often also effective in inducing supercontraction, actual or potential. The separation of the microfibrils would, of necessity, imply the breakdown of any linkages of the type considered.

With reference to the structure of the interfibrillar material there are two points to note. Very often, when distinct microfibrils can be seen in the electron micrographs, there also appears to be a filmy seemingly structureless material overlying them; more frequently, however, the sheets of microfibrils seem to have some sort of globular remains (similar to the material observed by Farrant, Rees, and Mercer [5]) scattered over them, and sometimes traces of regularity appear in the arrangement of these globules. This suggests that the matrix may consist, at least in part, of an orderly arrangement of globular material; if this is, in fact, the case it would seem that the globular matrix must be located between the sheets of microfibrils rather than between the microfibrils in the sheets, since no clear evidence has been found for interfibrillar globules in the sheets. The idea of an orderly globular matrix would, if accepted, lead to an alternative possible explanation of the "high period" X-ray reflections [4, 14]; it could thus give a histological interpretation of Astbury's idea of the existence of an "actin-like" component in keratin [2].

Summary

Examination in the electron microscope of keratin supercontracted by various techniques shows that no important deformation, other than shortening, occurs in the microfibrils. The supercontraction phenomena may depend on interactions between the microfibrils and an interfibrillar matrix, each component being contractile under suitable conditions. The possibility that the matrix located between microfibrillar sheets has an orderly globular configuration is suggested.

Acknowledgments

The authors wish to acknowledge their indebtedness to the Courtaulds' Scientific and Educational Trust Fund and to the International Wool Secretariat for financial help which enabled this work to be carried out.

Literature Cited

1. Alexander, Fox, and Hudson, *Biochem. J.* **49**, 554 (1951).
2. Astbury, *Proceedings of the 6th International Congress of Experimental Cytology*, Stockholm, p. 234 (1947).
3. Astbury and Woods, *Trans. Roy. Soc.* **A232**, 333 (1933).
4. Bear and Rugo, *Ann. N. Y. Acad. Sci.* **35**, 53 (1949).
5. Farrant, Rees, and Mercer, *Nature* (London) **159**, 535 (1947).
6. Hanson and Huxley, *Nature* (London) **173**, 973 (1954).
7. Jeffrey, Sikorski, and Woods, in preparation.
8. Kondo and Horio, TEXTILE RESEARCH JOURNAL **23**, 273 (1953).
9. Mercer, Ph. D. thesis, Leeds (1948).
10. Mercer, *Nature* (London) **163**, 18 (1949).

11. Mercer, TEXTILE RESEARCH JOURNAL **22**, 476 (1952).
12. Mercer, TEXTILE RESEARCH JOURNAL **23**, 380 (1953).
13. Mercer and Rees, *Australian J. Exp. Bio. Med. Sci.* **24**, 175 (1946).
14. McArthur, *Nature* (London) **152**, 38 (1943).
15. Rudall, "Fibrous Proteins, Symposium," *J. Soc. Dyers and Colourists*, p. 15 (1946).
16. Sikorski, Reports Conference on Electron Micr., *Brit. J. Appl. Phys.* **4**, 1 (1953).
17. Speakman and Whewell, *J. Soc. Dyers and Colourists* **52**, 380 (1936).
18. Stoves, *Trans. Faraday Soc.* **62B**, 245 (1946).
19. Whewell and Woods, "Fibrous Proteins, Symposium," Soc. Dyers and Colourists, p. 50, 1946.
20. Woods, *Proc. Roy. Soc.* (*London*) **A166**, 76 (1938).

Manuscript received February 9, 1955

Experimental Study of the Viscoelastic Properties of Textile Fibers

Dynamic Measurements from Subsonic to Supersonic Frequencies

K. Fujino, H. Kawai, and T. Horino[1]

Abstract

The viscoelastic properties of some commercial textile fibers were measured by means of several longitudinal-vibration methods over a range of frequency from 2×10^{-1} to 2×10^{5} cps at 20°C, 65% R.H., under a static tension of 0.4 g/den and a dynamic strain of less than 0.1%.

In the above experiments, the nonlinear characteristics of vibrational properties were negligibly small, and the experimental results were described by the complex dynamic modulus function $E^*(\omega)$ on the assumption that the Boltzmann superposition principle was valid.

Generally speaking, for all the textile fibers tested the real part of the complex dynamic modulus was found to be flat over this frequency range except there was some increase in the supersonic range. The imaginary part of the complex dynamic modulus, on the other hand, seemed to increase at both ends of the frequency range covered.

It was concluded from our experimental results that for any textile fiber there is not so anomalous a dispersion as that of various rubberlike materials found in the same frequency range.

Furthermore, according to the method of representation by a continuous distribution of relaxation times, the shape of the so-called "relaxation spectrum" of any textile fiber was found to be fairly flat over the relaxation-time range from 1×10^{-6} to 1×10^{0} sec. With the exception of slight increases at both ends of this relaxation-time range the spectrum can be represented by the so-called "box distribution." This is very different from the spectra of rubberlike materials over the same relaxation-time range.

Introduction

For linear viscoelastic substances, the mechanical behavior is fully described by any one of the following phenomenological functions, namely, the stress-relaxation function $\Psi(t)$, the creep function $\Phi(t)$, the complex dynamic modulus function $E^*(\omega)$, and the complex dynamic compliance function $J^*(\omega)$ [14, 25, 43]. As is well known, assuming a mechanical model of the generalized Maxwell or Voigt type in which the relaxation times τ_i or retardation times λ_i are continuously distributed from zero to infinity, the above-mentioned phenomenological functions are represented by the following respective mathematical expressions [1, 14, 25, 42]:

$$\Psi(t) = \int_0^\infty E(\tau) e^{-t/\tau} d\tau \qquad (1)$$

[1] Department of Textile Chemistry, Faculty of Engineering, Kyoto University, Kyoto, Japan.

$$E^*(\omega) = E_1(\omega) + iE_2(\omega) \tag{2}$$

where

$$E_1(\omega) = \int_0^\infty E(\tau) \frac{\omega^2\tau^2}{1 + \omega^2\tau^2} d\tau \tag{2'}$$

$$E_2(\omega) = \int_0^\infty E(\tau) \frac{\omega\tau}{1 + \omega^2\tau^2} d\tau \tag{2''}$$

and

$$E(\tau)\, d\tau = \sum_{\tau<\tau_i<\tau+d\tau} E_i \tag{3}$$

$$\Phi(t) = \int_0^\infty J(\lambda)(1 - e^{-t/\lambda})\, d\lambda \tag{4}$$

$$J^*(\omega) = J_1(\omega) - iJ_2(\omega) \tag{5}$$

where

$$J_1(\omega) = \int_0^\infty J(\lambda) \frac{1}{1 + \omega^2\lambda^2} d\lambda \tag{5'}$$

$$J_2(\omega) = \int_0^\infty J(\lambda) \frac{\omega\lambda}{1 + \omega^2\lambda^2} d\lambda \tag{5''}$$

and

$$J(\lambda)\, d\lambda = \sum_{\lambda<\lambda_i<\lambda+d\lambda} J_i \tag{6}$$

where E_i and J_i are partial modulus and partial compliance which correspond to τ_i and λ_i in the generalized Maxwell and Voigt models respectively.

The functions $E(\tau)$ and $J(\lambda)$, which are defined by equations (3) and (6) and which are related by the above-mentioned integral equations with the phenomenological functions, are generally called the "relaxation spectrum" and the "retardation spectrum," or sometimes the distribution function of relaxation times and that of retardation times, respectively. But this latter terminology might seem unsuitable because, as defined by equations (3) and (6), they are not the distribution functions in the usual sense and express directly neither the distribution density of relaxation times nor that of retardation times.

These new functions, nevertheless, have many advantages over the phenomenological functions not only in the description of viscoelastic behavior of materials but also in the consideration of correlation between the mechanical behavior and its molecular significance. Namely, once any one of these spectra is determined, all other phenomenological functions and quantities, such as the relaxation function, the creep function, the steady-flow viscosity, and the instantaneous elasticity can be predicted [1, 2, 16, 23, 46]. Furthermore, these spectra can easily be represented by a mechanical model consisting of springs and dashpots and are also represented as a function of relaxation time or of retardation time, which can be considered as an "internal time scale," characteristic of the relaxation or of the retardation of the internal structural elements.

The determination of the spectrum from one of these phenomenological functions is just the solution of these integral equations which are formally Fredholm's linear integral equations of the first kind. This had been performed rigorously by Gross [14, 15] and by Gross and Pelzer [17], using inverted Laplace transformations. But this can only be done when a phenomenological function is given as an analytical function, which never occurs in practice, and so some approximate methods are usually adopted to determine the spectrum.

In the present paper, the relaxation spectra of several commercial textile fibers, which are typical high-polymeric solids, are determined by means of the so-called "zeroth order approximation method" from the imaginary part of the complex dynamic modulus obtained from several longitudinal-vibration experiments over a relatively wide frequency range, and then they are compared with those of several rubberlike materials reported by other authors.

At present, there is no definite foundation by which the spectra can be explained in terms of the molecular structure, while the spectra have many advantages over the phenomenological functions, as mentioned above. To enable us to progress and to understand the relation between molecular structure and mechanical behavior, it is absolutely necessary not only to develop the molecular theories of viscoelastic behavior, which have been recently proposed again, although these may be still crude, by some authors [5, 37, 41, 49], but also to accumulate experimental results on several typical high polymers under a wide range of conditions where the distinctions of molecular structure may be represented.

General Procedure

In all the experiments, the vibrational strain was always limited to pure longitudinal mode only and was kept smaller than 0.2% to simplify the mathematical description of results. But it is well known that on account of the special shape of textile fibers; that is to say, the length of a specimen is very great compared to its cross-sectional dimension, compressional deformation is not realizable. Consequently, in order to avoid this drawback, as in several individual experimental procedures mentioned subsequently, the initial static strain should always be kept larger than the vibrational strain by application

of a definite static load upon the sample strips. But, strictly speaking, this initial static condition depends upon the actual construction of the individual apparatus and upon the procedures for using it. For example, the sample strip must be fixed in length during the experiment with one apparatus, and hence the initial definite static tension would be relaxed gradually. On the other hand, a constant tension is used with another apparatus, and so the static creep caused by the static tension is unavoidable. In other words, the former is a vibrational experiment under stress relaxation and the latter is one under creep of strain.

The magnitude of the dynamic-strain amplitude itself was always kept smaller than 0.2%, as mentioned above, but the actual magnitude varied in the opposite direction to the frequency range of the apparatus.

As mentioned in the introduction, to determine the relaxation spectrum from dynamic measurements, it is necessary to describe the experimental results by the complex dynamic modulus $E^*(\omega)$ as a function of angular frequency ω over as wide a range as possible. For linear viscoelastic substances, the complex dynamic modulus is defined by the ratio of complex amplitude of sinusoidal stress to that of strain. If the mechanical behavior under a given angular frequency ω is described by a single retarded elastic model, that is to say, a single Voigt element, the following simple mathematical relations can easily be obtained:

$$E_1(\omega) = E$$
$$E_2(\omega) = \xi\omega \qquad (7)$$

and

$$\tan \delta(\omega) = E_2(\omega)/E_1(\omega)$$

where $E_1(\omega)$ and $E_2(\omega)$ are the real and imaginary parts of the complex dynamic modulus; E and ξ, the tensile modulus of elasticity and the coefficient of normal viscosity, respectively, in a single Voigt element; and tan δ the so-called mechanical-loss tangent in which δ is the phase difference between stress and strain amplitudes.

Our experimental objective was to determine $E_1(\omega)$ and $E_2(\omega)$ as a function of applied angular frequency over as wide a range as possible by means of several suitable experimental methods. The theory of each type of measurement given subsequently has been derived on the assumption that the material

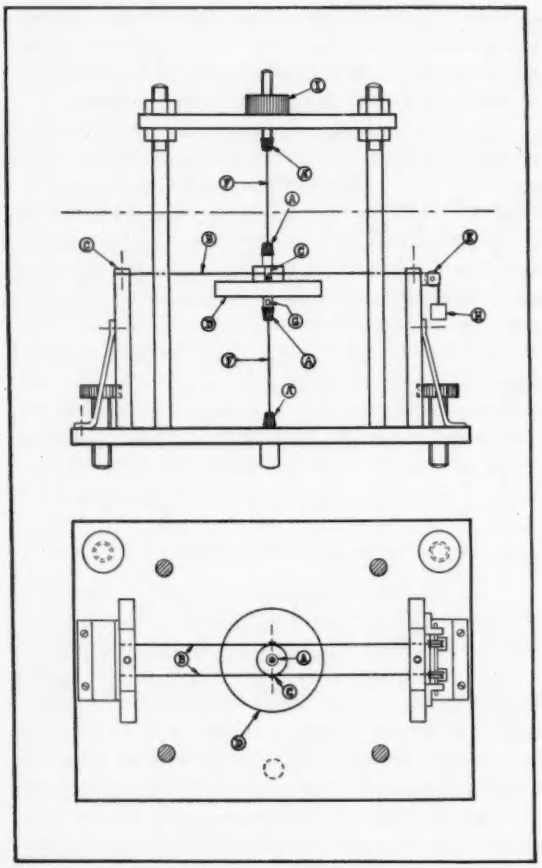

Fig. 1. Apparatus used in the subsonic frequency range.

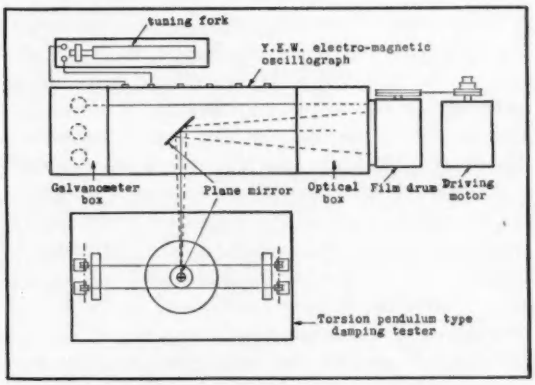

Fig. 2. Arrangement of the same apparatus.

under test behaved like a single Voigt element. The experimental results showed in fact that $E_1(\omega)$ and $E_2(\omega)/\omega$ were not independent of frequency, as was assumed. However, it can be shown that even when the viscoelastic properties must be represented by a spectrum the above assumption does in fact lead to the correct values of $E_1(\omega)$ and $E_2(\omega)$ [28].

By reason that the deformation of the sample strip was of a simple tensile mode and that the dimensions of a single textile fiber were too small for accurate experimentation, the sample strips, except in the case of raw silk, were always prepared as a bundle of single fibers by untwisting ordinary commercial multiple-filaments yarn of about 100 den. Sample strips were preconditioned under standard air conditions, 20°C, 65% R.H., for several days, and the experiments were also carried out under these same air conditions.

Apparatus and Experimental Procedures

In order to obtain the relaxation spectrum, it is necessary to carry out the vibration experiment over as wide as possible a range of frequency. A single apparatus, however, is not available for such a wide-range experiment; several types of apparatus were constructed, and they offered in these experiments a range of frequency from 2×10^{-1} to 2×10^{5} cps.

1. *Apparatus Employed in the Subsonic Range*

The measurements over this frequency range were carried out by means of the free damping vibration method, and the frequency range could cover from 2×10^{-1} to 2×10^{1} cps.

The drawing of the construction of the apparatus employed is shown in Figure 1, where D is a circular disc which has a known moment of inertia referred to its rotational axis. The circular disc is also fixed tightly by two chucks, A's, to a piece of piano wire, F, which is vertically stretched by an adjustable screw I between two chucks, A''s, of which the bottom one is fixed to the foundation and the upper one to the upper platform through the adjustable screw I. B's are sample strips which are horizontally stretched by a definite dead weight, H, through the idler pulleys, E's, and which are fixed at each end and at the center of their effective length by the sample clamps, C's, to the foundations and to the circular disc respectively. G is a small plane mirror cemented on the circular disc. Consequently, this forms a combined oscillation system in which the torsional oscillation system, consisting of a circular disc and a piano wire, is restrained by tensile alternating deformation of parallel sample strips. This is similar in principle to that adopted by Künzle [24], Nielsen [30], Schmieder et al. [38], and Heyboer et al. [18] for torsional experiments.

Figure 2 is a schematic diagram showing the general arrangement of the apparatus. The torsional free-damping oscillation of the circular disc is started by a mechanical exciter from a definite angular displacement. This oscillation is recorded together with a time signal generated from the tuning fork on the film drum by the aid of an optical system consisting of the two plane mirrors and the optical box of a Y.E.W. N-3 type electromagnetic oscillograph, as illustrated in Figure 2.

Figure 3 shows the calibration diagrams of the angle of oscillation of the circular disc against the displacement of spot on the film drum and the longitudinal-strain amplitude of the sample strip under the actual procedures. As illustrated in this figure,

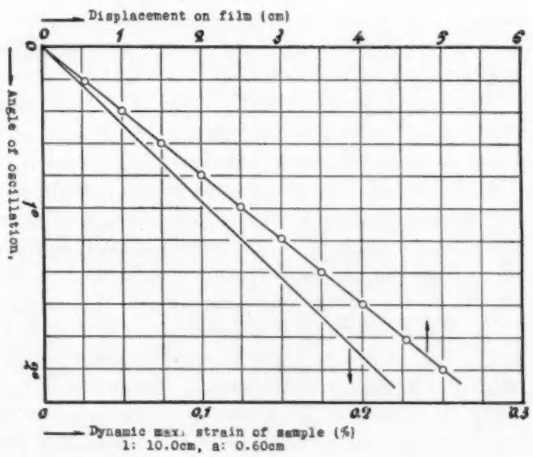

Fig. 3. Calibration diagram for the same apparatus.

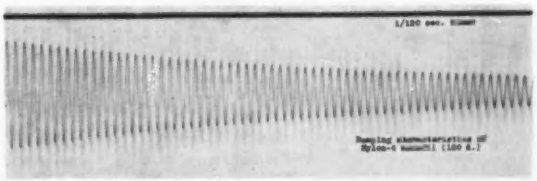

Fig. 4. Record obtained from the same apparatus.

good linear relations between them are obtained when the oscillation angle is kept smaller than 2°, which always corresponds to the starting angle of oscillation of the circular disc under actual conditions.

Figure 4 is one of the typical records obtained by this apparatus. On analyzing the amplitude dependences both of the logarithmic decrement of the amplitude and of the period of oscillation, it is found that there are hardly any striking amplitude dependences in them with the exception of slight decrease of logarithmic decrement with decreasing amplitude; this is, however, somewhat marked in regenerated cellulose fibers.

Then, considering the nonlinear effects, the fundamental equation of angular motion of the system referring to the axis of rotation may be given as follows:

$$\alpha\ddot{\theta} + \beta f(\theta, \dot{\theta}) + \gamma\theta = 0 \qquad (8)^2$$

In an approximate representation by which the damped oscillation just mentioned is reduced to a linear one with neglect of nonlinear effects, equation (8) may be written as follows:

$$\alpha\ddot{\theta} + \beta\dot{\theta} + \gamma\theta = 0 \qquad (8')$$

where θ is the angular displacement of the circular disc at time t; α is the effective moment of inertia of the system referred to the axis of rotation and is approximately equivalent to that of the circular disc; β is the coefficient of nonrestored torque which is proportional to the angular velocity and which may be due to internal friction of the sample strips and of the piano wire as well as to air friction resulting from the rotation. It is possible to make the latter two frictional effects negligibly small by the suitable choice of the material, of the conditions for supporting the piano wire, and of the shape of the rotating parts of the apparatus which give rise to air friction. The parameter γ is the coefficient of restored torque, which is proportional to angular displacement and which arises from the linear elastic properties of the piano wire and the sample strips.

Since the angular displacement θ is always kept very small, equation (8′) may be rewritten as follows by substituting the actual dimensions of the apparatus and the sample strips:

$$I\ddot{\theta} + (\xi(4S/l)a^2)\dot{\theta} + (E(4S/l)a^2 + b)\theta = 0 \qquad (9)$$

where E is the tensile modulus of elasticity of the sample strip; ξ, its coefficient of normal viscosity; l, its effective length between the clamps; s, its effective cross-sectional area; I, the moment of inertia of the circular disc referring to its axis; a, the distance between the rotational axis and the sample clamp; and b, the torsional constant of the piano wire.

From the solution of equation (9) under the condition of free damped oscillation, the following mathematical expressions for E and ξ can easily be obtained:

$$E = lI/Sa^2\{\pi^2 + (\ln \Delta)^2/T^2 - \pi^2/T_0^2\} \qquad (10)$$

and

$$\xi = lI/Sa^2 \ln \Delta/T \qquad (10')$$

where T and T_0 are oscillating periods of the system containing the sample strips and that of the system not containing them, respectively; and $\ln \Delta$ is the logarithmic decrement of the amplitude in damped oscillation. Thus the two mechanical parameters, E and ξ, can be determined from the measurable quantities T, T_0, and $\ln \Delta$.

As mentioned previously, equations (10) and (10′) give correctly the values of $E_1(\omega)$ and $E_2(\omega)/\omega$ when these are functions of frequency.

As to the practical procedures in this experiment, the maximum angular displacement of the circular disc was always kept at 2°; this was equivalent to about 0.2% longitudinal dynamic strain of the sample strip; the initial static tension of the sample strip was always kept at a definite value, about 0.4 g/den, by applying a dead weight to the sample strip; and changing of the angular frequency of the system was carried out by changing the moment of inertia of the circular disc from 3×10^2 to 3×10^5 cgs or by changing the diameter of piano wire from

[2] One of concrete forms of the equation may be represented as follows [11]:

$$\alpha\ddot{\theta} + \sum_i \sum_j \beta_{ij}\dot{\theta}|\dot{\theta}|^{p_i}|\theta|^{q_j} + \sum_k \gamma_k\theta|\theta|^{r_k} = 0 \qquad (8'')$$

where β_{ij} and γ_k are the coefficients of a nonrestored torque and of a restored one respectively; and p_i, q_j, and r_k are constants and are assumed, for convenience's sake, to be integers where $p_i + 1$, q_j and $r_k + 1 \geqq 0$.

In a first-order approximation in which the second and third terms on the left-hand side of equation (8″) are limited by one term and in which p_1, q_1 and r_1 are equalized to 0, the equation is identical to equation (8′).

0.3 to 1.5 mm, instead of changing the shape factor of the sample strip.

2. *Apparatus Employed in the Low-Audio Range*

In order to extend the frequency range of the experiment, the forced longitudinal-vibration method was adopted, and thus the frequency range could be increased up to about 5×10^2 cps.

Because the apparatus and the principle employed here are essentially the same as that which had been adopted by Gehman et al. for various gum stocks [13], by Lyons et al. for the strips of textiles in the so-called "stretch vibrometer" [27], by Dunell et al. for a single filament [6], and by Palandri for various tire cords [36], it may be unnecessary to describe the details with the exception of some modifications.

Figure 5 is the schematic diagram of the apparatus and Figure 6 is the drawing of its driving part rebuilt from a loud-speaker unit, where the A's represent sample strips stretched by a definite dead weight, D, through the idler pulleys, C's. The sample strips are also connected to both the ends of a horizontally movable light spindle, F, and they can be clamped at any point along their length by means of the movable clamps, B's. H is a removable mass loading the whole vibrator unit from about 8 to 50 g. E is a solenoid coil cemented on the spindle, F, and is located in the radial magnetic field which traverses an annular space between both poles of a magnetic core, I, and L is the exciting coil of this magnetic core. A horizontal movable spindle, F, is hung at each end and aligned by the aid of fine nylon threads of about 15 den, which are radially stretched by the adjustable screws, K's, mounted on the ring, J.

When direct and alternating currents are imposed on the exciting coil, L, and the driving coil, E, respectively, the longitudinal forced vibration of the system is excited.

Figure 7 shows the general arrangement of the whole apparatus. The above-mentioned vibrating system is built onto a lathe bed and is located across the optical system which measures the amplitude of vibration of the spindle by means of a photoelectric method. Since the driving of spindle, F, is effected by supplying the alternating current from the audio-frequency power amplifier to the solenoid coil, the amplitude of this driving force can be determined by measuring the current through this coil, namely, by measuring the voltage difference between the ends of a pure resistance coupled in series with the solenoid coil.

Figure 8 is the calibration diagram to determine the actual amplitudes of the driving force and of the displacement of the vibrating spindle from readings of the vacuum-tube voltmeter by means of the double-pole double-throw switch; the latter amplitude must be divided by the frequency characteristic factor of the phototube amplifier shown in Figure 9.

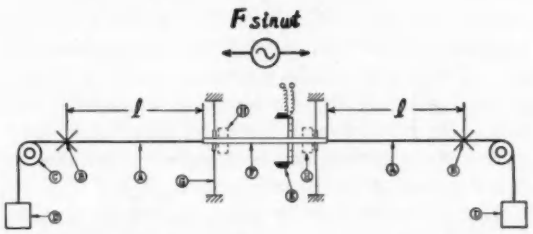

Fig. 5. Diagram of apparatus used in the low audio frequency range.

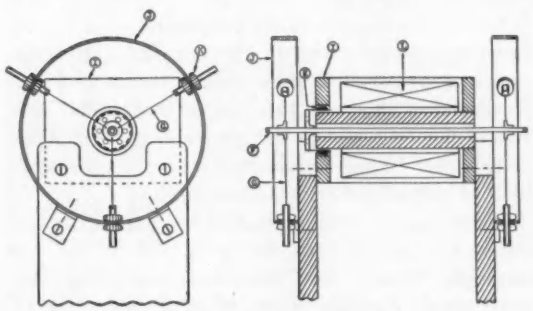

Fig. 6. Driving part of the same apparatus.

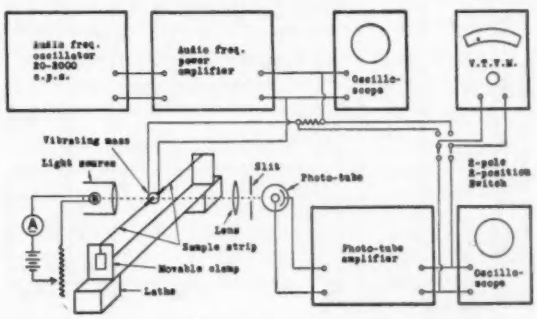

Fig. 7. General arrangement of the same apparatus.

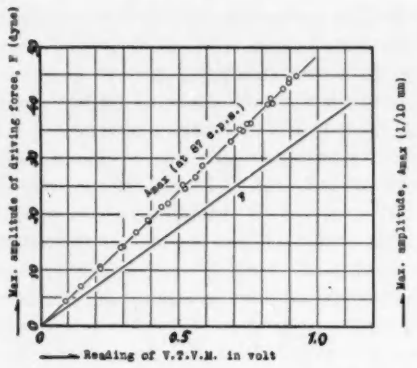

Fig. 8. Calibration diagram for the same apparatus.

The slit arranged before the phototube, as illustrated in Figure 7, can be revolved from its normal vertical position to a horizontal one to examine a vibration pattern of the spindle.

The mechanical behavior of the sample strips under a small harmonic driving strain may well be represented by a single Voigt element. Again, when the amplitude of the vibrator itself is kept relatively small, there is hardly any noticeable nonlinear behavior. Hence the fundamental equation of motion of the vibrator under a harmonic driving force, $F \sin \omega t$, can be approximated as follows:

$$\alpha\ddot{\chi} + \beta\dot{\chi} + \gamma\chi = F \sin \omega t \qquad (11)$$

where χ is displacement of the vibrator at time t; α is the effective mass of the vibrating system; β is the coefficient of nonrestored force proportional to the velocity of the vibrator; and γ is the coefficient of restored force proportional to the displacement of the vibrator.

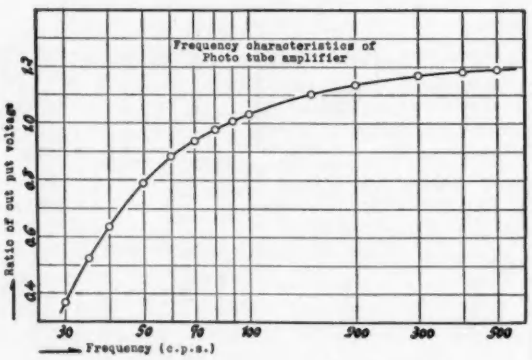

Fig. 9. Phototube amplifier of the same apparatus.

By substituting the resonance conditions of the system into the steady-state solution of equation (11), the final mathematical relations between two coefficients, β and γ, and measurable quantities are obtained under some adequate assumptions as follows:

$$\gamma = M\omega_0^2 \qquad (12)$$

and

$$\beta = F/(A_{\max} \cdot \omega_0) \qquad (13)$$

or

$$\gamma = M_0\omega^2 \qquad (12')$$

and

$$\beta = F/(A_{\max} \cdot \omega) \qquad (13')$$

Equations (12) and (13) are for a frequency-tuning experiment and equations (12′) and (13′) for a mass-tuning one. $A_{\max}$ in equations (13) and (13′) is the maximum amplitude of the vibrator at resonance; ω_0, the resonance angular frequency in a constant mass experiment; and M_0 the resonance mass in a constant angular-frequency experiment.

Now, as already mentioned by Dunell et al. [6], the effective mass of the system is not merely equivalent to the algebraic sum of the masses of the system but to the sum of mass of the vibrator itself and the effective mass of the appendages. But the mass of the appendages is very small in comparison with that of the vibrator, and, therefore, the effective mass of the whole system may be approximately taken as equal to that of the vibrator itself.

The two coefficients, β and γ, appear to be composed of contributions not only from the sample strip here represented by a single Voigt element but also from the appendages, particularly the spindle suspensions at each end. But, strictly speaking, it is very doubtful that the latter contribution can be represented only by a simple mathematical representation such as equation (11) without nonlinear terms. Nevertheless, the fact that no noticeable nonlinear effects can be found in the vibration pattern of the system may be merely ascribed to the small magnitude of the vibration amplitude itself.

Some experimental evaluation concerning the restored and nonrestored forces caused by the appendages showed that these forces are negligibly small compared to those caused by the sample strip. Hence equations (12) and (13) may be rewritten

as follows by assuming β and γ to be equivalent to the coefficients of the sample strip:

$$2SE/l = M\omega_0^2 \qquad (12'')$$

and

$$2S\xi/l = F/(A_{max}\cdot\omega_0) \qquad (13'')$$

Thus, the two mechanical parameters, E and ξ, can be determined from the measurable quantities, ω_0, F, and A_{max}, at the resonance of the system. It seems necessary, however, to check the validity of neglecting nonlinear forces caused by the suspensions, especially in the experiments at relatively large vibration amplitudes.

In practice, the experimental conditions were as in the previous apparatus; namely, the longitudinal dynamic strain and the initial static tension were always kept at definite values, 0.1% and about 0.4 g/den respectively, and the experimental frequency, that is to say, a resonance frequency of the system, was changed by altering the effective mass of the system from 8 to 50 g and by changing either the length of the strips from 5 to 25 cm or the number of strips from one to several. Thus, the frequency range could cover from 5×10 to 5×10^2 cps.

3. *Apparatus Employed in the Frequency Range from Higher Audio to Supersonic*

By means of the longitudinal forced vibration method just mentioned, it was in practice difficult to experiment at higher frequencies than several hundred cycles per second on account of the various restrictions concerning the effective mass of the system, the shape factor of sample strips, and some disturbances of vibration. It was then necessary once again to change the experimental method to reach a higher frequency range.

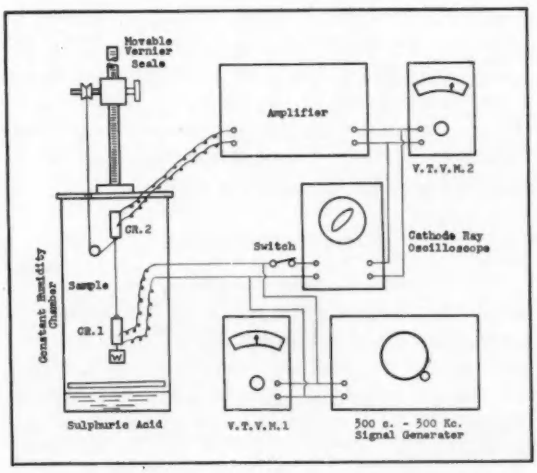

Fig. 10. Arrangement of the apparatus used in the frequency range from high audio to supersonic.

The experimental frequency range was expanded by means of the longitudinal wave resonance method mainly in the higher-audio frequency range and by means of the longitudinal wave propagation method mainly in the supersonic range, respectively; consequently the frequency range could cover from 2×10^3 to 2×10^5 cps.

Although the principles employed here are essentially the same as those mentioned by Nolle [33] in 1948, the apparatus is of a vertical type similar to that used by Kawai and Tokita [22, 47] and different from the horizontal one used by Ballou and Silverman et al. [3, 4, 19, 20, 32, 33, 48] since 1944 for the propagation method. The conventional one has an unavoidable defect that a contact condition between sample strip and wave detector is hardly kept constant during observation and consequently high accuracy of determination of attenuation constant is not expected.

Figure 10 is the general arrangement of apparatus, where *CR.1* and *CR.2* are the driving and receiving crystals respectively, which are cut out from a single crystal of Rochelle salt to be available for longitudinal-vibration experiments. The sample strip is connected at one end to the driving crystal and at the other to the vertically movable vernier scale, which is used for changing the effective length of the sample strip through an idler pulley and a hook cemented on the receiving crystal. The driving crystal is not only driven by the output from the variable-frequency signal generator but is also used as a dead weight together with the additional weight W. The cathode-ray oscilloscope is used to measure the phase difference between the voltages on the sending and receiving crystals to determine the wave length. Again, the two vacuum-tube voltmeters, *V.T.V.M.* 1 and *V.T.V.M.* 2, are also used to measure the relative values of voltage amplitudes on sending and receiving crystals respectively.

Therefore, this apparatus can be used for both the above-mentioned methods. For the longitudinal wave resonance method the so-called resonance curve of the output voltage is obtained from *CR.2* against

the driving frequency on *CR*.1 while keeping the length of sample strip constant; for the longitudinal wave propagation method the output voltage on *CR*.2 is measured while keeping the driving frequency and voltage on *CR*.1 constant.

When one assumes here again that the nonrestored force is proportional to the rate of change of strain and that the restored force is proportional to the strain itself, the following well-known wave equation results:

$$\rho(\partial^2\mu/\partial t^2) = E(\partial^2\mu/\partial\chi^2) + \xi(\partial^3\mu/\partial\chi^2\,\partial t) \quad (14)$$

where μ is the instantaneous displacement of a cross-section of the sample strip in the χ direction; E, the tensile modulus of elasticity; ξ, the coefficient of normal viscosity; and ρ, the density of the material.

Assuming that the driving force on the sample is a sinusoidal one of angular frequency ω, then the steady-state solution of equation (14) is given by the well-known equation as follows:

$$\mu = (A_1 e^{c\chi + id\chi} + A_2 e^{-(c\chi + id\chi)})e^{i\omega t} \quad (15)$$

where A_1 and A_2 are constants which must be determined from the initial and boundary conditions of the experiments and c and d are attenuation constant and factor of phase shift respectively, and they are represented as follows:

$$c^2 = (\rho\omega^2/2)\{(E^2 + \omega^2\xi^2)^{\frac{1}{2}} - E\}/(E^2 + \omega^2\xi^2) \quad (16)$$

and

$$d^2 = (\rho\omega^2/2)\{(E^2 + \omega^2\xi^2)^{\frac{1}{2}} + E\}/(E^2 + \omega^2\xi^2) \quad (17)$$

Furthermore, the two mechanical parameters of the sample strip, E and ξ, are introduced from equations (16) and (17) as follows:

$$E = \rho v^2\omega^2(\omega^2 - c^2v^2)/(\omega^2 + c^2v^2)^2 \quad (18)$$

and

$$\xi = 2\rho cv(\omega v)^2/(\omega^2 + c^2v^2)^2 \quad (19)$$

For $(cv)^2 \ll \omega^2$, $E \simeq \rho v^2$ (18′)

and

$$\xi \simeq 2\rho cv^3/\omega^2 \quad (19')$$

where v is propagation wave velocity and is equal to ω/d.

Equations (18) and (19) relate the normal viscosity coefficient ξ and the tensile modulus of elasticity E to the propagation constants, c and v, at a given angular frequency ω.

The final equations, which are available for the determination of propagation constants, can be introduced by substituting suitable experimental conditions into equation (15). It had been done by Nolle [33] for the longitudinal wave resonance method and by Ballou and Smith [4] and Hillier and Kolsky [19] for the longitudinal wave propagation one, respectively. Hence, it seems unnecessary to describe the details again here.

Both the upper and lower limits of the frequency range covered by these experimental methods are determined theoretically by the acoustical shape of the sample strip and practically by the dimension of the apparatus, respectively. The upper limit in our experiments, however, was in practice about 200 kc, which was appreciably lower than the theoretical one on account of some experimental difficulties. On the other hand, the lower limit was about 40 kc for the propagation method and about 2 kc for the resonance one, being limited by the effective height of the closed vessel in which the sample strip was maintained. Hence experiments in the higher frequency range were carried out mainly by the former method; those in the lower frequency range, mainly by the latter.

The static tension of the sample strip was as nearly as possible the same as in the previous experiments. However, in this case the dynamic experiment was under creep and the previous experiments were under stress relaxation caused by clamping the sample during vibration. The dynamic-strain amplitudes were extremely small compared with those in the previous experiments. These differences in the experimental conditions should be taken into account in comparing the results obtained by the different methods.

Experimental Results

The complex dynamic modulus $E^*(\omega)$ was evaluated by substituting the results of two mechanical parameters, E and ξ, into equation (7) and was represented by the real and imaginary parts, $E_1(\omega)$ and $E_2(\omega)$, in d/cm^2. The results are plotted in Figures 11–16 as a function of applied frequency for each fiber.

In any figure, the region lower than 30 cps is the result obtained by the first free-damping method;

the next region, from 40 to 400 cps, by the forced-vibration method; and the region higher than 1 kc by the acoustic methods.

The results of raw silk in the highest frequency range are plotted as open circles. This is because the accuracy of measurement was somewhat low on account of multiple reflections.

As illustrated in these figures, some discontinuities between each region are observed, which may be caused by the difference between each experimental

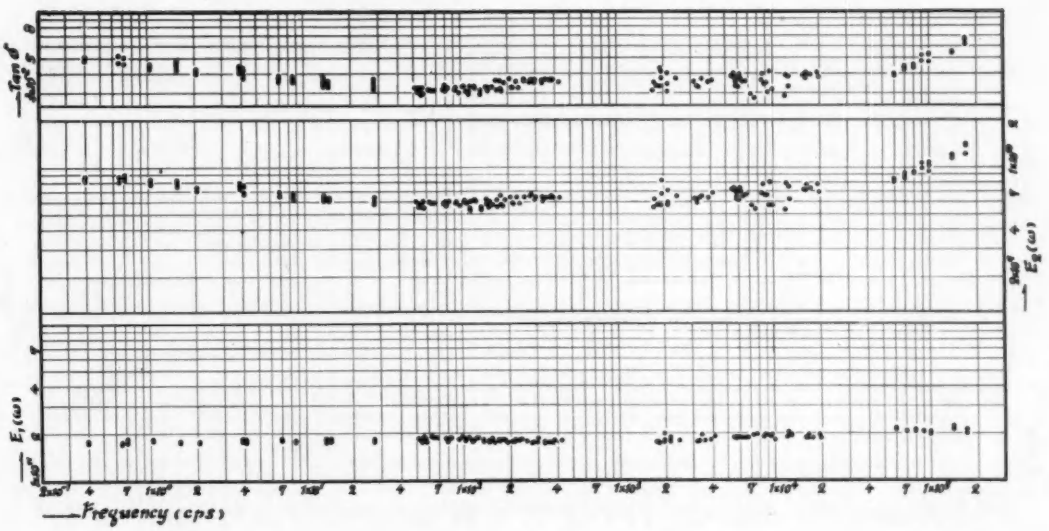

Fig. 11. Bemberg rayon at 20°C, 65% R.H., under static tension of 0.50 g/den.

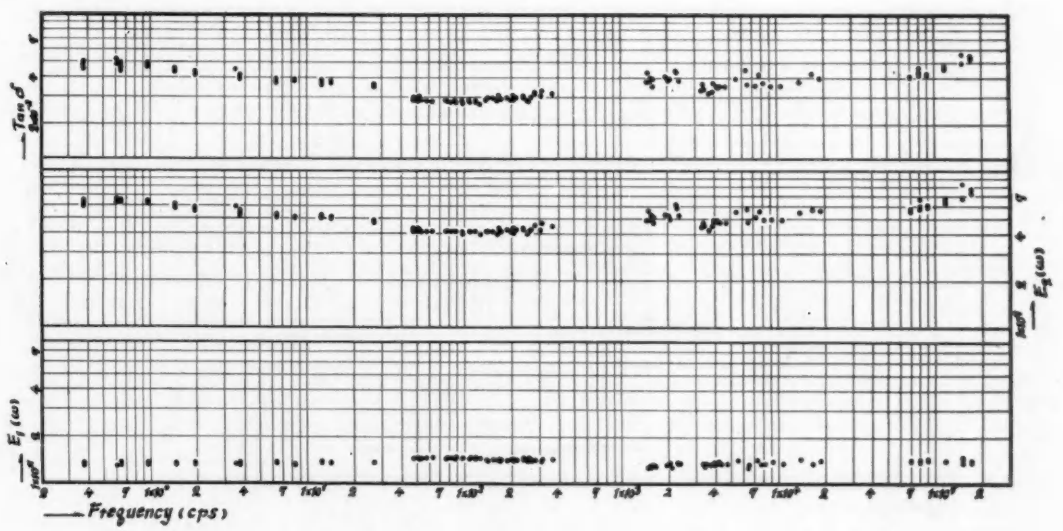

Fig. 12. Viscose rayon (normal) at 20°C, 65% R.H., under static tension of 0.47 g/den.

arrangement with reference to the nature of the applied static tension and to the magnitude of dynamic-strain amplitude. But these discontinuities seem to be too small to separate these whole results into two different categories, namely, the one obtained by the former two methods and the other obtained by the latter two acoustic methods.

In any fiber, the real part of the complex dynamic modulus $E_1(\omega)$ seems to increase very slightly with increase of the frequency except with some increase in the supersonic range, but the experimental errors are too serious to determine the exact frequency dependence. The results obtained by the longitudinal forced vibration method, as shown in some figures,

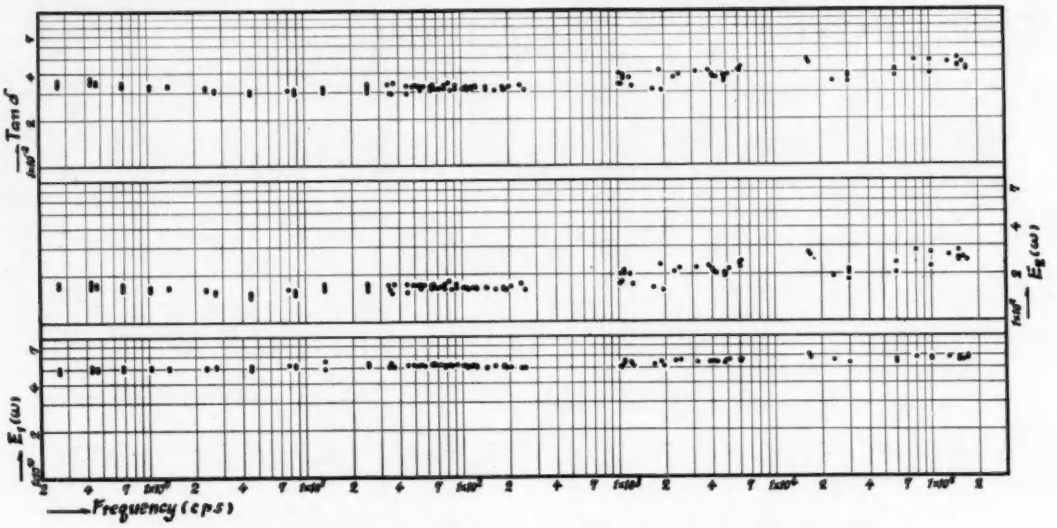

Fig. 13. Acetate rayon (normal) at 20°C, 65% R.H., under static tension of 0.35 g/den.

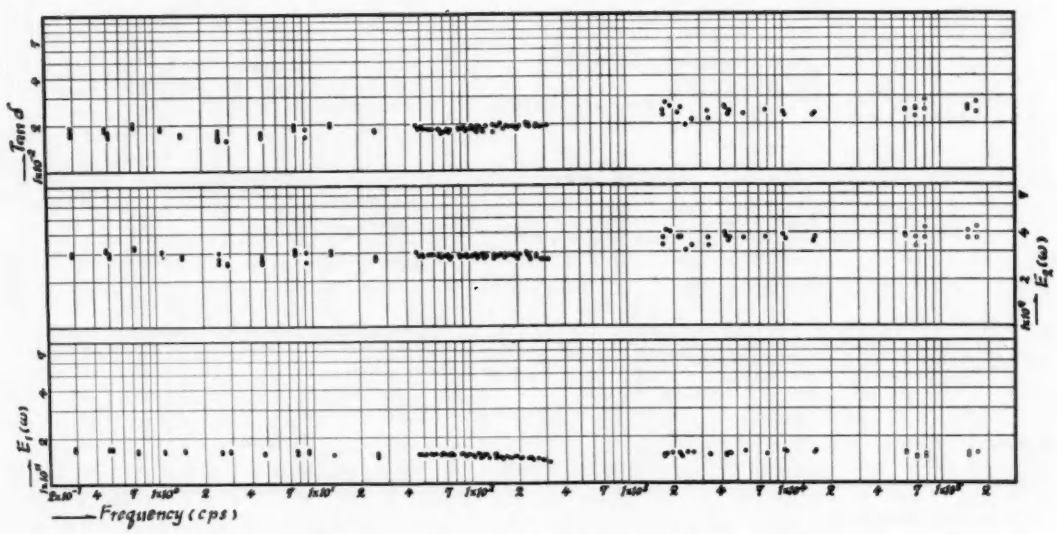

Fig. 14. Raw silk at 20°C, 65% R.H., under static tension of 0.42 g/den.

have usually a somewhat opposite tendency. This may be caused not by the property of the sample strip itself but rather by the instrument habits and may be attributed to the nonlinear restoring force caused by the vibrator suspension; the nonlinear restoring force may not be neglected for experiments at relatively lower frequencies where the magnitude of vibration amplitude necessarily becomes large.

The imaginary part of the complex dynamic modulus $E_2(\omega)$ has generally two different tendencies, namely, to increase with increasing frequency in the supersonic range and to increase with decreas-

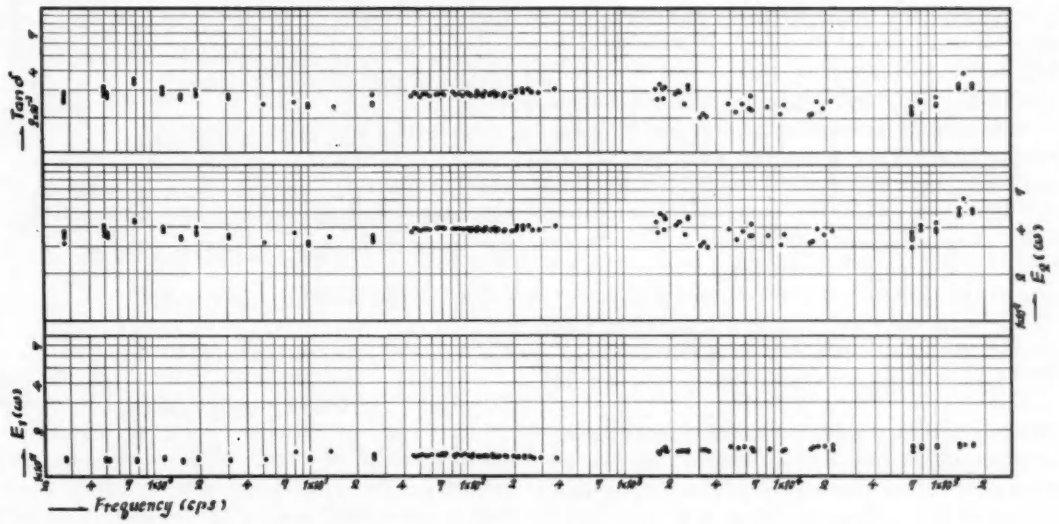

Fig. 15. Degummed silk at 20°C, 65% R.H., under static tension of 0.44 g/den.

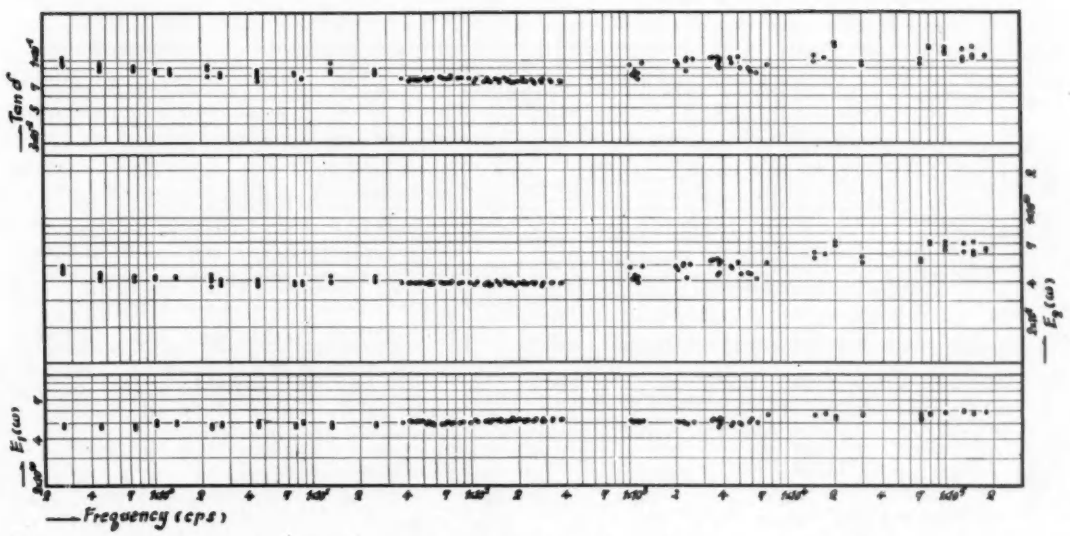

Fig. 16. Nylon-6 (polycapramide) at 20°C, 65% R.H., under static tension of 0.40 g/den.

ing frequency in the subsonic range. The former tendency generally appeared in all the fibers, and the latter is especially noticeable in regenerated cellulose fiber.

The frequency dependence of mechanical loss tangent, tan δ, is similar to that of the imaginary part of the complex dynamic modulus.

The striking anomalous dispersion of the complex dynamic modulus that was discovered for several rubberlike materials by Ivey et al. [21] and by Nolle [34] in the same frequency range is not detected in these textile fibers, but the real part of the complex dynamic modulus increases gradually, and the imaginary part has an almost constant value over several logarithmic decades of the frequency, suggesting that the dispersion occurs over nearly the whole range. Accordingly, it is reasonable to describe the results by the continuous distribution of relaxation times rather than by a few relaxation times.

Then, it is necessary to obtain a complete spectrum of relaxation times adopting equations (2′) and (2″) in order to explain the mechanism involved.

The approximate methods classified from "zeroth" to higher-order approximations, which determine the spectrum from the phenomenological functions, have been presented by many authors [1, 2, 7, 8, 9, 12, 23, 26, 34, 39, 40, 44], and the determination of the relaxation spectrum from the dynamic-modulus function is usually done by differentiating the real part, $E_1(\omega)$, with respect to the logarithm of angular frequency. This conventional procedure is not very suitable for our results because, as mentioned above, the experimental results of any fiber do not give a sufficiently precise frequency dependence of the real part of complex dynamic modulus. Hence, in spite of somewhat lower accuracy theoretically, the approximate method of zeroth order to determine the spectrum from the imaginary part was adopted according to the following equation:

$$E'(\ln \tau) \simeq 2/\pi[E_2(\omega)]_{\omega=1/\tau} \tag{20}$$

where $E'(\ln \tau)$ is the relaxation spectrum in the logarithmic time scale and is related to the relaxation spectrum in linear time scale $E(\tau)$ as follows:

$$E'(\ln \tau) = \tau E(\tau) \tag{21}$$

which follows from the fact that by definition

$$E'(\ln \tau)\, d \ln \tau = E(\tau)\, d\tau \tag{22}$$

In Figure 17, the final results of the relaxation spectrum $E'(\ln \tau)$, in d/cm², are plotted as a function of relaxation time τ in seconds. Generally speaking, for any textile fiber, the spectrum seems to increase slightly at both ends of this relaxation

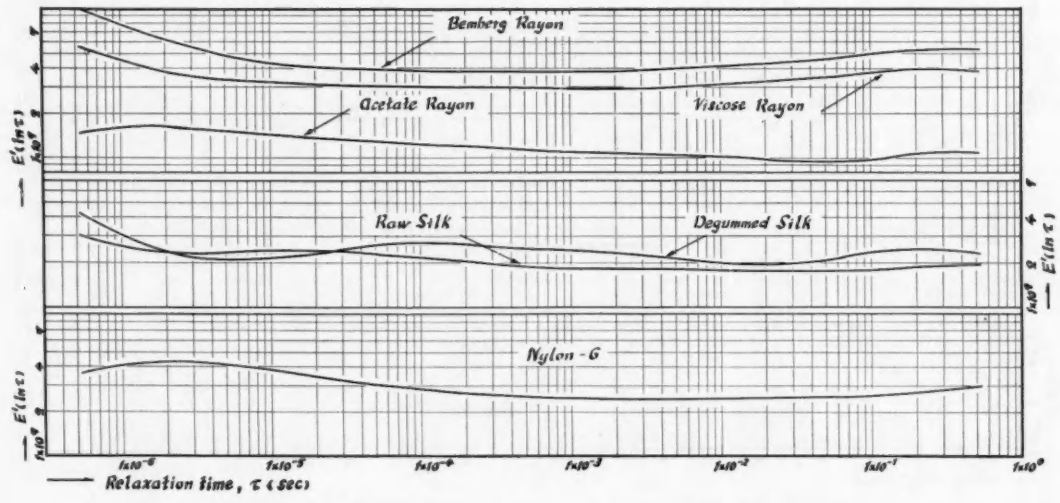

Fig. 17. Final results of the relaxation spectrum as a function of relaxation time.

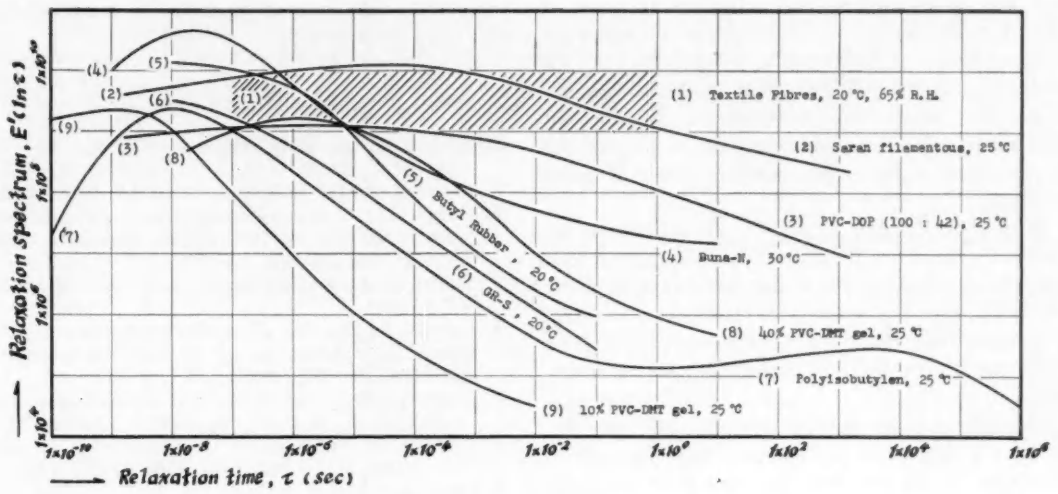
Relaxation spectrum, E'(ln τ)
Relaxation time, τ (sec)
(1) Textile Fibres, 20 °C, 65% R.H.
(2) Saran filamentous, 25 °C
(3) PVC-DOP (100 : 42), 25 °C
(4) Buna-N, 30 °C
(5) Butyl Rubber, 20 °C
(6) GR-S, 20 °C
(7) Polyisobutylen, 25 °C
(8) 40% PVC-DMT gel, 25 °C
(9) 10% PVC-DMT gel, 25 °C

Fig. 18. Recent data on relaxation spectra.

time range, but its general shape may belong to the category of so-called "box distribution."

Figure 18 [3] is a collection of recent data of relaxation spectra reported by several authors for some high-polymeric materials in which the results by Ferry et al., Nohara, and Onogi were obtained not from the measurements over a wide frequency range but from those over a wide temperature range, reducing the temperature to the frequency on the basis of the so-called "thermo-rheological simplicity."

As is well known from tests with line spectra corresponding to a few relaxation mechanisms, the relaxation spectrum thus approximately determined does not exactly agree with its real form but is a somewhat broader one. However, as illustrated in the figure, the greatest difference is found between the spectrum of the textile fiber and that of the rubberlike material. That is, the spectrum of the textile fiber is represented by the so-called "box-distribution," at least in the range of relaxation time from 1×10^{-6} to 1 sec, while that of the rubberlike material is represented by the so-called "wedge-distribution" in the same range.

The fact that the real part of the complex dynamic modulus of the textile fiber at the lowest frequency attained in our experiment is still very large when compared to that of the rubberlike material suggests that the relaxation spectrum of the textile fiber at even longer relaxation times than 1 sec may be higher than that of the rubberlike material, although its exact form cannot be predicted. Since the real part of the complex dynamic modulus at a frequency ω is approximately represented in terms of the relaxation spectrum by the following equation,

$$E_1(\omega) \simeq \int_{1/\omega}^{\infty} E(\tau)\, d\tau \tag{23}$$

Furthermore, as also recognized from the definition of the relaxation spectrum given in equation (3), the quantity $E(\tau)d\tau$ represents only the total sum of partial moduli of relaxation mechanisms falling into the relaxation-time interval from τ to $\tau + d\tau$. Strictly speaking, the quantity specifies only the contribution to the total instantaneous modulus which is given approximately by

$$\lim_{\omega \to \infty} \int_{1/\omega}^{\infty} E(\tau)\, d\tau,$$

[3] The relaxation spectra E' (ln τ) of various high polymers where (1), the area marked by inclined lines, corresponds to our results; (2) is Saran fiber (Onogi [35]); (3) PVC-DOP (100:42), by Nohara [31], is reduced to 25°C by Onogi [35]; (4) Buna-N vulcanizate containing carbon-black, by Nolle [34]; (5) butyl rubber vulcanizate, by Ivey et al. [21]; (6) GR-S vulcanizate, by Ivey et al. [21]; (7) Polyisbutylene, collected by Marvin [29]; and (8) and (9) 40% and 10% PVC-DMT gels respectively by Ferry et al. [10].

and represents neither the individual quantity of partial modulus nor its distribution density separately. Again, as mentioned in the introduction, the relaxation spectrum is indeed a mathematical representation which can conveniently describe the viscoelastic behavior of materials and is nothing but a phenomenological representation which is never essential.

It may be plausible to explain the differences between the spectra of these two typical high-polymeric materials in terms of the molecular structures under the guidance of a viscoelastic structural "picture" which has been described by Tobolsky and Eyring [45], but the explanation cannot help but be speculative.

Nevertheless, we believe that the difference between the spectra of the extreme high polymers is ascribable to the difference between their molecular structures. It is of much interest that the spectrum intensities of all the high-polymeric materials illustrated in the figure are almost equal in the range of relaxation time from 1×10^{-8} to 1×10^{-6} sec and that the spectrum changes its shape from the so-called "wedge distribution" to the "box distribution" in accordance with the change in the nature of materials to be tested from rubbery to highly oriented crystalline ones in the range of relaxation time from 1×10^{-6} to 1 sec.

For model filaments of several high polymers, some experimental researches have been in progress to clarify the relationship between the spectrum and the molecular structure, especially molecular orientation and crystallization. The results of these will be published later.

Acknowledgment

In concluding this paper the authors wish to express their cordial thanks to the members of the high-polymer research group in our university for their valuable suggestions and discussions given throughout the course of this work and to Dr. H. Leaderman of the National Bureau of Standards, who reviewed the manuscript of this paper and gave valuable suggestions.

The authors are also indebted to Dr. H. Kawai and Mr. N. Tokita of the Kobayashi Institute of Physical Research, Kokubunji, Tokyo, who advised them on the constructions of apparatus and to the Minister of Education of Japan for his financial support from 1951 to 1952.

Literature Cited

1. Alfrey, T., and Doty, P., *J. Appl. Phys.* **16**, 700 (1945).
2. Andrews, R. D., *Ind. Eng. Chem.* **44**, 707 (1952).
3. Ballou, J. W., and Silverman, S., *J. Acoust. Soc. Amer.* **16**, 113 (1944); TEXTILE RESEARCH JOURNAL **14**, 282 (1944).
4. Ballou, J. W., and Smith, J. C., *J. Appl. Phys.* **20**, 493 (1949).
5. Bueche, F., *J. Chem. Phys.* **22**, 603 (1954).
6. Dunell, B. A., and Dillon, J. H., TEXTILE RESEARCH JOURNAL **21**, 393 (1951).
7. Ferry, J. D., Sawyer, W. N., Browing, G. V., and Groth, L. D., *J. Appl. Phys.* **21**, 513 (1950).
8. Ferry, J. D., Fitzgerald, E. R., Grandine, L. D., and Williams, M. L., *Ind. Eng. Chem.* **44**, 703 (1952).
9. Ferry, J. D., and Williams, M. L., *J. Colloid Sci.* **7**, 347 (1952).
10. Ferry, J. D., and Fitzgerald, E. R., *Proc. of 2nd International Congress on Rheology*, London, Butterworths, p. 140 (1954).
11. Fujino, K., Kawai, H., and Horino, T., *J. Text. Mach. Soc. Japan* **1**, 9 (1955).
12. Fujita, H.. *Busseiron Kenkyu* 63: 48 (1953).
13. Gehman, S. D., Woodford, D. E., and Stambaugh, R. B., *Ind. Eng. Chem.* **33**, 1032 (1941).
14. Gross, B., *J. Appl. Phys.* **18**, 212 (1947); **19**, 257 (1948).
15. Gross, B., *J. Poly. Sci.* **6**, 123 (1951).
16. Gross, B., *Mathematical Structure of the Theories of Viscoelasticity*, Paris, Hermann et Cie (1953).
17. Gross, B., and Pelzer, H., *J. Appl. Phys.* **22**, 1035 (1951).
18. Heyboer, J., Dekking, P., and Staverman, A. J., *Proc. 2nd International Congress on Rheology*, London, Butterworths, p. 123 (1954).
19. Hillier, K. W., and Kolsky, H., *Proc. Phys. Soc. (London), B* **62**, 111 (1949).
20. Hillier, K. W., *Proc. Phys. Soc. (London), B* **62**, 701 (1949).
21. Ivey, D. G., Mrowca, B. A., and Guth, E., *J. App. Phys.* **22**, 486 (1949).
22. Kawai, H., and Tokita, N., *Report of the Kobayashi Institute of Phys. Res.* **1**, 265 (1951).
23. Kuhn, W., Künzle, O., and Preissmann, A., *Helv, Chim. Acta.* **30**, 307, 464, 487 (1947).
24. Künzle, O., *Helv. Chim. Acta.* **30**, 840 (1947).
25. Leaderman, H., *Elastic and Creep Properties of Filamentous Materials and Other High Polymers*, Washington, D. C., Textile Foundation (1943).
26. Leaderman, H., *J. Appl. Phys.* **25**, 294 (1954).
27. Lyons, W. J., and Prettyman, I. B., *J. Appl. Phys.* **19**, 473 (1947); TEXTILE RESEARCH JOURNAL **19**, 123 (1949).
28. Marvin, R. S., *Ind. Eng. Chem.* **44**, 696 (1952).

29. Marvin, R. S., *Proc. of 2nd International Congress on Rheology*, London, Butterworths, p. 156 (1954).
30. Nielsen, L. E., *Bull. Am. Soc. Test. Mat.* **165**, 48 (1950).
31. Nohara, S., *Chem. of High Polymers, Japan*, **10**, 326 (1953).
32. Nolle, A. W., *J. Acoust. Soc. Amer.* **19**, 194 (1948).
33. Nolle, A. W., *J. Appl. Phys.* **19**, 753 (1948).
34. Nolle, A. W., *J. Poly. Sci.* **5**, 1 (1950).
35. Onogi, S., unpublished data.
36. Palandri, G., *Rubber Age* **64**, 45 (1948).
37. Rouse, P. E., *J. Chem. Phys.* **21**, 1272 (1953).
38. Schmieder, K., and Wolf, K., *Kolloid. Z.* **127**, 65 (1952).
39. Schwarzl, F., *Physica* **17**, 830, 923 (1951).
40. Schwarzl, F., and Staverman, A. J., *Physica* **18**, 791 (1952); *Proc. of 2nd International Congress on Rheology*, London, Butterworths p. 197 (1954).
41. Scott, K. W., and Stein, R. S., *J. Chem. Phys.* **21**, 1291 (1953).
42. Simha, R., *J. App. Phys.* **13**, 201 (1942).
43. Sips, R., *J. Poly. Sci.* **5**, 69 (1950).
44. Haar, D., *Physica* **16**, 719, 738, 839 (1950); *J. Poly. Sci.* **6**, 247 (1951).
45. Tobolsky, A. V., and Eyring, H., *J. Chem. Phys.* **11**, 125 (1943).
46. Tobolsky, A. V., Dunell, B. A., and Andrews, R. D., TEXTILE RESEARCH JOURNAL **21**, 404 (1951).
47. Tokita, N., *Journal of Japan Society for Testing Materials* **2**, 14 (1953).
48. Witte, R. S., Mrowca, B. A., and Guth, E., *J. Appl. Phys.* **22**, 481 (1949).
49. Yamamoto, M., *Report of the Kobayashi Institute of Phys. Res.* **3**, 140 (1953).

Manuscript received October 20, 1954

Correction

The Diffusion of Water Vapor through Laminae with Particular Reference to Textile Fabrics. Part II: A Study of the Transmission of Water Vapor by Diffusion through Perforated Metal Plates

M. E. Whelan, L. E. MacHattie, A. C. Goodings, and L. H. Turl

March 1955 **Volume XXV, No. 3** **Page 205**

Line 7 of the abstract should read β = fractional area of perforation.

Letters to the Editor

Short communications in the form of Letters to the Editor are intended to provide prompt publication of significant new research results and to permit an exchange of views on papers previously published in the JOURNAL. These communications are not submitted to formal review as are research papers, and the editors do not assume any share of the author's responsibility for the information given or the opinions expressed. When work previously published in the JOURNAL is the subject of critical comment, the authors of the original paper are given an opportunity to submit a reply, which will be published concurrently when possible.

Studies on Wool Gelatin: Isolation of Acid Peptides from Room-Temperature Extracts[1]

UNIVERSITY OF HEIDELBERG
Chemical Institute
May 2, 1955

To the Editor
TEXTILE RESEARCH JOURNAL

Dear Sir:

On treating wool with water protein-containing substances are solved. These substances which are called wool gelatin are of some significance in dyeing processes. The literature contains contradictory reports on the treating of wool with water with regard to the *p*H values of solutions, the evolution of NH_3 and H_2S, and the quantity being solved [1–5]. Most authors examined only the reaction of boiling water with wool. More detailed investigation at different temperatures has been carried out by Zahn [6]. These experiments have now been repeated and continued. Suint wool (Cape Merino) was thoroughly cleaned in six steps: continuous extraction for 48 hr each with ethanol, ether, ethanol, ether; stirring in ethanol above a perforated plate in order to remove sand; and picking out of parts of plants by hand. Analysis of the cleaned wool was as shown in Table I.

This wool was now treated successively with distilled water twice at room temperature, twice at 50°C, and three times at 100°C. The extracts were filtered and evaporated in vacuo at 40°C to a small volume (Vol_{conc}). On evaporation the *p*H value increased and was then brought to *p*H 4.5 with acetic acid. The appearing precipitates were removed by centrifuging. The nitrogen contents of the solutions were determined by the micro-Kjeldahl method. The multiplication of the nitrogen value by the factor 6.2 gave a rough value for the protein contents. The results are summarized in Table II. A test investigation revealed that the amino acid composition of the room-temperature extract differed most from wool. The wool gelatins isolated after boiling wool with water became more and more similar to wool with duration of treatment. The amino acid composition of wool gelatin resulting after boiling for 25 hr was close to the amino acid composition of untreated wool with the exception of the cystin contents.

Further investigation was made on room-temperature extracts. The concentrated solutions were dialyzed for 70 hr by means of a parchment membrane to remove inorganic material. Thirty-seven per cent of the protein substances also passed through the membrane. Investigation of the outside solution by paper chromatography showed glutamic acid, aspartic acid, and some lower peptides to be present. The inside substance was ninhydrine negative on paper chromatographic test. The reaction with Cl_2/KJ-starch was positive. This made the existence of higher peptides probable. The solution was now gently evaporated to dryness. The product was a brown glassy brittle mass containing 25% of protein substances and 75% of impurities according to nitrogen analysis. Paper chromatography (solvent: SBA,[2] Whitman Nr.1) gave evidence that the

[1] Presented to the International Wool Textile Research Conference, Australia, 1955.

[2] Mixture of 75% sec. Butanol, 15% formic acid 90%, 10% water.

TABLE I

Ashes	3.47%	Acid solubility	10.40%
Grease	0.47%	Cystin	11.49%
Alkali solubility	12.75%	Mean diameter of fibers	18.5μ

TABLE II

Extract	Temp.	Liquor	Time (h)	*p*H Sol.	Vol_{conc} (mc)	*p*H Conc.	g N	Protein Quantity (g)	Per Cent of Wool
1	20	1:30	74	5.8	280	10	0.236	1.46	0.36
2	20	1:25	65	5.8	328	9	0.019	0.12	0.03
3	50	1:35	48	5.8	250	6.6	0.172	1.07	0.27
4	50	1:30	96	5.8	270	5.8	0.080	0.50	0.12
5	100	1:60*	4	5.4	250	6.4	0.216	1.62	0.41
6	100	1:75*	4	5.6	250	6.4	0.372	2.30	0.58
7	100	1:75*	4	5.6	250	6.4	0.373	2.31	0.58

Total yield of wool-gelatin: 2.35 %

* The washing machine made necessary these high solution/wool ratios.

TABLE III

Isolated Peptide	Amino Acid Composition
PI	Asp, Glu, Ser, Gly, Val, Leu, Ala
PII	Asp, Glu, Ser, Gly, Leu, Thr, Ala
PIII	Asp, Glu, Gly, Thr, Ala

substance was composed of three parts: PI, PII, and PIII. PI remained on the starting point; PII ran 70 mm within 10 days; PIII, 150 mm. Enough substance was put on 60 × 60 cm sheets to isolate after eluation a quantity of 2–3 mg each of the three peptides. The amino acid composition of PI, PII, and PIII was now investigated separately by hydrolizing then with 6 *N* HCl for 12 hr in a sealed tube. No basic amino acids could be found in the three peptides. The results are given in Table III.

On continuing this work the extracts at 50°C and 100°C are to be examined.

Literature Cited

1. E. Clayton, *J. Soc. Dyers Col.* **52**, 86 (1936).
2. Gardner and Carter, *J. Soc. Dyers Col.* **14**, 167 (1898).
3. P. Gelmo and W. Suida, *Monatshefte Chemie* **27**, 225 (1906).
4. W. Pässler and W. König, *Z. angew Chem.* **44**, 288 (1931).
5. A. Schöberl, P. Rambacher, *Biochem. Z.* **306**, 279 (1940).
6. H. Zahn, *Melliand Textil Ber.* **31**, 484 (1950).

HELMUT ZAHN
JOHANNES MEIENHOFER [3]

[3] IWS Fellow.

The Relationship of Aqueous-Extract *p*H to Grade in Raw Cotton of the U. S. Crop of 1954

FIELD CROPS RESEARCH BRANCH
Agricultural Research Service
U. S. Dept. of Agriculture
Beltsville, Maryland
February 16, 1955

To the Editor
TEXTILE RESEARCH JOURNAL

Dear Sir:

Certain observations have been made here recently which may interest your readers as information supplementary to that contained in four earlier papers in TEXTILE RESEARCH JOURNAL [1, 2, 3, 4]. In 1951, Hall and Elting [1] reported a high *p*H of aqueous extracts of raw cotton to be frequently indicative of certain undesirable use-value properties in the fiber and noted with some concern the existence of quite considerable percentages of high-*p*H cotton among white Middling bales in the crops of 1949 and 1950. At the same time a paper from this Laboratory detailed some of the relationships of high *p*H to preharvest weathering of the fiber and to microbial activity and pointed out that the *p*H response is a highly sensitive one which might not indicate significant fiber damage in all cases [2], the latter point being expanded in a subsequent paper [3]. Recently, Wakeham and coworkers [4] conducted extensive fiber and commercial-scale spinning tests

on a pair of low-pH and high-pH samples and reported more short fibers, more waste and end breakage in spinning, and somewhat weaker yarns for the high-pH sample. Information on the relationship of pH to grade has been extremely limited, all reported pH data on graded samples having been confined to white Middling cotton [1, 4]. The objective of the observations to be described here was to determine for a series of samples from the crop of 1954 whether or not any relationship existed between the pH and the grade.

In the months of October, November, and December of 1954, 2350 classer's samples were obtained from the cotton crop of that year in the several cotton-growing states of the United States. Of these samples 1040 were obtained and tested for pH in October, 884 in November, and 426 in December. The numbers of samples tested within each grade are shown in Table I. Of the total number of samples, 42.9% were in the grades of Middling or better. The total number of samples from each of the several states was as follows: Alabama, 134; Arizona, 89; Arkansas, 200; California, 225; Georgia, 185; Louisiana, 199; Mississippi, 235; Missouri, 69; North Carolina, 103; New Mexico, 123; Oklahoma, 132; South Carolina, 40; Tennessee, 47; Texas, 569. Samples were chosen at random at frequent intervals, usually daily, between October 1 and December 31 from a much larger series of randomly selected samples being received by Dorothy Nickerson in the U. S. Department of Agriculture, Washington, D. C. The pH test was carried out essentially as previously described [2]: Add 7.5 cc of boiled-and-cooled distilled water to 500 mg of fiber, tamp and knead for about 1 min, place 5 cc of the supernatant liquid in a test tube of 13-mm outside diameter, add 0.25 cc of Gramercy universal pH indicator, mix, and estimate pH to the nearest 0.1 pH unit from the color chart supplied with the indicator.

Reference is made first to certain relationships between pH and grade which may be noted in the data of Table I. Both the average pH and the percentage of high-pH samples increased from the better to the poorer grades. The designation "high pH" is used here to refer to pH values of 8.0 and higher. In the white samples of the four highest grades from all areas, i.e., Good Middling, Strict Middling, Middling Plus, and Middling, the percentages of high-pH samples were 0, 2.1, 4.3, and 7.1, respectively, whereas in the remaining or lower grades the percentages of high-pH samples were in general much higher. It was noted that in the higher grades such high-pH values as were found occurred principally in the samples classed as gray or spotted.

The data of Table I also bring out the fact that the relationship of pH to grade may vary from one part of the country to another. When the percentages of high-pH samples for the white grades were calculated for the samples from the southeast-and-

TABLE I. Summary of Data on Aqueous-Extract pH and Grade of 2350 Classer's Samples of Cotton Fiber, U. S. Crop of 1954

Grade	Numbers of Samples Tested			Average pH (all samples, all areas)	Percentage of High-pH Samples in Each Grade*				Percentage of Samples in Different pH Groups for Each Grade (White Grades Only) (all areas)			
					White Grades Only							
	White	Spotted and Gray	Tinged		All Areas	Southeast and Mid-south	Tex., Okla., and Western	Spotted and Gray, All Areas	6.0–6.9	7.0–7.9	8.0–8.9	9.0 and up
Good Middling	37	15	—	6.54	0	0	0	26.4	97.3	2.7	0	0
Strict Middling	227	86	6	6.63	2.1	2.8	1.9	14.0	92.1	5.7	1.7	0.4
Middling Plus*	95	—	—	6.72	4.3	3.3	4.7	—	86.3	9.5	3.2	1.1
Middling	379	160	3	6.88	7.1	9.6	5.6	26.4	76.8	16.1	6.6	0.5
Strict Low Middling Plus*	141	—	—	6.74	4.9	4.3	5.6	—	78.0	17.0	4.2	0.7
Strict Low Middling	395	129	4	7.36	30.6	48.2	14.0	23.2	47.1	22.3	22.5	8.1
Low Middling Plus*	126	—	—	7.28	25.4	32.9	11.1	—	51.6	23.0	20.6	4.8
Low Middling	270	60	3	7.83	52.7	65.8	22.0	36.7	22.2	25.2	39.7	13.0
Strict Good Ordinary Plus*	67	—	—	7.72	41.8	44.0	21.4	—	22.5	35.8	31.4	10.4
Strict Good Ordinary	114	—	—	8.18	64.9	66.7	61.1	—	7.0	28.1	52.6	12.3
Good Ordinary Plus*	7	—	—	8.30	85.7	100.0	0	—	0	14.3	85.7	0
Good Ordinary	26	—	—	7.96	50.0	48.0	50.0	—	15.4	34.6	42.3	7.7

* Samples of pH 8.0 or higher.

midsouth area and compared with the same percentages for the Texas-Oklahoma-and-western samples, it was found that the former area generally had a higher percentage of high-*p*H samples than the latter, especially in Strict Low Middling and the lower grades (Table I). It was thought probable that, in the Texas-Oklahoma-and-western samples of lower grades, the lower percentage of high-*p*H cotton resulted from the fact that there was simply less microbial growth on the fiber than in the corresponding grades in the southeast and midsouth, the lowered grade in the Texas-Oklahoma-and-western area being probably more strongly associated with the presence of leaf fragments, twigs, and other nonfibrous material. This interpretation was supported by the results of tests (not shown) in which the southeast-and-midsouth samples had definitely and consistently lower amounts of reducing constituents in a copper-reduction test. This test is very responsive to microbial growth [3]. Another possible interpretation which came to mind was that for some reason the western samples simply did not have the capacity to increase in *p*H under the influence of microbial growth as the midsouth-and-southeastern samples did. Although such an explanation was considered of questionable validity, an experiment was carried out to test the point. Twenty-four Strict Middling samples of *p*H 6.3–6.7 from Arizona, California, New Mexico, Oklahoma, and Texas were incubated for 2 weeks in a water-vapor-saturated atmosphere with a pure culture of a fungus, *Alternaria,* as previously described [2]. After incubation, all but one of the samples had a *p*H of 10.0, a single sample having a *p*H of 9.5. It was obvious, therefore, that the western samples did not lack the capacity for increasing in *p*H under the influence of microbial growth.

Hall and Elting [1] reported definitely higher percentages of high-*p*H samples in the white Middling grade in 1949 and 1950 than were observed in our laboratory, as reported in Table I for 1954. They found 15, 65, and 61% of southeastern Middling cotton of good color to be of *p*H 8.0 or higher for the crops of 1948, 1949, and 1950, respectively, and 18, 43, and 63% for Middling white midsouth cotton of the same crops. It seemed worth while to be certain that this difference in results was not due to a difference in the method of making the *p*H determinations. In the Kendall method of *p*H determination [1], 3 cc of hot water is added to 1 g of cotton, the wet fiber centrifuged, and the *p*H of the centrifugate estimated to the nearest half-*p*H unit by the use of a drop of Gramercy universal indicator. When this method was compared with the method this Laboratory employed, it was found that, in samples which tended toward a yellowish fiber color, the hot water extracted a good deal of the color, which interfered with the colorimetric *p*H determination, this effect also being accentuated by the low water-to-fiber ratio used. As a result, the Kendall-method *p*H's were difficult to estimate but in some cases much lower (approximately 0.3 to 1.3 *p*H units) than the USDA-method *p*H's and never higher. When the two types of extracts were tested with the glass-electrode *p*H meter instead of by indicator, it was observed that the hot-water (3:1) centrifugate was only slightly lower in *p*H than the cold-water (15:1) extract.

In a personal letter to the writer, Dr. Elting has kindly communicated the fact that data from Kendall Mills' tests on the *p*H of Middling grade white cotton of the crop of 1954 is in substantial agreement with that reported here in our Table I. He states "Of the cotton which we tested from the 1954 crop (1,389 samples, consisting of Eastern and Central points) 137 were alkaline. This we believe compares favorably with the 9.6% shown in your table for Middling cotton under the column headed 'Southeast and Mid-south.' While our data showing 10% and yours 9.6% may be a somewhat fortuitous agreement . . . our data and yours yield results of the same order of magnitude." As a result of the foregoing data on comparative results by the Kendall and U.S.D.A. test methods and of the close agreement in results between the two laboratories on the 1954 crop, it seems clear that the differences in numbers of high-*p*H samples between the 1949 and 1950 crops on the one hand [1] and the 1954 crop on the other cannot be ascribed to differences in the method of *p*H determination.

It is suggested that the reason for the existence of a relationship between aqueous-extract *p*H and grade is to be found in the facts that preharvest microbial growth on the fiber induces both an increase in *p*H and a darkening in color and that the latter property is an important element in the determination of grade. No explanation is advanced as to the cause of the above-discussed differences in the prevalence of high-*p*H samples in Middling cotton between the data of Hall and Elting [1] and those here reported, further investigation of the point appearing desirable.

Acknowledgment

The writer wishes to record his gratitude to Miss Dorothy Nickerson, Standards and Testing Branch, Agricultural Marketing Service, U. S. Department of Agriculture, Washington, D. C., for her kind assistance in securing the samples and for helpful comments during the work; also to Mrs. M. L. Butler for carrying out the *p*H determinations.

Literature Cited

1. Hall, L. T., and Elting, J. P., "Cavitomic Cotton; A Progress Report," TEXTILE RESEARCH JOURNAL **21**, 580–590 (1951).
2. Marsh, P. B., Guthrie, L. R., and Butler, M. L., "The Influence of Weathering and of Microorganisms on the Aqueous-Extract *p*H of Cotton Fiber," TEXTILE RESEARCH JOURNAL **21**, 565–579 (1951).
3. Marsh, P. B., Bollenbacher, K., Butler, M. L., and Merola, G. V., "The Relative Responsiveness of Certain Properties of Cotton Fiber to Microbial Action," TEXTILE RESEARCH JOURNAL **24**, 31–38 (1954).
4. Wakeham, H., Stickley, H., and Spicer, N., "Cotton Quality and Fiber Properties. Part II: Cavitomic Cotton," TEXTILE RESEARCH JOURNAL **24**, 1037–1047 (1954).

PAUL B. MARSH

you can't sit this one out...

Pleats that won't sit out when they're sat *on* are a boon that women have learned to look for—and are willing to pay for! And they're just one of many pace-setting advantages you can build into the fabrics you create by using Du Pont's "modern-living" fibers.

Other such exciting textile advances as thick and thin and crimpable yarns . . . and fibers that offer *built-in* shape retention, wrinkle resistance, and easy care . . . stem from Du Pont research for today's world. For today's customers *want* home furnishings and apparel that look better, wear longer, and require less care.

Use Du Pont modern-living fibers for the extras that spell a fabric success. Count on Du Pont's experience in fiber research to help you keep pace with the more demanding needs of today's customers.

Du Pont's Modern-Living Fibers

DU PONT
REG. U.S. PAT. OFF.

NYLON RAYON ACETATE ORLON® ACRYLIC FIBER DACRON® POLYESTER FIBER

BETTER THINGS FOR BETTER LIVING... *THROUGH CHEMISTRY*